UNIVERSITY OF COPENHAGEN

FACULTY OF SCIENCE

MASTER THESIS

Greenland in a warmer world

A MODELLING STUDY OF THE GREENLAND ICE SHEET

Author:
Helene Pehrsson

Supervisors:
Christine Schøtt Hvidberg
Anne Munck Solgaard
Nanna Bjørnholt Karlsson

May 20, 2022

Abstract

The goal of the project is to model the minimum ice sheet extent of the Greenland ice sheet during the Eemian interglacial and to figure out if including Canada in the computational domain, can make a difference for the ice extent in northern Greenland. Knowing more about the extent of the Eemian ice sheet, can give us invaluable insights, when it comes to predicting the future conditions of the Greenland ice sheet, if global temperatures continue to rise.
Further more the evolution of the present day ice sheet under warmer conditions is investigated, to determine the sea level rise related to the loss of mass. All the modeling is done using the ice flow modelling tool PISM and the climate forcing data comes from RACMO [Noël et al., 2018].
It is found that an increase in temperature over Greenland of 2°C results in an approximate increase of the global mean sea level of 1.29 m, when the ice sheet approaches a new steady state after 20,000 years and a temperature increase of 4°C results in an increase of 6.88 m and a drastic retreat of the ice sheet. It is also found that under present day conditions, the Greenland ice sheet will lose mass over time and reach steady state after approximately 20,000, after contributing around 0.36 m to the global mean sea level.
Further more it turns out that due to the bedrock conditions of the model, the Eemian ice sheet retreats too far south and has a hard time growing north again when the glacial period starts.
Due to a very low precipitation in the northern part of the domain, only very minor changes in the ice sheet evolution can be seen when including Canada in the computational domain, compared to when it is not included.

Acknowledgments

Firstly I would like to thank my wonderful supervisors Christine Schøtt Hvidberg from PICE and Anne Munck Solgaard and Nanna Bjørnholt Karlsson from GEUS. Their help and supervision has been invaluable to me throughout this project. They have provided data, motivation, PISM help and advice about the future over the course of this project and I am truly grateful for it all.

I would also like to thank Emily Wilbur, for being my partner in crime and going on this adventure with me. She has played a big role in the preprocessing of all the data and the understanding of PISM as an ice flow modelling tool.

A big thanks goes out to Mikkel Langgaard Lauritzen for all the help with CDO, NCO and PISM commands. I am really glad you got this Ph.d. position and that we got to work together. I know you will make a great glaciologist and I cannot wait to find out, what results your research will yield.

I would also like to thank Nicholas Rathmann for setting up PISM and generally helping with the understanding of how Computerome works, Signe Hillerup Larsen for helping with command lines and getting PISM running and Thea Quistgaard for proofreading my thesis and general emotional support.

Lastly I would like to thank Kasper Holst Lund for keeping everything together for me on the home front, especially these last few weeks. You have been my rock and deserve so much praise for all the late night rants you have had to endure and for keeping me sane and in a good mood throughout these past 9 months.

Contents

1 Introduction

The rising sea levels over the past decades, have sparked an increasing interest in the Arctic region and specifically the Greenland ice sheet. If temperatures in and around Greenland continue to rise, it could result in large loses of the ice mass and thereby an increase of the global sea level, which could affect areas all around the globe.
This project aims to model the potential mass loss from the Greenland ice sheet in the future, as well as the minimum extent of the Greenland ice sheet ice sheet during the last interglacial period. Understanding the climate conditions on Greenland during the last interglacial, could help us to understand the climate conditions we might encounter in a warmer future.

The main goal of this project is to model the minimum ice sheet extent, of the Greenland ice sheet during the Eemian interglacial (last interglacial) and to figure out if including Canada in the computational domain, can make a difference for the ice extent in northern Greenland.
To do this it is necessary to also model the end of the glacial period just before the Eemian, because the ice sheets at Greenland and Canada ware connected at the time [Cuffey and Paterson, 2010]. Therefore the project also includes a study in glacial climate conditions and how to recreate them in the model, as well as a study in how different temperature increases over Greenland can effect the global mean sea level.
All the ice flow modelling in this project is done using the ice sheet model PISM, a widely used open source model, suitable for large scale ice flow modelling.

In the following chapters can be found the ice dynamics theory that the model is build upon, as well as the theory needed to understand the motivation for the project and the results it yields. A description of the data sets used and how they were prepared can also be found, followed by a detailed description of the model dynamics.
Lastly the results of the studies conducted are presented, along with a discussion of the models validity and limitation. Finally, there is a short discussion of how the results can be used and possibly improved in the future.

2 Background

In this chapter the background is described, on which this thesis is built. This includes how Greenland fits into the global climate system and affects specifically the climate of Northern Europe. What the glacial cycle is and how it has changed over time, as well as an overview of the last glacial and interglacial and what results previous studies about Eemian Greenland have yielded and how the results of this study will differs from these studies.

2.1 Greenland in the climate system

The Greenland Ice Sheet (GrIS) is the second largest inland body of ice on Earth, only exceeded by the Antarctic ice sheet. The glaciarized area of Greenland is 1,710,000 km^2 and covers most of the landmass. The GrIS alone holds a mass equivalent to a global sea level rise of 7.42 m [Morlighem et al., 2017], if all the ice melted. Because of the enormous amount of ice, the GrIS holds a very central role in the climate system of the Earth and especially the Northern hemisphere.

The North Atlantic Current is an ocean current that together with the Gulf Stream transports warm ocean water from the Gulf of Mexico across the Atlantic ocean to Northern Europe. Essentially this flow of warm water from southern to northern latitudes, is what makes the northern European climate so warm and humid, creating great living conditions for humans compared to other places with the same latitude.
From northern Europe the water flows west and south along the eastern coast of Greenland. Here the water is cooled down again by the flux of fresh water, coming from the marine outlet glaciers in the area. This cold water then flows back south again to the Gulf of Mexico, this part of the current is called The North Atlantic Deep Water. An approximate map of the currents can be found in figure 1.

If the temperature in and around Greenland continues to rise, the GrIS will start to shrink due to surface melt, resulting in a retreat from the coast. This could result in a reduction or complete loss of fresh water flux into the Atlantic Ocean. If this is the case, it could ultimately result in the termination of the North Atlantic Deep Water current, which brings cold water south to the Gulf of Mexico. If there is no flow of cold water into the Gulf of Mexico, there will be no flow of hot water out of it, meaning no North Atlantic Current and thereby no transport of warm water to Northern Europe, effectively lowering the temperature of this part of the world.

Over the past decades there has been an increase in the mass loss of GrIS and the Antarctic ice sheet. This is likely due to the temperature rise over the two areas as well as the ocean's. This results in ice melting faster than before, both at the margins and on the surface of the ice sheets. It also means more calving of icebergs from the shelves and outlet glaciers. This also results in more precipitation coming down as rain and less as snow, effectively resulting in less accumulation of ice.

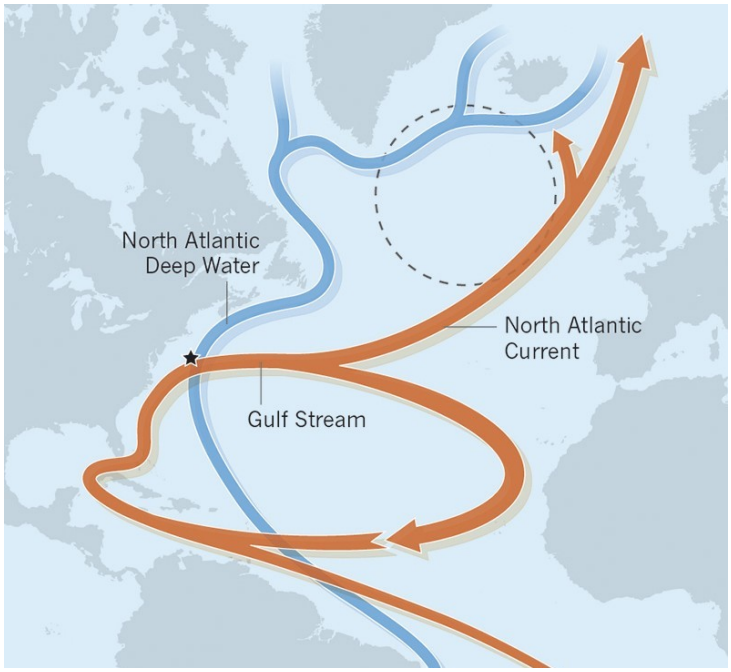

Figure 1: The large currents that control the flow of water in the Atlantic ocean [Praetorius, 2018].

The shrinking of the GrIS is also resulting in a lowering of the albedo in the area. Especially the surface melt on Greenland has a big part to play here, because snow has one of the highest percentages of diffusely reflected sunlight of all surfaces. This means that when ice and snow is melting in Greenland, less solar radiation is reflected and therefore the temperatures in the area increases even further, resulting in a feedback effect that could cause even more melting.

2.2 The glacial cycles

Oscillations in the temperature of Earth is no new concept, in fact they have been happening cyclically for more than 5,200,000 years [Lisiecki and Raymo, 2005]. These cyclical oscillations are called glacial cycles and consist of a cold period called a glacial followed by a warm period called an interglacial. These cycles have been following a pattern of approximately 40,000 years, which is the same frequency as the change in the Earth's axis tilt.
About 800,000 years ago the frequency of the glacial cycles changed to 100,000 years, which is the same frequency as the change in the Earth's Orbital eccentricity. Why this happened is still somewhat of a mystery and it is a question climate researchers all over the world are currently trying to answer [Cuffey and Paterson, 2010].

Figure 2 shows a graphic representation of the correlation of 57 globally distributed benthic $\delta^{18}O$ ocean sediment core records [Lisiecki and Raymo, 2005]. The plot shows the amount of $\delta^{18}O$ in the sediment, which is a proxy for the amount of ice bound on the continents at the time as well as the temperature. Low amounts of $\delta^{18}O$ mean large amounts ice on the continents, because $\delta^{18}O$ is bound in ice instead of the water in the ocean. This means that peaks in the figure represents interglacial periods, with little ice and valleys represent glacial periods, with lots of ice.

As it can be seen the climate has oscillated a lot, but ultimately it seems to follow a trend of cooling over time with an increase in the amplitude on the oscillations. This means that the temperature trend is falling and the difference between the warm and cold periods of Earth has gotten larger.

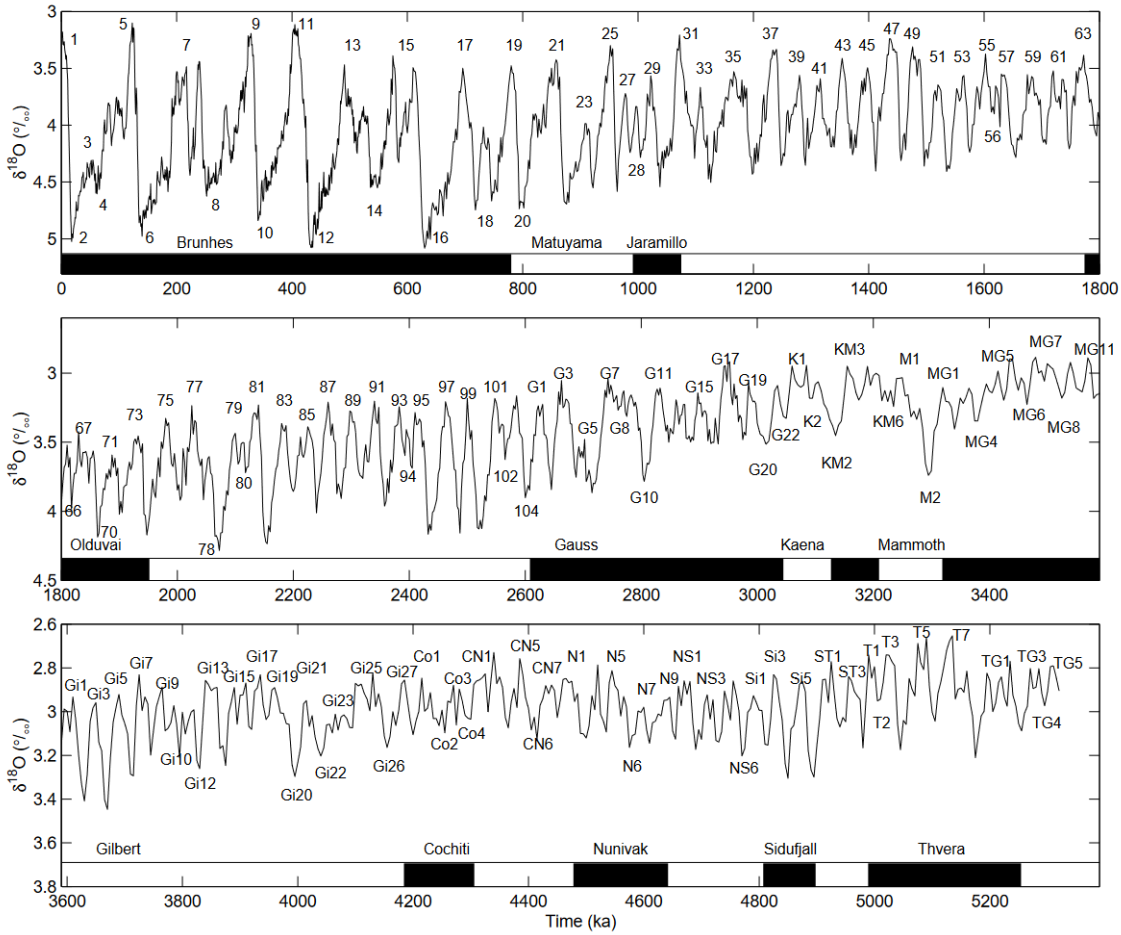

Figure 2: A graphic correlation of 57 globally distributed benthic $\delta^{18}O$ ocean sediment core records. On the y-axis is the amount of $\delta^{18}O$ found in the sediment and on the x-axis is time before present [Lisiecki and Raymo, 2005].

The focus of this thesis is on the last two glacial periods and the interglacial between the two called the Eemian and then of course the present day climate. In Greenlandic deep ice core records, it is only possible to go as far back as 130.000 years, and since the Eemian interglacial started around this time, it means that we have no data from before Eem and the Eemian data we do have is very limited. However we do have large amounts of data from the last glacial and at a very fine resolution [NEEM community members, 2013].

2.2.1 Last glacial

The last glacial period does not officially have a name, but in Northern Europe it is called The Weichselian glaciation and it took place from about 115,000 – 11,700 years ago. The last glacial period was filled with oscillations in temperature resulting in the ice advancing and retreating several times over the period [NorthGRIP members, 2004].

The maximum ice extent happened about 22,000 years ago [Cuffey and Paterson, 2010] and is called the Last Glacial Maximum (LGM). At this point the ice covered most of Northern Europe, including most of Denmark, and in Greenland it spread all the way to the continental shelf on both sides. The ice also created an ice bridge between northern Greenland and the north-eastern part of Canada [Cuffey and Paterson, 2010].

During LGM the climate in Greenland was very different from present day. The temperature over the area was $20 - 25^{\circ}C$ colder [Dahl-Jensen et al., 1998] and sea level was lower by approximately 130 m [Lambeck, 2004]. Precipitation was also lower, of around 20% to 25% of the present day precipitation [Johnsen et al., 1992].The pattern of rain and snow fall was most likely also different from today, but it is very hard to pinpoint what it looked like. Precipitation has a tendency to be higher along the margins of the ice sheet rather than on the top of the ice sheet, meaning that the snow would have most likely fallen further out than at present since the ice sheet extended over a much larger area.

2.3 Eemian interglacial

The Eemian interglacial was the last interglacial before the Holocene, the epoch we are in currently. The Eemian began around 130,000 years ago and lasted until 115,000 years ago. This period was characterized by warmer temperatures and higher sea levels than today. The global mean temperature during Eemian times was higher by approximately $2^{\circ}C$ [Kopp et al., 2009] and over Greenland specifically the temperature peaked at $8 \pm 4^{\circ}C$ warmer than present day [NEEM community members, 2013].
This means that the GrIS extent was most likely smaller, by possibly quite a lot more than today and a modelling study estimated that it contributed to the global sea level rise with about 0.6 m of the total 6-9 m, that the sea level was higher than the present day [Stone et al., 2012].

Not much is known about the Greenland ice sheet at this time, because all the evidence has either melted away at this point or is sediment that is currently covered by several kilometers of ice. Geologists are looking for sediment deposits along the coast of Greenland, to see if they can determine the extent of the ice sheet from those. But since the ice sheet was most likely smaller than it is at present time, all these deposits are probably located under the current ice sheet.

Climate researchers all over the world are however still very interested in finding out, what Greenland looked like at the time, as knowing more about Eem, could bring us closer to figuring out how our world might look in the future, if the global mean temperature and global sea level continues to rise.
The evidence we do have access to, points in the direction that the Eemian climate conditions are very close to present day conditions, especially if the present day temperature increases by just a few degrees. It is also the only period, with warmer temperatures than today, where we know with fair certainty how the world was in terms of climate, sea level and general living conditions. This means that if temperatures at present increase above the Eemian, we have no previous climate records to help figure out how the world will look in the future.

2.4 Previous studies

Several previous studies have been conducted regarding the Eemian ice sheet extent in Greenland. Figure 3 shows a collection of these studies [Plach et al., 2018]. These 10 studies all aim to model the minimum extent of the Eemian ice sheet and as it can be seen they all differ from each other and some of them by quite a lot. The two major differences between the studies are whether there was one large ice sheet or the ice sheet was split in two, creating a large northern ice sheet and a smaller southern one, as well as how far north the ice actually extended.
Some of the studies show the ice sheet mostly centered around the middle of Greenland, and some of them extent almost as far north as the present day ice sheet. Some of them reach almost all the way to southwestern coast, where as some of them only have ice in the eastern part. This a very accurate representation of how little we know about the size of the Eemian ice sheet.

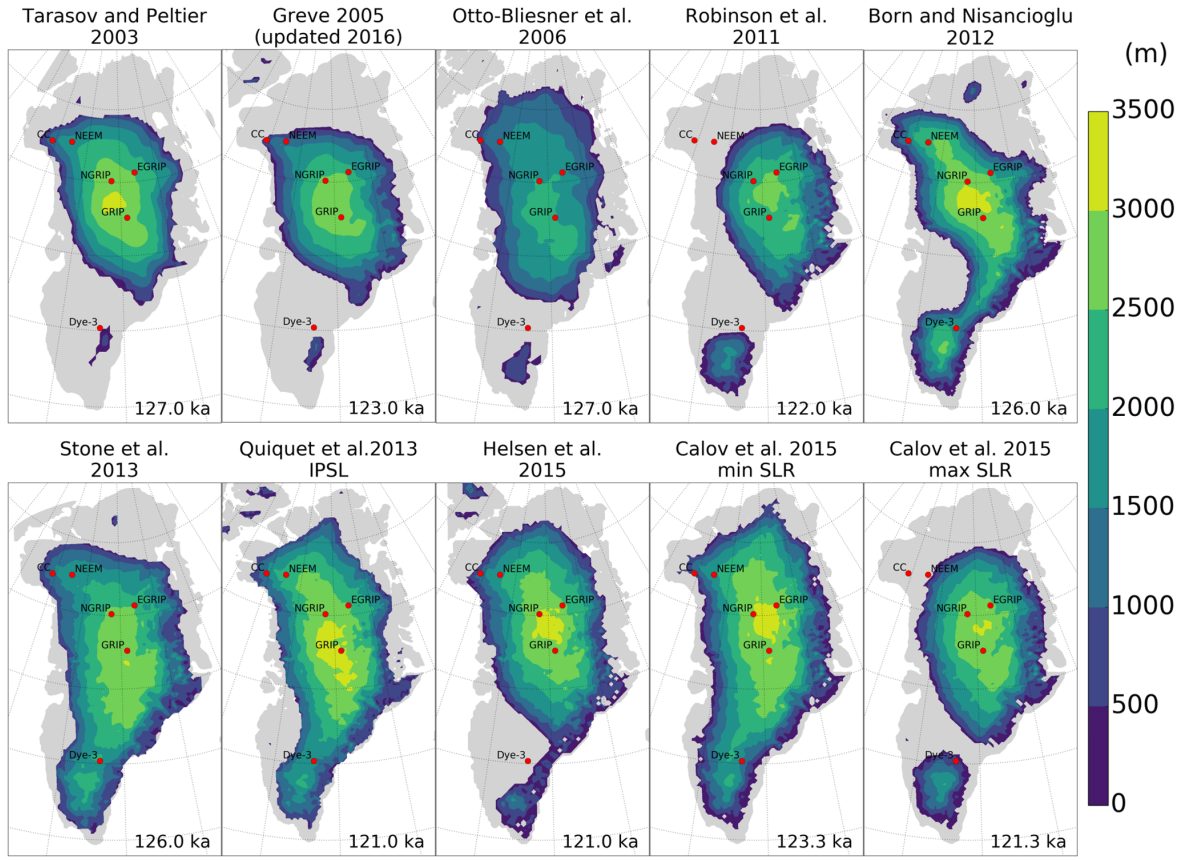

Figure 3: This figure contains a collection of plots, showing the minimum modelled ice extent in Eemian Greenland [Plach et al., 2018]. The red dots mark the deep ice core drill sites in Greenland.

All the studies showed in figure 3 are simulated using different ice flow models, but this is not the reason for the large differences in ice extent, since most ice flow models are build on the same assumptions and approximations of the real world. The main reason for these differences are the climate forcing parameters chosen. Here climate forcing refers to precipitation pattern and amount, air and ice temperature, melting and calving rates, sea level and ocean temperatures.

The differences in these parameters are fairly small among the studies, and it shows how sensitive the ice sheet is to a small change in the forcing, which can impact the overall result of a model run.

2.4.1 Evidence of Eemian ice

Researchers now believe that there is evidence of Eemian ice at the bottom of all the deep ice cores drilled in Greenland [Vinther and Johnsen, 2013]. This points to the conclusion that the Eemian ice was extended to all these locations, or it has moved to these locations since Eem due to ice dynamics. The location of the deep ice core drill sites in Greenland can be seen in figure 3.
This knowledge can be used as a forcing parameter when modelling the Eemian ice sheet, since the ice that survives within the ice sheet, must at present time be located at all the deep ice core drill sites in Greenland.

Figure 4 shows the results of a study that attempted to locate the current extent of Eemian ice, within the present day Greenland ice sheet [MacGregor et al., 2015]. This study was conducted using radiostratigraphy and points towards the conclusion, that there must have been at least some ice in northern Greenland during Eem, which speaks in contrary to some of the previous studies conducted shown in figure 3.

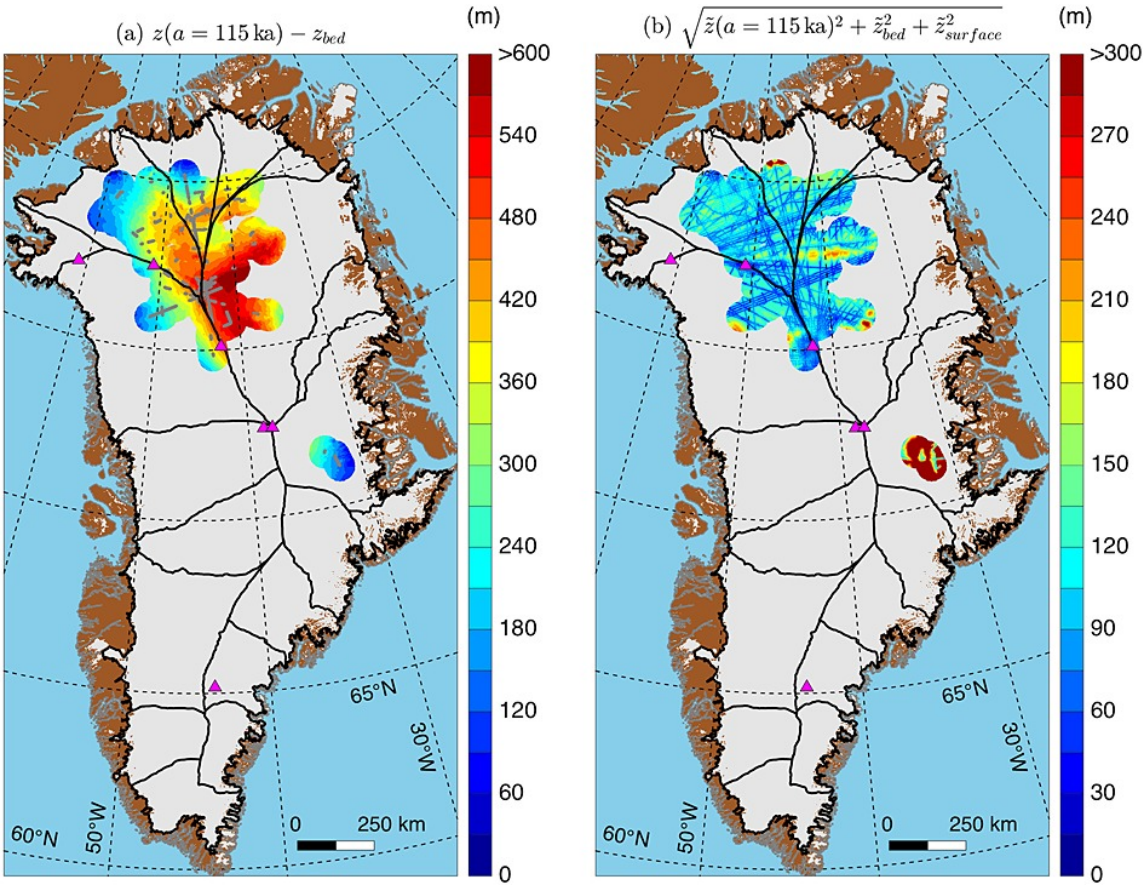

Figure 4: Radar data from Greenland, showing the distribution of Eemian ice [MacGregor et al., 2015].

2.4.2 How this project differs

A lot of previous studies have been conducted about the extent of the Eemian ice in Greenland. This project differs from former studies, as it aims to compare the model results with the results of [MacGregor et al., 2015], as well as testing what difference it makes including Canada in the computational domain.
As can be seen in figure 3, most of the previous studies do not include Canada in the computational domain and those that do only include the most eastern part of Greenland. We know that the ice sheet during LGM extended all the way to the continental shelf and included an ice bridge between Greenland and Canada in the Nares strait. Since the temperature during LGM and the glacial maximum before Eem are approximately the same [Lisiecki and Raymo, 2005], there is no reason to believe that the ice did not have a similar extent then.
If an ice bridge between Greenland and Canada was present during the glacial before Eem, including Canada and thereby this ice bridge in the computational domain, could make a major difference for the extent of the Eemian ice specifically in the northern part of Greenland.

3 Data

The following chapter contains a description of all the data sets used in this study and how they were preprocessed prior to use. The preprocessing includes regridding to a lower resolution, changing the map projection and stitching different data sets together. All the data sets ended up being regridded to 10 and 20 km resolution and was to be on polar stereographic projection, with a true scale of 75 ° N.

3.1 Topography

In this study the bedrock topography used for modelling, is from from The International Bathymetric Chart of the Arctic Ocean (IBCAO) v4.0 [Jakobsson et al., 2020]. IBCAO is a topography and ocean bathymetry mapping of the whole Arctic region surrounding the Arctic ocean. Figure 5 shows the bed topography and the surface elevation from IBCAO for the domain used in this thesis.

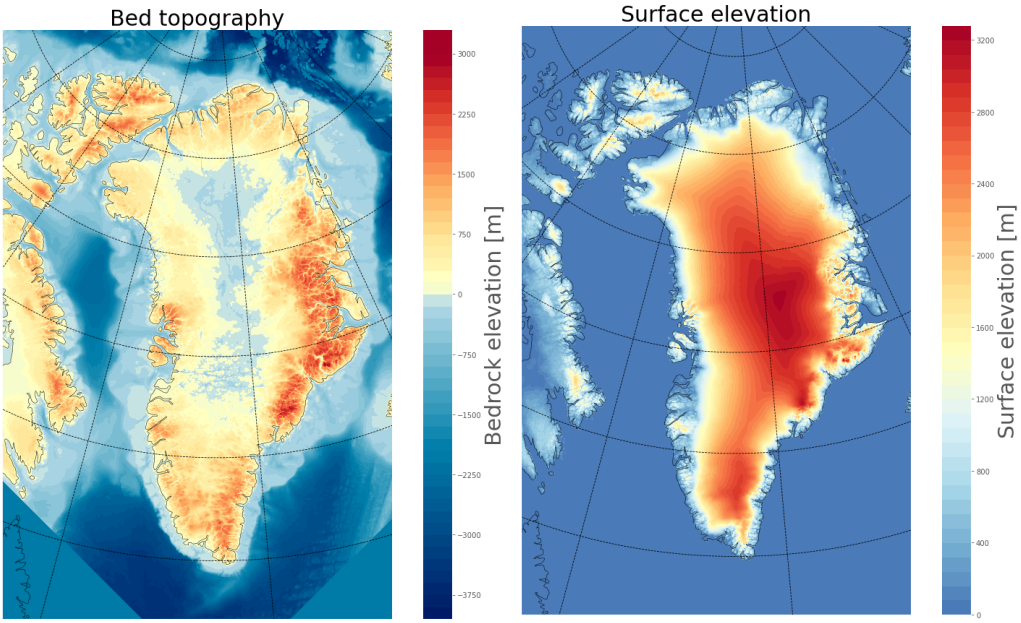

Figure 5: The bedrock topography and surface elevation, used in this study [Jakobsson et al., 2020], at 10 km resolution.

The IBCAO data set [Jakobsson et al., 2020], comes in two resolutions 200 m and 400 m, and because both these resolutions would require to much computational time, compared to what the aim of the project is, the resolution had to be lowered. The 400 m version of IBCAO is a regridded version of the 200 m version, so to lower the number of miscalculations and uncertainties related to regridding, the 200 m resolution map was used to do the regridding.
The projection of the IBCAO data set is polar stereographic, with the true scale set at 75 ° N. Which is the projection wanted for the data, so for this data set, nothing had to be done about the projection, just the resolution.

The first step in the preprocessing was to cut the data set, so that the domain, was not the whole Arctic region, but just the area around Greenland. The file came as four

tiles, and the entirety of the domain for this project was contained in one of the tiles. This tile was cut to fit the domain, but this left the domain without data in the southern corners, as can be seen in figure 5, because these are not a part of the IBCAO data set. After the whole regridding process of the data, these areas were set to be ocean of 2000 m depth to best match the surrounding elevation.
The data set was regridded using bi-linear interpolation, which is a method that uses repeated linear interpolation, first in one direction of the grid, and then again in the other direction. Meaning that although every step of the interpolation is linear for the position and the sampled values, the interpolation as a whole is not actually linear but rather quadratic in the sample location. This method is very useful, when working with functions sampled on a two dimensional rectilinear grid, like the IBCAO grid, and therefore it is also one of the most used interpolations for this grid type.

Part of this study consists of determining whether including Canada in the computational domain will make a difference. To test this there is a need for an identical set of maps to those in figure 5, where the only difference is the removal of all Canadian land from the map without changing the domain. This was accomplished by creating a version of the bed topography and surface elevation maps, where the domain is the same size, but Canada has been cut out and replaced with 1000m deep ocean, again to match the surrounding elevation. These maps can be seen in figure 6.

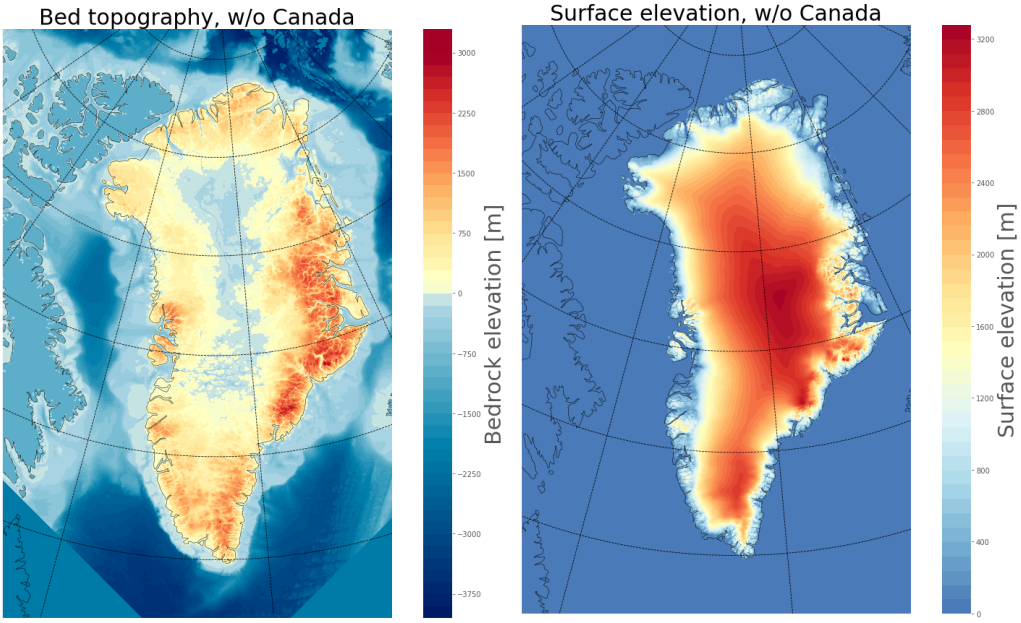

Figure 6: This plot shows the same maps as the first two in figure 5 from IBCAO v4.0 [Jakobsson et al., 2020], at 10 km resolution. The only difference is the removal of Canada. The land has been replaced with 1000m deep ocean.

3.2 Ice thickness

The ice thickness shown in figure 7 comes from BedMachine v3 [Morlighem et al., 2017]. This is a bed topography and ocean bathymetry mapping of Greenland, created using multi-beam echo sounding combined with mass conservation. In this study only the ice thickness from this data set will be used, not the topography and surface elevation.

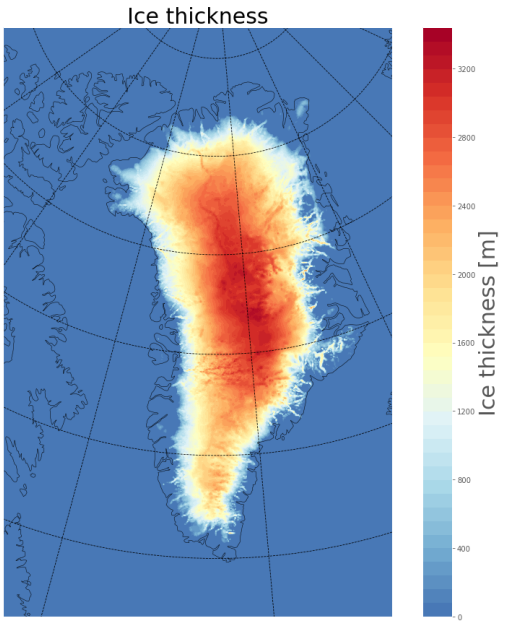

Figure 7: The ice thickness over Greenland used in this study [Morlighem et al., 2017], at 10 km resolution.

The BedMachine data [Morlighem et al., 2017] comes on a 150 m resolution and only covers an area that is Greenland and a very small part of Canada. The projection of this data set is polar stereographic, with a true scale of 70 ° N, rather than 75 ° N. This means that the resolution and the projection had to be changed and the domain had to be extended rather than cut.

The regridding of this data set was also done using bi-linear interpolation. It was done using CDO (Climate Data Operators) and NCO (netCDF Operators). When using these the true scale of a projection can be changed alongside the regridding process.
When the data was on the right resolution and projection, the Canadian part of the domain was cut out and replaced with zeros everywhere and the domain was extended to the same size as the preprocessed IBCAO data and filled in with zeros. Zeros were chosen, because PISM cannot deal with Nan values and the only variable used from BedMachine, is the ice thickness, which should for this purpose be zero everywhere but the GrIS.

3.3 Climate forcing

When modelling an ice sheet the main difference in final results comes from the climate forcing parameters chosen. This is because the temperature on top of an ice sheet and the precipitation falling over the area, are two of the main drivers for the evolution of an ice sheet. The RACMO data set used is an extension of the data set by [Noël et al., 2018]

RACMO consists of the monthly mean temperature and precipitation from 1959-2020. The model used in this study needs the monthly mean precipitation for every month and the mean annual and the mean summer temperature over the area. The maps in figure 8 shows the mean annual and the mean summer temperature. These temperature fields where created by taking the mean of the monthly data in RACMO over the whole period to create a mean annual and a mean summer temperature.
The mean summer temperature refers to the mean temperature in the month of July.

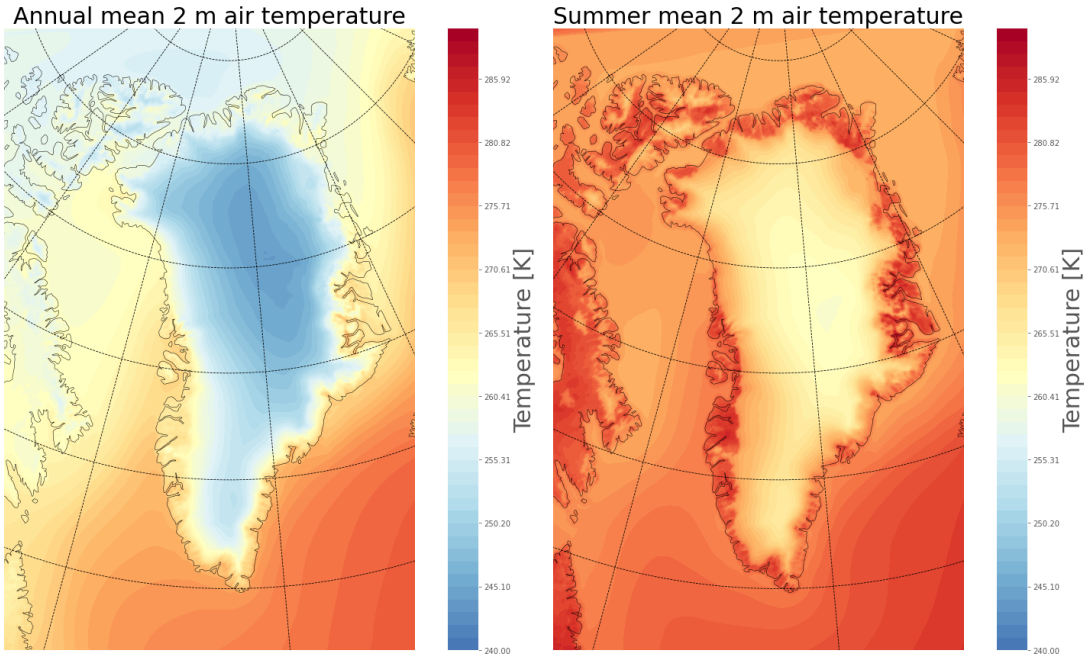

Figure 8: The mean annual and mean summer temperature, created from the monthly temperature form RACMO over the period 1959-2020 [Noël et al., 2018], plotted in 10 km resolution.

The precipitation used to force the model has to have the form of monthly mean values. Figure 9 contains the precipitation averaged over the whole RACMO period of 1959-2020 for each month of the year.

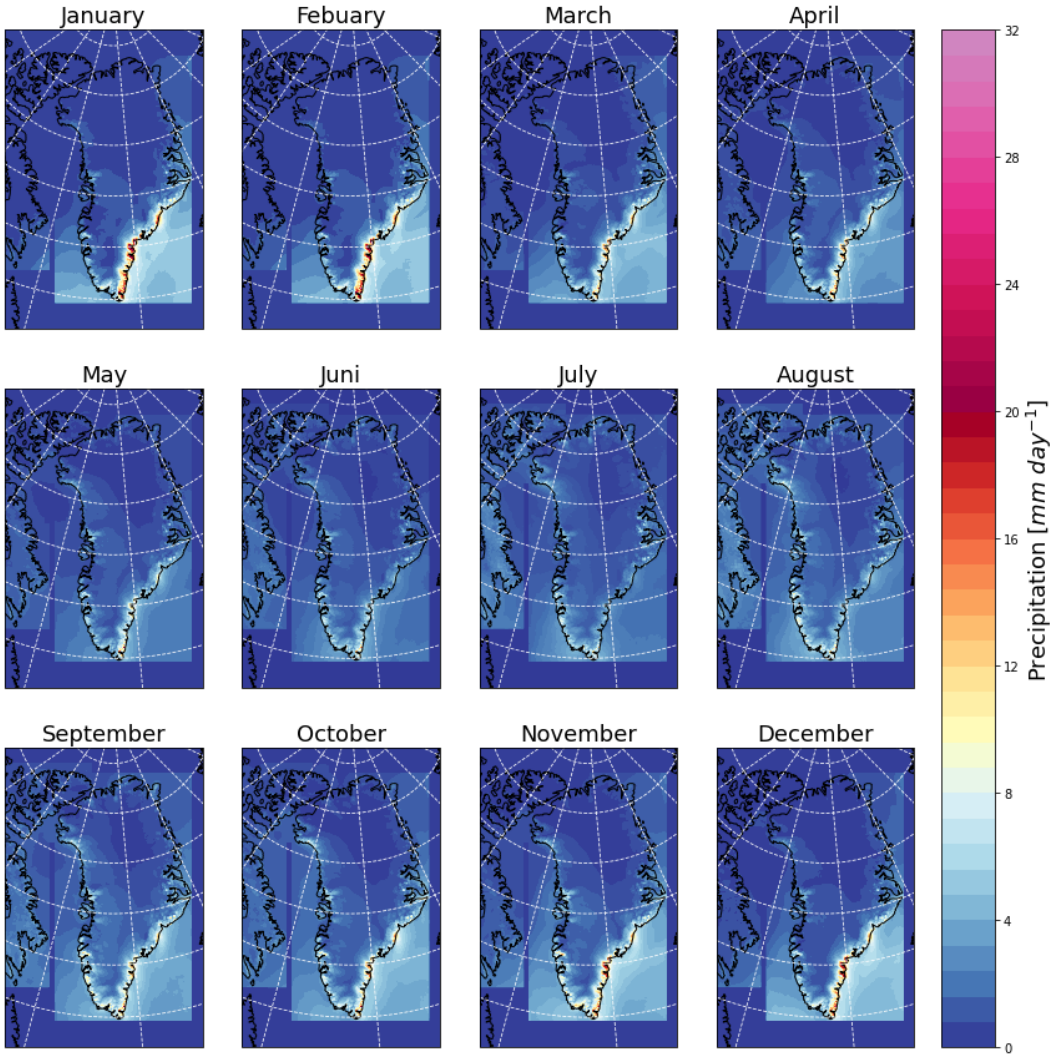

Figure 9: The mean monthly precipitation, for every month of the year, over Greenland for the period 1995-2020 [Noël et al., 2018], plotted in 10 km resolution.

As mentioned above is the data set an extension of the data set by [Noël et al., 2018]. It is stitched together from three tiles of data: the GrIS, the North (NCAA) and South Canadian Arctic Archipelago. The three tiles can be seen in figure 10. All the data was originally on 5.5 km resolution, but in the stitching processes the resolutions was increased to be 1 km. The data set was also on polar stereographic projection, with a true scale of 70 ° N, that had to be changed. The data was again regridded using bilinear interpolation in CDO and NCO, so the projection could be changed along with the regridding.

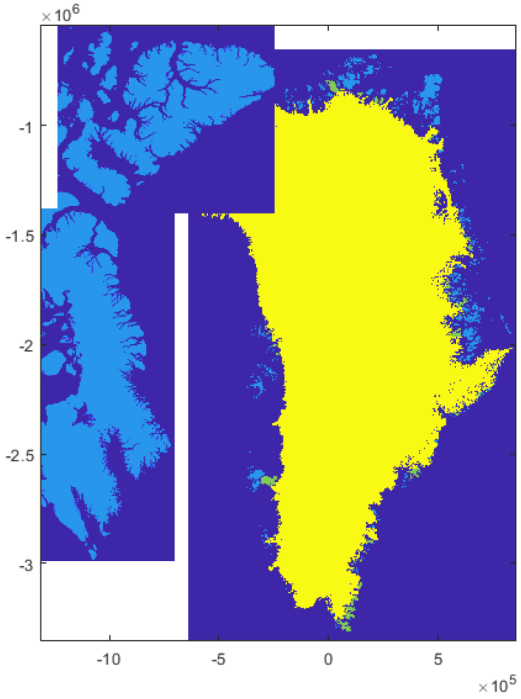

Figure 10: The three tiles containing the the GrIS, the North (NCAA) and South Canadian Arctic Archipelago, that are combined to make the climate forcing data set.

3.4 Basal heat flux

The basal melt of an ice sheet is determined by the basal heat flux coming from the bedrock. The basal heat flux is the amount of heat passing from the interior of the Earth to the surface and in this case to the bottom of the ice sheet. If the heat flux is sufficiently large it will create basal melt at the bottom of the ice sheet.

The basal heat flux used in this study comes from [Shapiro and Ritzwoller, 2004] and can be seen in figure 11. The basal heat flux map was created using a global seismic model of the Earth's crust and upper mantel to determine how much heat passes through to the surface.

The heat flux map from [Shapiro and Ritzwoller, 2004] is a model that covers the entire Earth on a 2x2 degree grid. This means that everything not in the domain of this project had to be removed and the grid type had to be changed and given a projection. The cutting and grid type change was done in Python, where everything not needed was removed and the grid was changed to lengths and not degrees over the domain. The regridding on projection assignment was done again using bi-linear interpolation in CDO and NCO.

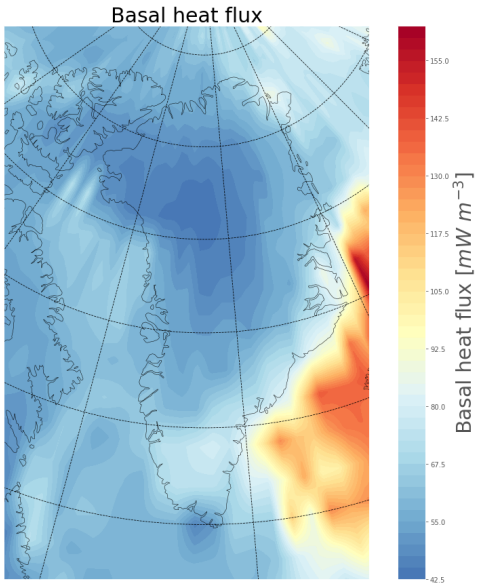

Figure 11: The basal heat flux map used in this project [Shapiro and Ritzwoller, 2004].

3.5 Paleoclimatic record

To provide the model with the correct forcing data for the climate over Greenland during the last 140,000 years, a paleoclimatic record is required. Since no climate record exists for Greenland this far back a record had to be stitched together.

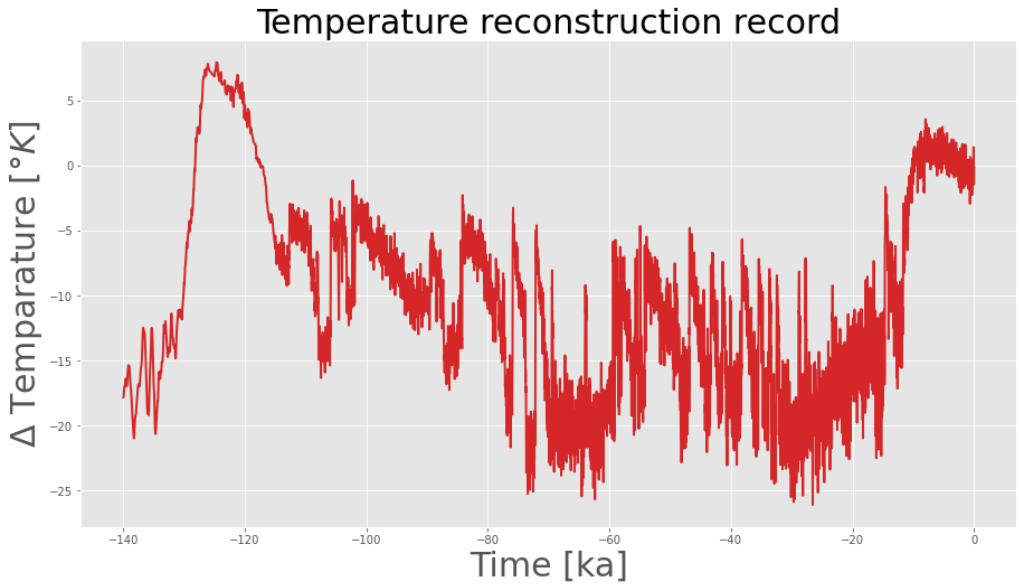

Figure 12: A temperature reconstruction that combines the NorthGRIP record [NorthGRIP members, 2004] from 0 to 115 ka before present, the NEEM record [NEEM community members, 2013] from 115 to 128 ka, and the synthetic Greenland record [Barker et al., 2011] before 128 ka.

The climate forcing record shown in figure 12 combines the NorthGRIP δ^{18}O ice core record [NorthGRIP members, 2004], the Eemian δ^{18}O ice core record and temperature reconstruction from the NEEM ice core [NEEM community members, 2013], with the synthetic Greenland climate record [Barker et al., 2011], that is derived from the

EPICA Dome C δD record [Jouzel J., 2007]. All the isotope ice core records are on a common timescale [Veres et al., 2013].
A new composite isotope record was created by combining the three records, so that the new record consisted of the NorthGRIP record from 0 to 115 ka, the NEEM record from 115 to 128 ka, and the synthetic Greenland record before 128 ka. This composite isotope record was then transferred to a temperature anomaly using the scaling from the NEEM reconstruction [NEEM community members, 2013].

The precipitation scaling shown in figure 13, is scaled to fit the present day precipitation. It was derived from the composite isotope record using the Central East Greenland scaling by [Buchardt et al., 2012]. An alternative precipitation scaling was derived as well using the scaling from the SeaRISE project [Huybrechts, 2002].
Notice that the precipitation is exponentially scaled to the temperature anomaly, which is due to the Clausius-Clapeyron relationship where humidity depends exponentially on temperature. In colder temperatures the precipitation is lower, and in warmer temperatures it is higher.
It is however, not confirmed that the scaling used for the glacial conditions also holds in a warmer climate and the pattern would most likely not be uniform. Climate model studies suggest higher precipitation in south Greenland during the Eemian, but lower precipitation in north Greenland [Plach et al., 2018].

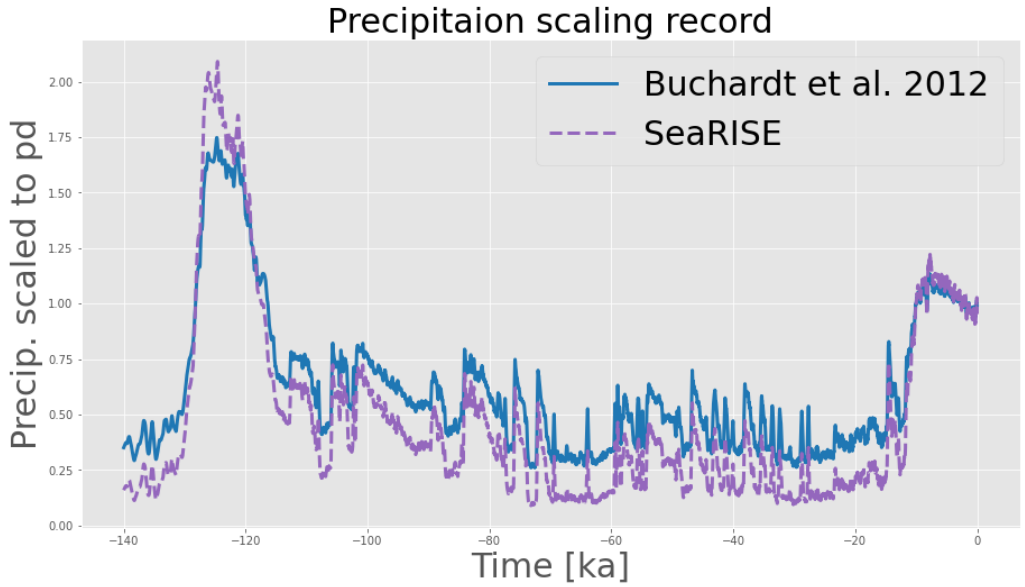

Figure 13: Two precipitation scaling reconstructions. Blue is the scaling from [Buchardt et al., 2012] for Central East Greenland and purple is the scaling from the SeaRISE project [Huybrechts, 2002].

The sea level forcing shown in figure 14 was derived from the benthic δ^{18}O marine record shown in figure 2 from[Lisiecki and Raymo, 2005], scaled to fit the sea level record for the last glacial from the SeaRISE project [Imbrie and McIntyre, 2006].

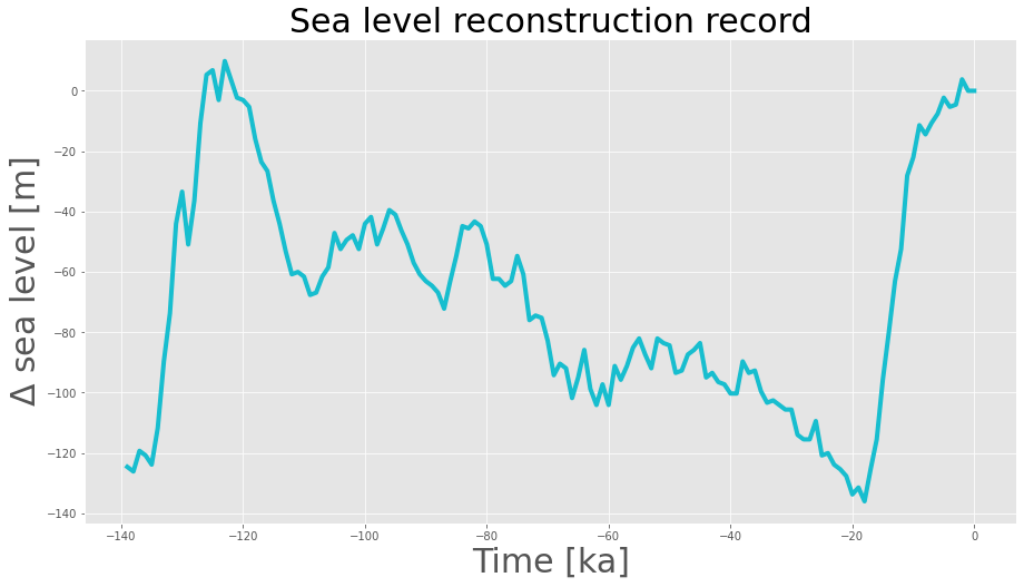

Figure 14: A paleoclimatic sea level reconstruction using the benthic δ^{18}O marine record from[Lisiecki and Raymo, 2005], scaled to fit the sea level record for the last glacial from the SeaRISE project [Imbrie and McIntyre, 2006].

4 Theory

This chapter contains a description of how large bodies of ice behave when exposed to the internal and external forces associated with ice dynamics as well as the most important approximations used in ice flow modelling.

4.1 Ice dynamics

Traditionally we think about ice as a solid matter, however when ice is exposed to internal and external forces it will display the properties of a viscous fluid. This can be characterized by a creeping flow, which is induced by gravitational forces. The ice sheet gains mass from accumulation of snow and freezing of rain on the surface. This mostly happens in the higher regions of the ice sheet, as seen in figure 15.

This gain of mass on top will cause a horizontal spreading of the ice towards the margins, resulting in thinning of the layers within the ice sheet. The ice sheet loses mass from ablation of ice at the margins, also illustrated in figure 15. The ablation is caused by induced subglacial and surface melt, as well as calving of icebergs at locations where outlet glaciers reach into the ocean.
When the accumulation of snow on top of the ice sheet is balanced out by the ablation at the margins, the ice sheet is at equilibrium, where the gain of mass is equal to the loss of mass. This state is called steady state.

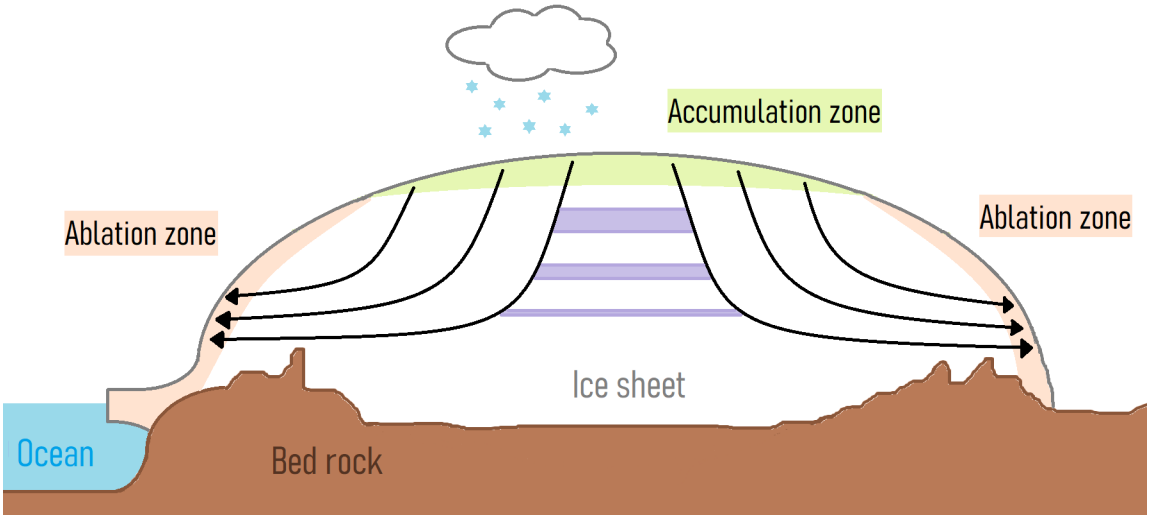

Figure 15: This figure shows the movement of ice inside of an ice sheet. On top of the ice an accumulation of ice and snow happens. The gravitational force causes the ice to sink, thin and spread, and flow horizontally towards the margins. At the margins the ice sheet loses mass from ablation in the form of basal and surface melt and calving of icebergs into the ocean.

The processes that determine the evolution of an ice sheet are numerous and can be complicated and not all of them are well described at this time. These processes include thermomechanically coupled non-linear flow of ice, with complex processes at the bed, depending on basal water and the basal material.

The goal in ice sheet modelling is always to make the model as realistic and accurate as possible, but often it is necessary to make approximations to minimize the complexity of the models. This is both a question of time and the amount of computational power needed to run these models.

4.1.1 Stress

Stress is the measure of how much a parcel in a continuum is pushed or pulled by the external forces applied to the material. The mechanical deformation of ice caused by these external stresses was first described in [Glen, 1955]. Stress is defined as force per area

$$\sigma_{ij} = \lim_{A \to 0} \frac{F_i}{A_j}. \tag{1}$$

If we look at an infinitesimal small cube of ice inside the ice column, the stress can be described as a tensor given as

$$\boldsymbol{\sigma} = \begin{pmatrix} \sigma_{xx} & \sigma_{xy} & \sigma_{xz} \\ \sigma_{yx} & \sigma_{yy} & \sigma_{yz} \\ \sigma_{zx} & \sigma_{zy} & \sigma_{zz} \end{pmatrix}. \tag{2}$$

The diagonal components of the stress tensor are the normal stresses and the remaining components are the shear stresses. The different components can be seen with respect to an ice parcel, shown in figure 16. It is assumed that that the material is a continuum, and therefore the parcel does not rotate around itself. For this to be true, it is required that the tensor is symmetric, meaning that $\sigma_{ij} = \sigma_{ji}$.

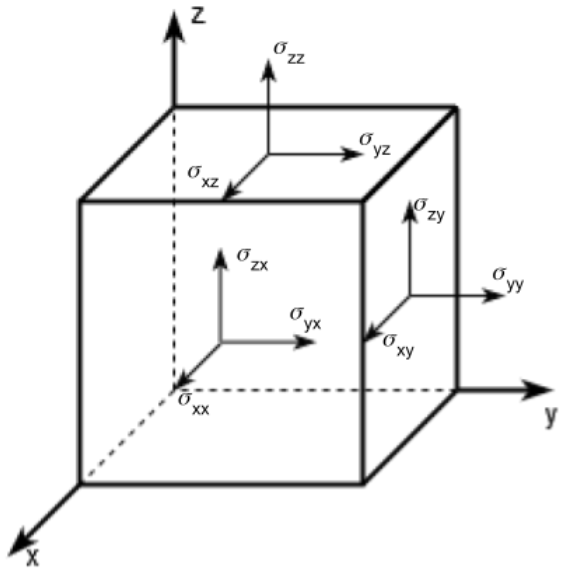

Figure 16: Components of the stress tensor.

Assuming that the stress is comprised of the pressure P and the deviatoric stress $\boldsymbol{\tau}$, the stress is then given as

$$\boldsymbol{\sigma} = \boldsymbol{\tau} - P\mathbf{I}. \tag{3}$$

Here **I** is the identity matrix. Pressure is the force applied perpendicular to the sides of the cube in figure 16 and if only isotropical pressure influences the parcel, the stress tensor is reduced to

$$\boldsymbol{\sigma} = -P\mathbf{I}, \tag{4}$$

which means that the pressure can be defined from the trace of the stress tensor, as so

$$P = -\frac{1}{3}tr(\boldsymbol{\sigma}) = -\frac{1}{3}(\sigma_{xx} + \sigma_{yy} + \sigma_{zz}). \tag{5}$$

Since ice is often considered an incompressible material, meaning that pressure does not contribute to the deformation of the ice, it is often simpler to deal with the other part of the stress tensor: the deviatoric stress or the stress deviator. The stress deviator describes the part of the stress that deviates from the hydrostatic pressure. The shear stresses from the stress tensor and the deviatoric stress are the same, and the stress deviator is therefore given as

$$\boldsymbol{\tau} = \boldsymbol{\sigma} - tr(\boldsymbol{\sigma})\mathbf{I}. \tag{6}$$

4.1.2 Strain

Ice deforms like all other materials do, when subjected to external forces. This deformation is called the strain ϵ and can be split into normal and shear strain, just as the stress can.
For a small deformation the normal strain is the change in length of a parcel of ice, when the parcel is under influence of a normal force. The normal strain in the x-direction can then be described as

$$\epsilon_{xx} = \frac{\Delta L}{L}. \tag{7}$$

The deformation of the ice is in itself not of much interest, when working with ice flow; the interesting part is the change in deformation over time. This is called the strain rate $\dot{\epsilon}$ and it describes the rate, with which the length of a parcel changes within a respective period of time. The strain rate in the x-direction is defined as

$$\dot{\epsilon}_{xx} = \frac{\epsilon_{xx}}{\Delta t} = \frac{\Delta L}{L\Delta t}. \tag{8}$$

Shear strain, on the other hand, is the ratio of displacement relative to the parcels original dimensions due to stress. It is also the amount of deformation happening perpendicular to a given line rather than parallel to it.

4.1.3 Flow law

The relationship between stress and strain can very simply be described using Glen's flow law [Glen, 1955], which is defined as

$$\dot{\epsilon}_{ij} = A\tau_{ij}^{n} \tag{9}$$

This equation is used to describe the relationship between the dominant shear stress $\dot{\epsilon}$ and the corresponding strain rate τ. The creep parameter A, is dependent mostly on the temperature and fabric of the ice, but also crystal orientation and amount of

debris in the ice. This means that the flow parameter differs from ice sheet to ice sheet. The creep component n, is usually approximated to a constant of n = 3, which is consistent with field and laboratory data, but in reality it can range from about 1.5 to 4.2 [Cuffey and Paterson, 2010].

Glen's flow law, equation 9, can be generalized to a relation called the Nye-Glen creep relation, where more than one component of stress can be applied at a time [Cuffey and Paterson, 2010]. The relation is given as

$$\dot{\epsilon}_{ij} = A\tau^{n-1}\tau_{ij}, \quad \tau = \sqrt{\frac{1}{2}\tau_{ij}\tau_{ij}}, \tag{10}$$

where τ is the second invariant of the stress tensor and τ_{ij} is a deviatoric stress, on which on the effective viscosity of the ice is dependent [Fowler and Ng, 2021]. τ_{ij} can also be written like

$$\tau_{ij} = 2\eta\dot{\epsilon}_{ij}, \text{ where } \eta = \frac{1}{2A\tau^{n-1}} = \frac{1}{2}A^{-\frac{1}{n}}\epsilon_e^{\frac{1}{n}-1}, \text{ where } \epsilon_e = \sqrt{\frac{1}{2}\epsilon_{ij}\epsilon_{ij}}. \tag{11}$$

The variations of the strain rate are not fully explained by the Nye-Glen creep relation. To resolve this there is a need to introduce the enhancement factor E. E is not an actual physical variable, but rather a measure of the inability to predict the strain rate in a situation [Cuffey and Paterson, 2010]. The enhancement factor is defined as

$$E = \frac{\dot{\epsilon}_m}{\dot{\epsilon}_0}. \tag{12}$$

Here $\dot{\epsilon}_m$ is the measured strain rate and $\dot{\epsilon}_0$ is the strain rate calculated using equation 10. The value for E is dependent on the orientation of the deformation. This means that E should not be regarded as a property of the ice however, in this study E is used to adjust the rate factor A uniformly for all strain rate, i.e. replace A with EA in equation 10, and assume that E is related to crystal orientation and impurity content of the ice.

4.1.4 The Shallow Ice Approximation

The Shallow Ice Approximation (SIA) is one of the most widely used approximations in ice flow modelling. It is built on the assumptions that the horizontal extent of the ice sheet is much greater than the thickness and that the surface and bedrock slopes are small relative to the size of the ice sheet.
As a result of this, the only relevant components of the stress deviator, are the vertical shear stresses τ_{xz} and τ_{yz}. The ice is assumed to be incompressible, and the continuity equation can therefore be written as

$$\frac{\partial u}{\partial x} + \frac{\partial v}{\partial y} + \frac{\partial w}{\partial z} = 0, \tag{13}$$

and the momentum equations can be approximated as follows [Fowler and Ng, 2021]

$$0 = -\frac{\partial P}{\partial x} + \frac{\partial \tau_{xz}}{\partial z}, \quad 0 = -\frac{\partial P}{\partial y} + \frac{\partial \tau_{yz}}{\partial z}, \quad 0 = -\frac{\partial P}{\partial z} - \rho g. \tag{14}$$

It is also assumed that there is no sliding at the bottom of the ice, meaning that the ice is frozen to the bedrock. As a result of this, the horizontal velocity of the interior of the ice sheet must be determined by the surface slope of the ice. This means that the ice will flow in the direction of the steepest surface slope, regardless of the geometry of the bedrock.
Essentially this means that the deformation of the ice sheet is only dependent on the local surface geometry and nothing else, greatly simplifying the complexity of the problem and thereby lowering the computational time and power needed. Figure 17 shows the velocity profile of SIA.

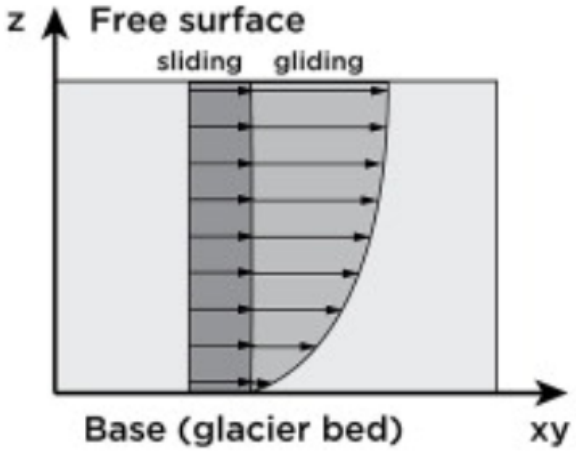

Figure 17: This figure shows how the ice flows and deforms according to the Shallow Ice Approximation, with an added component of basal sliding [Kirchner et al., 2011].

The Shallow Ice Approximation holds for large areas of the GrIS and this makes it one of the most commonly used approximations in ice flow modelling. It does however not hold everywhere. As illustrated in figure 15, the ice at the ice dome clearly has vertical velocities, in fact most of the velocities are vertical rather than horizontal at this point.
The assumption that the ice is frozen to the bedrock and therefore there is no basal sliding also only holds for some parts of the ice sheet. In ice streams and at outlet glaciers basal sliding plays a big role in the motion of the ice. Also at the margins of the ice sheet, SIA breaks down, because here the surface slope is usually very steep.
These are still relatively small parts of the GrIS, meaning that SIA is a good approximation for large parts of what is to be modelled.

4.1.5 The Shallow Shelf Approximation

The Shallow Shelf Approximation (SSA) was created as a way of describing the flow of ice in ice shelves. Here stress at the base of the ice is negligible, due to the amount of basal melt and that the stress is mostly applied from the sides of the shelf, where it connects to the coast line.
It turns out that SSA can also be used to describe grounded parts of an ice sheet where basal sliding plays a big role, such as outlet glaciers and fast flowing ice streams. This mostly occurs at the margins of the ice sheet, where the basal temperature is high and causes basal melt [Fowler and Ng, 2021].

SSA is built on the assumption that there is no vertical shear happening in the interior of the ice. This means that the shear stresses are negligible compared to the normal stress. The velocity of the ice only varies spatially in the x-y-plane, so the horizontal velocity is constant over the entire depth of the ice. Figure 18 shows the vertical velocity profile of SSA.

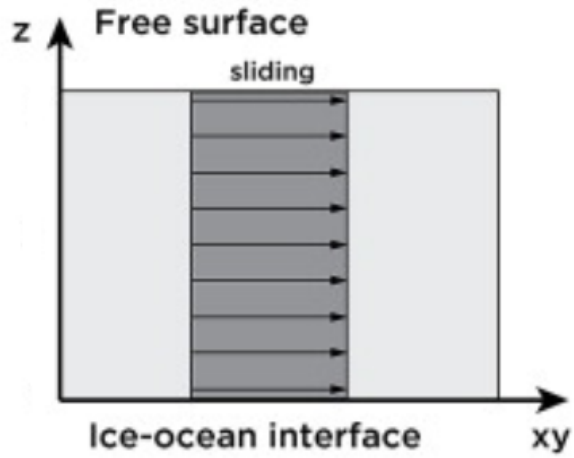

Figure 18: This figure shows how the ice flows as the so-called block-flow, according to the Shallow Shelf Approximation [Kirchner et al., 2011].

In the SSA, it is assumed that the motion is due to deformation of the basal till. The yield stress of the till is partly determined by the amount of basal water present. The yield stress can be found as a function of the till fraction angle ϕ, a strength parameter for the till [Clark et al., 2020]. The relation is given as

$$\tau_c = c_0 + \tan\phi \, \left(\rho g H - p_w\right), \tag{15}$$

where c_0 is the till cohesion, and can in most cases for simplicity be approximated to 0 [Bueler and Brown, 2008]. p_w is the pore water pressure and when this is equal to the downward pressure on the ice $\rho g H$ then the ice starts to float. Here H is ice thickness, ρ is ice density and g is the gravitational acceleration.

5 Parallel Ice Sheet Model

Parallel Ice Sheet model (PISM) is an open-source modelling framework that can be used for modelling ice sheets as well as glaciers. It is a 3 dimensional model with a time dependency and it is very useful for modelling both on large scale or more locally. The version of PISM used in this thesis is v1.2 [The PISM authors, 2020].
This chapter contains the description of how (PISM) works. This includes how the model is build and what boundaries and limitations it has and how the model applies the physical approximations described earlier to compute the evolution of an ice sheet or glacier.

5.1 Grid and spatial domain

In PISM the spacial domain consists of a 3 dimensional grid. The grid cells are equally spaced in the horizontal xy-plane and the vertical spacing is quadratic by default, but can be chosen as equal spacing. The z-coordinates are measured as positive upward from the base of the ice, so that $z = 0$ represents the base on the ice. The computational box can extend downward into the bedrock, but since $z = 0$ is the base of the ice, the bedrock will correspond to negative z values regardless of its true elevation z'.
The gravitational force is represented by a vector in the negative z-direction and the surface $z = 0$ is the base of the ice both when the ice is grounded and when it is floating.

Where ever the ice is grounded, the true vertical coordinate z, is given as the following function of z and the bedrock topography $b(x, y)$

$$z' = z + b(x, y). \tag{16}$$

The top surface of the ice $h(x, y)$ is described by

$$h(x, y) = H(x, y) + b(x, y), \tag{17}$$

where $H(x, y)$ is the ice thickness.

In cases of floating ice, the true vertical coordinate is

$$z' = z + z_{sl} - \frac{\rho_i}{\rho_w} H(x, y). \tag{18}$$

Here z_{sl} is the sea level elevation, ρ_i is the density of ice and ρ_w the density of sea water. The floating criteria of the model is

$$z_{sl} - \frac{\rho_i}{\rho_w} H(x, y) > b(x, y). \tag{19}$$

The grid is defined by four numbers, the number of grid points in the x-direction Mx, the number of grid points in the y-direction My, the number of grid points within the ice in the z-direction Mz and the number of points in the z-direction within the bedrocks thermal layer Mbz.
The horizontal computational grid in PISM, is uniform and cell-centered, by default. It is not the only possible interpretation, but it is consistent with the finite-volume handling of mass evolution in PISM and is the interpretation used in this thesis.

5.2 Boundary conditions

PISM's job is to approximate the ice flow in an ice sheet, this mean that the model is only centered around ice dynamics and the lithosphere below the ice. In reality, the evolution of an ice sheet, is also dependent on conditions outside this, such as atmospheric and oceanic conditions.
The constant accumulation and ablation of mass, results in a continuous replacement of ice. The rate of this replacement has a great dependency on the weather conditions on top of and around the ice sheet, as well as the temperature and height of the ocean and the change in temperature at the base of the ice sheet, due to geothermal heat flux. All these things are not build in processes in PISM, but are included as boundary conditions for the model. This means that these data will have to be provided, if the standard values in PISM do not seem efficient.

There are four boundary surfaces in PISM and they are shown in figure 19. The first boundary condition is the ice surface (green in figure 19). By this is meant the surface of the actual ice, which starts below a layer of snow and firn. This boundary requires the surface mass balance of the ice sheet (the mass flux into and out of the ice) and the ice surface temperature. This boundary condition is implemented all over the surface of the ice sheet.

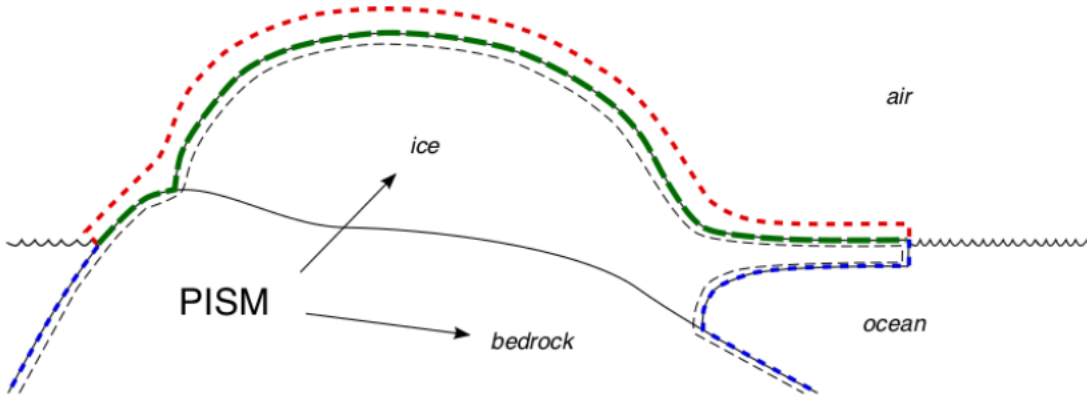

Figure 19: This figure show the four boundary surfaces of the PISM. These boundaries represent the processes that influences the ice sheet evolution, but are not included as part of the model. Atmospheric boundary (red), ice surface (green) and oceanic boundary (blue) [The PISM authors, 2020].

The second boundary is the atmospheric boundary (red in figure 19). This boundary is only necessary if one does not provide a sufficient set of data for the surface boundary. For this project there was not a sufficient amount of data of the ice surface, so the atmospheric boundary was chosen, because when this is used there is no need for the ice surface boundary.
For this boundary the model requires a precipitation field and a temperature field, PISM can then reinterpret these data sets as a surface mass balance and ice surface temperature for the domain. PISM interprets snow as precipitation happening at temperatures below $0°C$ and rain as precipitation happening at temperatures above.
The melt rate is calculated using a positive-degree-day scheme (PDD). This method calculates the number of days with average temperatures above 0°C, resulting in surface melt, over a given time period. The probability of surface melt is calculated from

the probability distribution around the mean annual and mean summer temperature. A more detailed describtion of how the surface mass balance is calculated can be found i section 5.3.5. This boundary condition is also implemented all over the surface of the ice sheet.

The third boundary is the bedrock (solid black in figure 19). Here the model requires a geothermal heat flux, that supplies additional energy and possibly raises the temperature at the bottom of the ice sheet. This boundary is applied at all areas where the ice sheet is grounded, both on land and at grounded marine outlet glaciers.

The last boundary is the ocean (blue in figure 19) and requires a ocean temperature forcing field and a mass flux into the ocean. If no temperature field is provided for the model, it will keep the temperature constant at the pressure melting point. The mass flux into the ocean can be set by choosing a calving parameter. This is described in more detail in section 5.3.2. This boundary is implemented over all areas, where the ice sheet comes into contact with the ocean. This includes ice shelves and marine outlet glacier.
A visual representation of the data needed and how the flow of data into PISM works, can be found in figure 20.

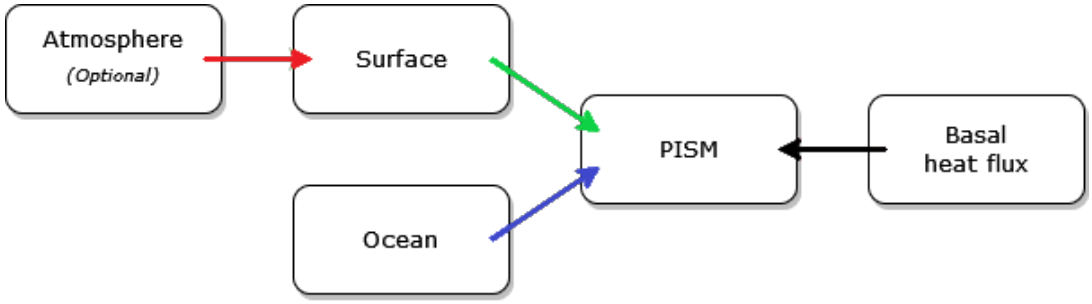

Figure 20: The flow of boundary data into PISM.

5.3 Model dynamics

5.3.1 Stress balance regime

In PISM one can freely chose between three different stress balance regimes. The first one is using just SIA, with no basal sliding, this is useful if one is modelling an area, that has no ice shelf or ice streams and the whole domain can then be approximated by just SIA. The second option is using just the SSA. This is very useful when modeling an ice stream or outlet glacier, where basal sliding plays an important part in the ice dynamics, or when modelling ice shelves , which the approximation was created for.
The last option is using a combination of the two, including both SIA and SSA over the domain. This is very useful when modelling a larger area or an entire ice sheet, where some areas are frozen to the bedrock and some areas have large amounts of basal sliding. Figure 21 shows how the different stress balance regimes are calculated in PISM.
The stress balance regime used in this project is the hybrid of the Shallow Ice Approximation and the Shallow Shelf Approximation. SIA is applied to the domain, where

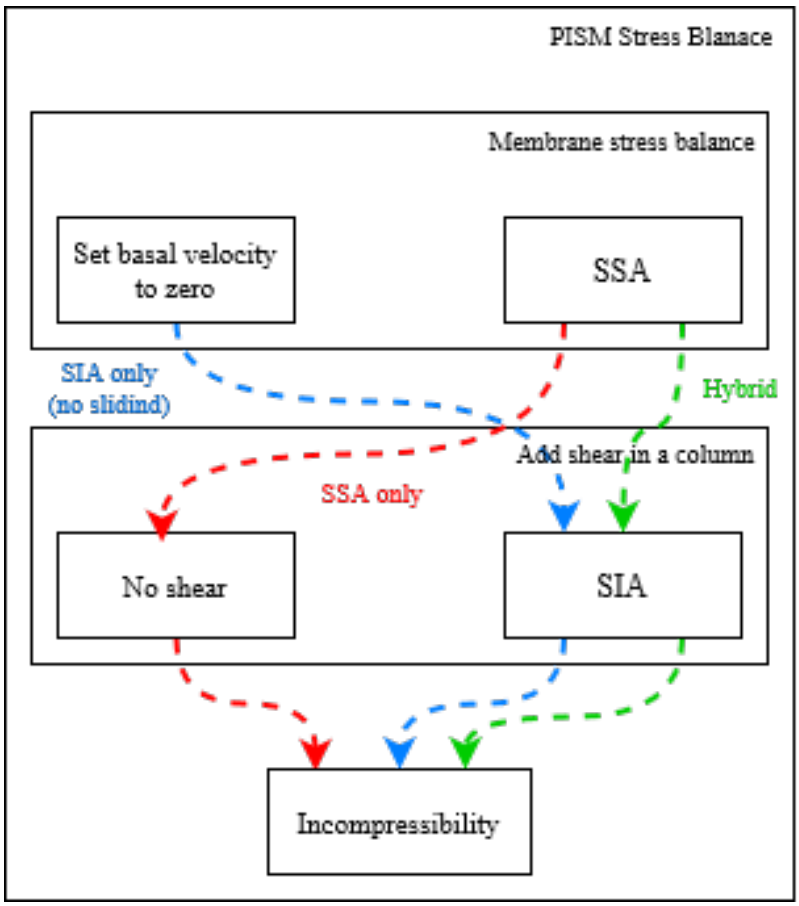

Figure 21: The stress balance regime chosen results in different routes taken for the calculations. In blue sees the route for SIA with no sliding, red is the route for SSA and in green is shown the hybrid route.

the ice is frozen to the bedrock and there occurs no basal sliding. SSA is applied to ice shelves, and in areas of low basal resistance, where sliding can occur. This allows the model to simulate fast flowing areas like ice streams and outlet glaciers, where the motion of the ice at the bedrock, contributes to a significant part of the ice velocity. Figure 22 shows an example of where the two approximations are used.

The field equations, SIA and SSH are solved numerically in each grid cell, based on the differences between neighboring cells. The velocities found using the two approximations SIA and SSH are combined into a total horizontal velocity $\mathbf{v}$ using the following function [Bueler and Brown, 2008]

$$\mathbf{u} = f(|\mathbf{u}_{SSA}|)\mathbf{u}_{SIA} + (1 - f(|\mathbf{u}_{SSA}|))\mathbf{u}_{SSA}. \tag{20}$$

Here $\mathbf{u}_{SIA}$ is the horizontal velocity from SIA, $\mathbf{u}_{SSA}$ is the SSA velocity and $|\mathbf{u}_{SSA}| = \mathbf{u}^2_{SSA_x} + \mathbf{u}^2_{SSA_y}$ and $f(|\mathbf{u}_{SSA}|)$ is a weight function, that ensures a continuous solution of the velocity reigning from the interior of the ice sheet across the grounding line and on to the ice shelves. The function is defined as follows

$$f(|\mathbf{u}_{SSA}|) = 1 - \frac{2}{\pi}\arctan\left(\frac{|\mathbf{u}_{SSA}|^2}{100^2}\right) \tag{21}$$

[Bueler and Brown, 2008]. $f(|\mathbf{u}_{SSA}|)$ is approximately 1 for small values of $|\mathbf{u}_{SSA}|$ and approximately 0 for large values. Figure 23 shows the weighting $f(|\mathbf{u}_{SSA}|)$ versus the sliding velocity $\mathbf{u}_{SSA}$. For the lower sliding velocities, approximately below 100 $\frac{m}{yr}$, SIA is the dominant stress balance and above this SSA is the dominant one.

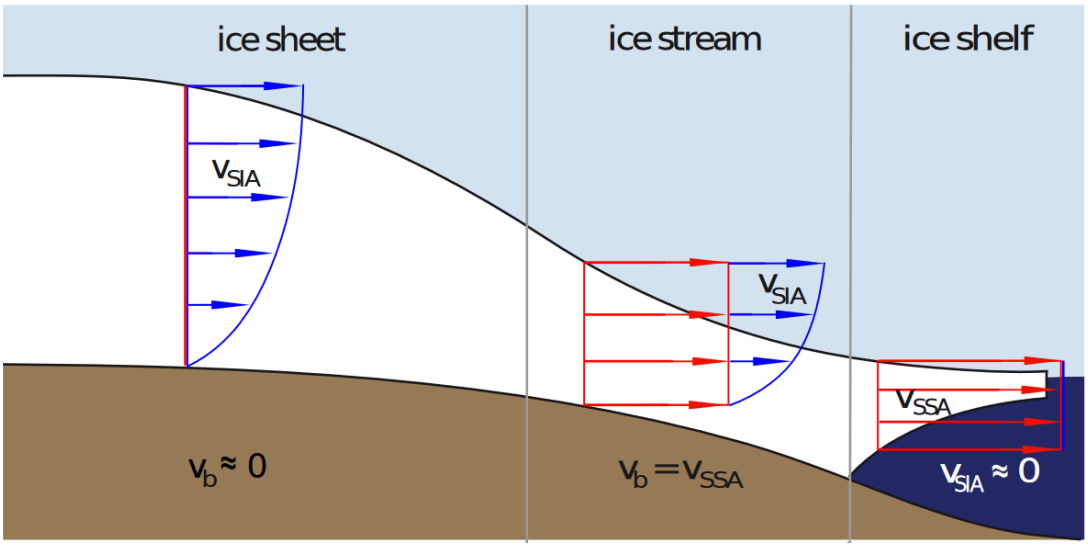

Figure 22: This figure shows where PISM applies the Shallow Ice and the Shallow Shelf Approximations to the modeled ice [Winkelmann et al., 2010].

PISM uses the two shallow approximations to determine the basal velocities of the ice sheet. When there is no basal velocity, SIA is applied, because it assumes no basal velocity. In cases with basal velocities PISM uses SSA as a sliding law, to determine the basal velocity [Bueler and Brown, 2008].

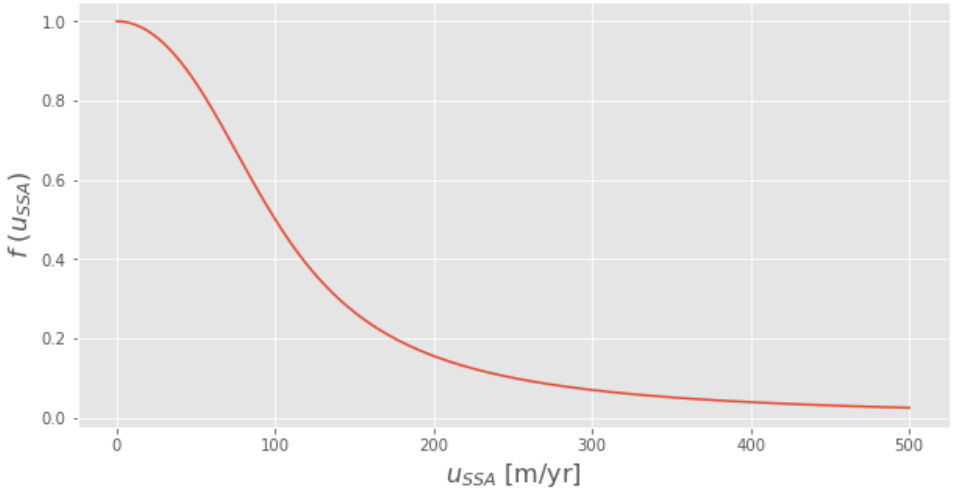

Figure 23: the weighting $f(|\mathbf{u}_{SSA}|)$ versus the sliding velocity $\mathbf{u}_{SSA}$.

5.3.2 Enhancement factor and sliding law exponent

In the Shallow Ice Approximation, the softness of the ice, has a big impact on how much the ice deforms. This softness can be changed using an enhancement factor E.

An increase of the enhancement factor will lead to a larger shearing from SSA and potentially higher horizontal velocities, in areas where basal motion is present.
In a study by [Aschwanden et al., 2016], they tested different values of $E = [1, 3]$ at intervals of 0.25. They found that for a higher enhancement factor the surface speed increases and the ice sheet becomes thicker. They ended up using en enhancement factor of $E = 1.25$ to avoid overestimating the vertical shearing, but in this project where the velocities and the shearing are not at the center, the most commonly used enhancement factor of $E = 3$ was chosen, to ensure that the ice thickness would not become to small.

PISM uses the following power law to describe the basal sliding τ_b of the ice, wherever the SSA is applied

$$\tau_b = -\tau_y \frac{\mathbf{u}}{u_t^q |\mathbf{u}|^{1-q}}. \tag{22}$$

Here u_t is the threshold velocity, where the basal sliding equals the yield stress τ_y. q is the sliding law exponent which has a direct impact on the SSA. Because the magnitude of τ_b, relative to the driving stress, is the determining factor in where SSA is applied, as well as the velocities due to the horizontal shear in these areas.
In the same study by [Aschwanden et al., 2016], they also tested different values of the sliding law exponent an found that for $q = 0.6$, the model is able to capture some of the larger ice streams, that are not captured with smaller values, and still not overestimate the the velocities at the margins of the ice sheet. Therefore the sliding law exponent was chosen to be $q = 0.6$ in this project as well.

5.3.3 Yield stress and till friction angle

The yield stress is defined as

$$\tau_y = \tan\phi N_{till}, \tag{23}$$

where ϕ is the till fraction angle, $\tan\phi$ is till friction factor and N_{till} is the effective pressure on the till. The till friction angle is based primarily on the topography of an area. It is justified bu the fact that deeper areas in the topography has a lower friction angle, in order to mimic the effects of weaker sediments collecting in the deeper valleys [Clark et al., 2020].
IN PISM the parameterization of the till friction angle is $\phi_{min}, \phi_{max}, h_{min}, h_{max}$, where h is the elevation.
The till friction angles and elevations used in the project is 10.0,30.0,-300.0 m,300.0m , which comes from the study by [Clark et al., 2020], where they found this to be the most realistic values for simulations over Greenland.

5.3.4 Calving

Through out the evolution of an ice sheet, ice will break of ice shelves and marine outlet glaciers and float into the ocean, this process is called calving. In reality this is a complex process that has to do with melt, ocean temperature and thickness of the ice, just to name a few. In PISM this process is however approximated with simpler solutions than reality.
PISM has schemes for defining when glaciers has to calve ice, into the ocean, relating to thickness, stress or plainly just cutting of ice, when it passes a certain margin. In

this project the calving used is called float kill and as the name suggests it cut of the ice when it starts floating.
Float kill is not strictly physically accurate, since shelves cannot really form using this scheme. Shelves form where outlet glaciers terminates into the ocean and the coastline holds the ice floating on water, without calving completely. Ice shelves are very important when modelling the Antarctic ice sheet, because it has so many very large ones. But Greenland does not really have these large ice shelves and therefore this calving scheme is appropriate here.

5.3.5 Surface mass balance

As mentioned earlier PISM can calculate a surface mass balance (SMB) if one is not provided. For this PISM will need the monthly precipitation and the mean annual and the mean summer temperature over the area. From this PISM can calculate a SMB using a PDD scheme. This method is derived from the statistical relationship between the melting of snow and ice and positive air temperatures. The percentage of days with surface melt, is assumed to be the same as the probability that the air temperature close to the surface exceeds $0^{\circ}C$, and that the PDD factors can be related to this temperature. This is calculated on a monthly basis.

The number PDDs during the years, found from the normal probability distribution around the monthly mean temperatures, is defined as

$$PDD = \frac{1}{\sigma_{PDD}\sqrt{2\pi}} \int_0^A dt \int_0^\infty T \, \exp\left(- \frac{\big(T - T_a(t)\big)^2}{2\sigma_{PDD}^2} \right) dT, \tag{24}$$

where σ_{PDD} is the standard deviation, t is time, A is one year, T is the near-surface temperature and T_a is the annual near-surface temperature cycle [Fausto et al., 2007]. T_a is assumed to oscillate like a sine wave over time, like so

$$T_a(t) = T_{ma} + \big(T_{ms} - T_{ma}\big) \cos\left(\frac{2\pi t}{A}\right), \tag{25}$$

where T_{ma} is mean annual temperature and T_{ms} is the mean summer temperature. When the number of positive degree days is found, the melt M can be calculated as the product of PDD's and the PDD factors for both ice and snow β_{ice} and β_{snow}

$$M = \beta_{ice}\, PDD + \beta_{snow}\, PDD. \tag{26}$$

PISM starts by melting the snow, and if all the snow melts it starts to melt the ice, meaning that the ice related melt is only part of equation 26 if all the snow melts away. Now that PISM has a melt rate and precipitation field, it can combine the two to construct the surface mass balance needed to run the model, because the SMB is essentially just the flux into and out of the ice surface, which is just surface melt and snow and ice accumulation.

5.3.6 Historical climate offset

It is possible to provide PISM with an offset for one or more of the input data files. For instance it is possible to provide a temperature offset, if one would like to model

a warmer or colder version of the temperature field, to see how big of a difference, a small perturbation in temperature, could do to the evolution of the ice sheet. To do this one would have to provide PISM with a file including the offset ΔT and a time series consistent with the time series PISM has to run.
It is also possible to do this for a non constant offset. This could be useful when running PISM through one or more glacial cycles. To do this PISM would need the temperature offset ΔT as a function of time and then again the time series PISM has to run over. An example of this could be the paleoclimatic temperature reconstruction seen in figure 12.

It is also possible to do the same thing for sea level changes over time, if one would like to emulate the rising sea level of the future or the lower sea levels of past glacial periods. Here PISM will need the same files but for Δ sea level instead.

5.4 Bootstrapping

Starting a PISM run can be done two ways, either with a new set of initial data fields or starting from a previously saved PISM run, that contains a complete set of new input fields. When starting from a previously created PISM run, PISM has already provided a complete set on new input fields to run from, and so PISM will not need to do any reprocessing on the files to start the run.
If one starts from a new set of input data field, they are bound to be incomplete, compared to what PISM requires to run. What PISM will do here is fill in the missing fields itself using a process called bootstrapping. PISM is build to this, because a lot of the input fields it requires, cannot be observed in real life. This is for instance everything that happens below the surface of the ice sheet. These fields are created using heuristic models and are filled in to fit the data of the available field, provide for PISM. These heuristic methods are applied before the first time step of the model, so they are part of an initialization process and not the actual model run.

5.5 Command line

Below can be found an example of a PISM command line, for a run with constant climate, at 10 km resolution and a SIA-SSA hybrid stress balance regime. At the very top of the code is written ”mpiexec - n 20 pismr”, this means that PISM is executing pismr and running it in parallel. ”-n 20” notes the number of processes set to run parallel, in this case 20.
Next the input topography file is loaded, this file must contain the bedrock topography, the surface elevation and the ice thickness over the domain. After this comes the bootstrapping, which creates the mathematical initial conditions required for the model to run. Then comes the definition of the grid. Here ”Mx” and ”My” is used to define a horizontal grid of 221×333, consistent with a 10 km resolution over the domain used in this project. ”Mz” is the number of grid points in the vertical direction upwards and ”Lz” is the size of the upwards vertical domain.”Mbz” is the number of grid points downwards and ”Lbz” is then the size of the downward vertical domain.
Afterwards PISM is told not to recompute the longitudes and latitudes in the topography file using the command ”-grid.recompute_longitude_and_latitude false”. Next PISM needs to calculate the grid, ”-grid.registration corner” tells PISM to calculate the

grid relative to the corners and to the center as is the default option. This means that each grid point represents the corner of a grid cell and not the center of it.
"ys" denotes the starting year of the simulation in this case 22,000 years ago and "ye" denotes the ending year, in this case present day. Remember PISM can only run forward in time.

```
mpiexec -n 20 pismr \
-i topgrafy.nc -bootstrap -Mx 221 -My 333 \
-Mz 101 -Mbz 11 -z_spacing equal -Lz 4300 -Lbz 2000 -skip -skip_max 10 \
-grid.recompute_longitude_and_latitude false -grid.registration corner \
-ys -22000 -ye -0 \
-atmosphere yearly_cycle -atmosphere_yearly_cycle_file atmosphere.nc \
-surface pdd \
-calving float_kill \
-sia_e 3.0 -stress_balance ssa+sia \
-pseudo_plastic -pseudo_plastic_q 0.5 \
-topg_to_phi 10.0,30.0,-300.0,300.0 \
-till_effective_fraction_overburden 0.02 -tauc_slippery_grounding_lines \
-energy.bedrock_thermal.file basal_heatflux.nc \
-ts_file ts_outfile.nc -ts_times -22000:1:0 \
-extra_file ex_outfile.nc -extra_times -22000:10:0 \
-extra_vars diffusivity,temppabase,tempicethk_basal,bmelt,tillwat,velsurf_mag,mask,thk,topg,usurf,hardav,velbase_mag,tauc \
-o outfile.nc
```

The atmospheric scheme used for this run is a yearly cycle and is chosen using "-atmosphere yearly_cycle", followed by the yearly cycle input file, containing the monthly precipitation, mean annual and mean summer temperature. PISM then needs to know how to interpret these data to a SMB. In this case it is done using a PDD scheme and the calving is chosen to be float kill.
Next the SIA enhancement factor is set to 3.0 using the command "-sia_e 3.0", and the stress balance regime is set to be a hybrid of SIA and SSA, "-stress_balance ssa+sia". After this the flow is set to be pseudo plastic and the sliding law exponent is set to be $q = 0.5$ using "-pseudo_plastic -pseudo_plastic_q 0.5".
Next the till friction angle and over burden is defined. Choosing the till friction, enhancement factor and sliding law exponent, is only necessary if one wishes different values from the default PISM values.
Now "-energy.bedrock_thermal.file basal_heatflux.nc" is used to read in the the basal heat flux map. If a basal heat flux map is not provided, PISM will use a constant value over the entire domain.

Lastly the output files are defined. The ts file contains all the outputs that are just a single value for every time step, this includes things like ice volume, ice mass, surface accumulation rate and surface melt rate. "-ts_times" is used to define for what time steps PISM has to save the data. It is written on the form "start_year:frequency:end_year", in this case "-22000:1:0" meaning PISM saves every year in the output file.
The ex file holds all the outputs that has a spacial range, such as ice thickness, diffusivity and velocity fields. Again "-ex_times" is used to define, with what frequency PISM should save the time steps, in this case it is every 10 years. "-extra_vars" is used to tell PISM what variables it should save. "-o outfile.nc" is the name of the output file.

To apply an atmospheric laps rate corrections, one will need to add a map for elevation change over the domain, this file has to contain the surface elevation (including ice) over the whole domain and then PISM will need a value for the lapse rate correction. The new command concerning the atmosphere can be seen below.

```
-atmosphere yearly_cycle,elevation_change \
-atmosphere.elevation_change.file atmosphere_elevation_change.nc \
-temp_lapse_rate 6.5 \
```

To have a time depended temperature offset, all that is needed is a file containing the offset and the time series for the PISM run. Then add ”delta_T” after the other atmospheric choices and load the offset file. An example of how this is done is shown below.

```
-atmosphere yearly_cycle,elevation_change,delta_T \
-atmosphere_delta_T_file paleoclimate_temperature.nc \
```

If one desires to change the sea level over time all that is needed is a file containing the sea level change and the time series for the PISM run. The ocean parameters are then defined like the code snipped below.

```
-ocean constant -sea_level constant,delta_SL \
-ocean_delta_SL_file paleoclimate_sea_level.nc \
```

6 Initialization

This chapter contains the description of the initialization of PISM and the number of runs done to better understand the dynamics of the model. To understand the model and how it reacts to different changes, a number of initial runs were made. The PISM manual [The PISM authors, 2020] provides a number of test runs to carry out with a data set that has been preprocessed, to already work with the model. These runs were executed firstly, but this section only contains the initial runs performed using the data sets described in chapter 3.

6.1 SIA stress balance regime

The first run was a very simple run, where the only thing different from the example runs provided in PISM [The PISM authors, 2020], was that the data is the data from this project and not the data provided for the PISM examples.
The only things provided to PISM, were the needed topography fields and climate forcing and then the SMB was calculated using a PDD scheme. For simplicity the stress balance regime was set to be only SIA. The command line from this run can be found in appendix A.
Figure 24 shows the ice volume evolution and the ice thickness, after running the simple SIA stress balance regime run, for 5000 years at 10 km resolution.

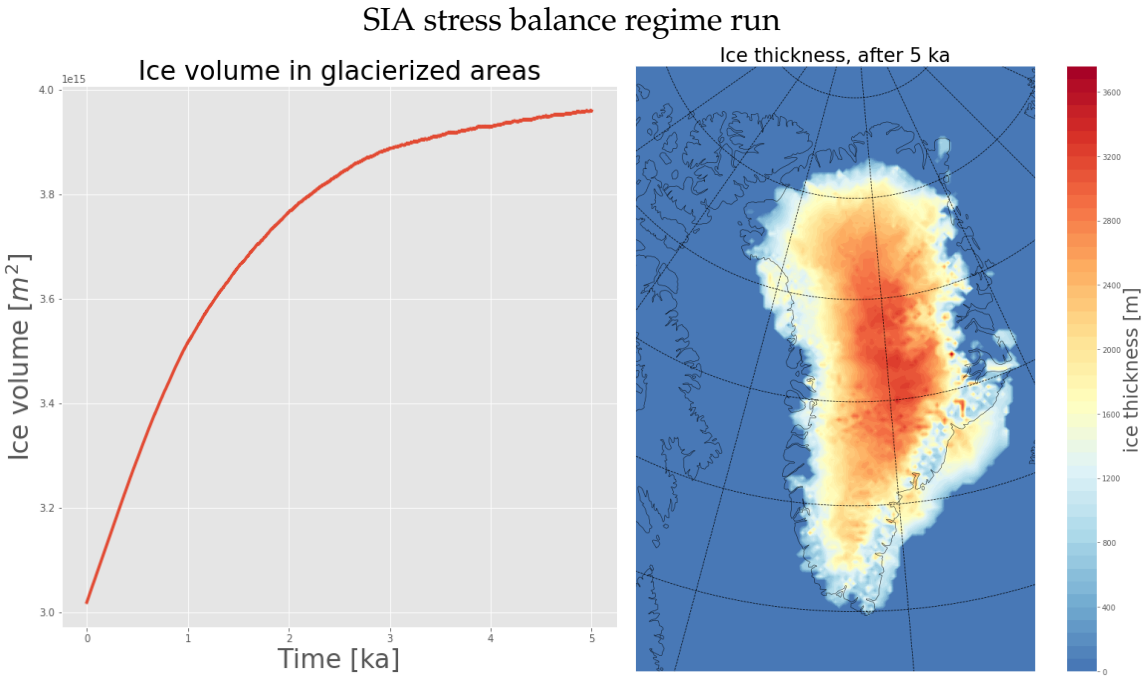

Figure 24: The results from a 5000 year run with only SIA as the stress balance regime. The first tile shows the evolution of the ice volume in the glacierized area and the second shows the ice thickness after 5000 years at 10 km resolution.

To make sure that the model uses only the SIA as the stress balance regime, the basal velocity has to be zero, all over the ice sheet, and as it can be seen from figure 25 this is the case. This means that there is no basal motion happening in the model anywhere, because the model could not allow basal sliding.

Figure 25 also shows the surface velocities over the ice sheet. Here the velocities are very small in the center of the ice sheet and get drastically larger when approaching the ice margins. At the margins the ice velocities get very large, that is however expected, since the only transport of ice, from the ice dome to the margins of the ice sheet, happens through internal velocities forced by the driving stress $\tau_d = \rho g H \sin$, i.e. most flow occurs when the surface is steep.

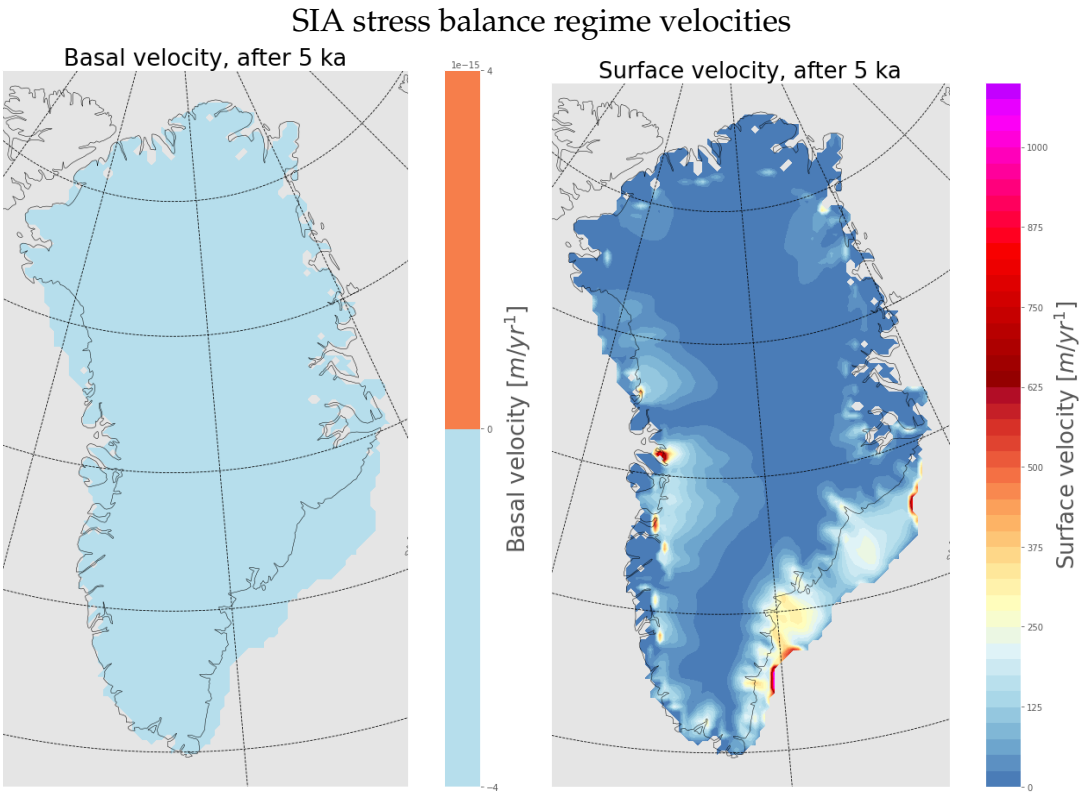

Figure 25: The basal and surface velocity of the ice after 5000 year with only SIA as the stress balance regime, at 10 km resolution. The basal velocity is zero everywhere as no basal motion is allowed by the model.

6.2 Hybrid stress balance regime

The next step was adding the SSA approximation to the stress balance regime. Again PISM was only provided with the needed topography fields and climate forcing and then the SMB was calculated using a PDD scheme, meaning that the only thing changed from the previous run was the stress balance regime. The command line from this run can be found in appendix B.
Figure 26 shows the ice volume evolution and the ice thickness for the hybrid stress balance regime run. As can be seen the ice volume is not quite as big as for the SIA only stress balance. This is because the ice does not grow quite as far out or get as thick near the margins, when adding SSA to the stress balance, since the basal sliding results in thinning and surface melt at the margins.
The two ice sheets are however very similar after 5000 years, they have almost the same ice thickness and extend. The pattern they follow when growing is the same, with a lot of ice front extending in the south-eastern part of Greenland and not a lot every where else.

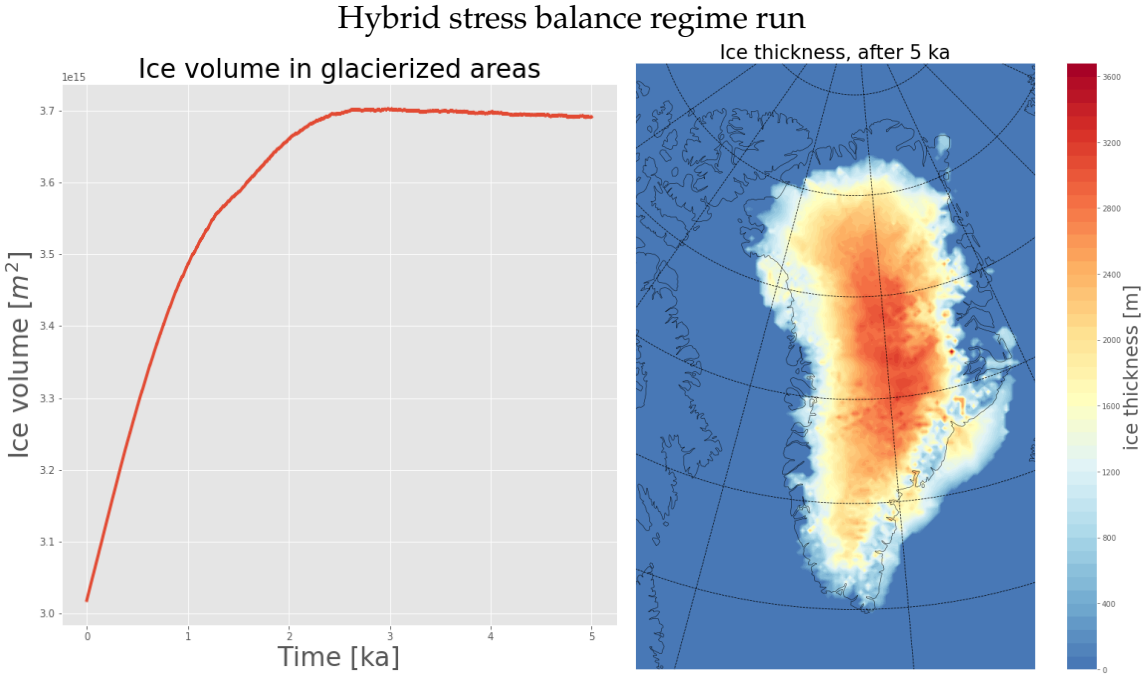

Figure 26: The results from a 5000 year run with a hybrid stress balance regime. The first tile shows the evolution of the ice volume in the glacierized area and the second shows the ice thickness after 5000 years at 10 km resolution.

Figure 27 shows the basal and surface velocities of the hybrid run. Now the basal velocities are still zero almost everywhere, but along the coastline they are larger non-zero, meaning that there is now basal sliding happening in the model. The reason that basal sliding is mostly happening near the coastline, is because this is where the larges bedrock slopes are located, meaning that this is where SSA is applied in the model.

Figure 27 also contains the surface velocities of the model. The surface velocities follow the same pattern as the SIA balance regime in figure 25, but the magnitude of the velocities are much smaller. This is because the model no longer has to transport all the ice through only the surface velocities, but it can now also use do it through basal sliding.

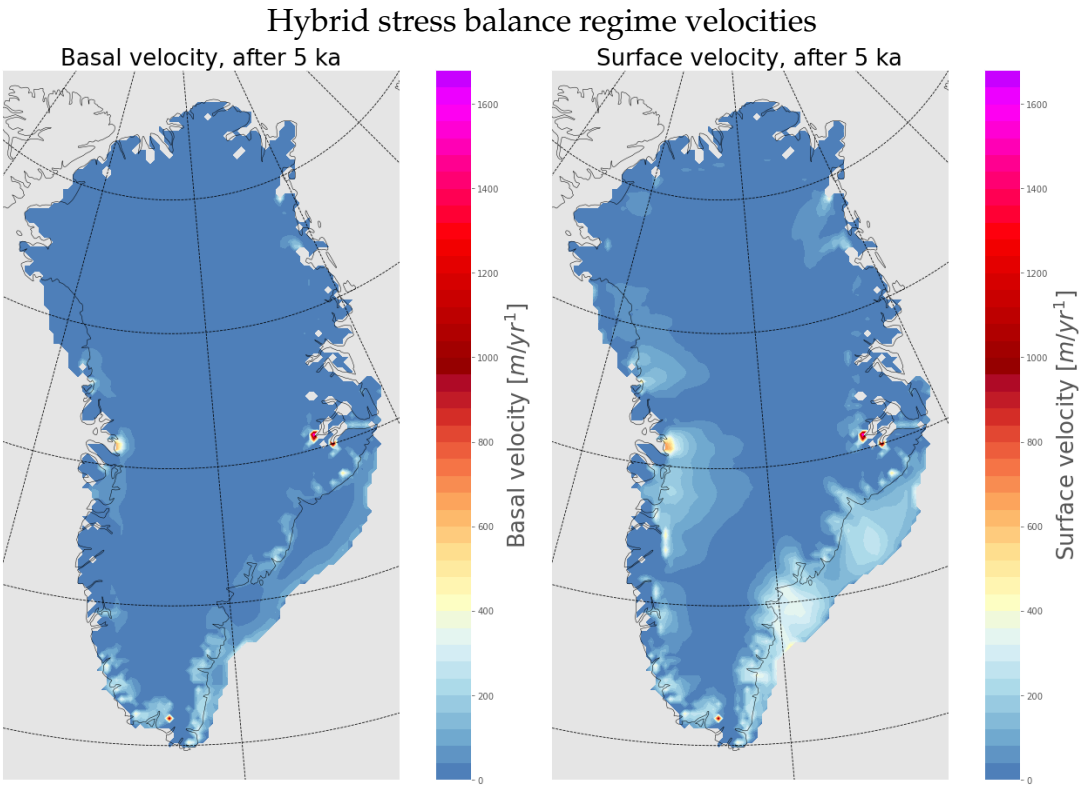

Figure 27: The basal and surface velocity of the ice after 5000 year with a hybrid stress balance regime, at 10 km resolution.

6.3 Lapse rate correction

In the next run a lapse rate correction was added. This was done to make the temperature field more realistic compared to the real world. The temperature in the atmosphere varies with height and lapse rate refers to the rate at which the temperature falls with altitude. Since the GrIS has quite a significant change in altitude it is necessary to add a lapse rate correction to try and make the model as physically correct as possible. Therefore a lapse rate correction of $6.5\frac{^{\circ}C}{km}$ was applied. This specific lapse rate is called the normal or environmental lapse rate. The command line for this run can be found in appendix C.

Figure 28 shows the evolution of the ice volume and the ice thickness after running the model for 5000 years. As it can be seen the ice volume becomes bigger than for the two previous runs and the ice sheet extent is also quite a bit larger along both the eastern and western coast lines.
The thickness of the ice sheet however is similar to the thickness of the ice sheet in both of the previous runs, meaning that the increase in mass is not coming from a vertical growth of the ice sheet, but only a horizontal growth.

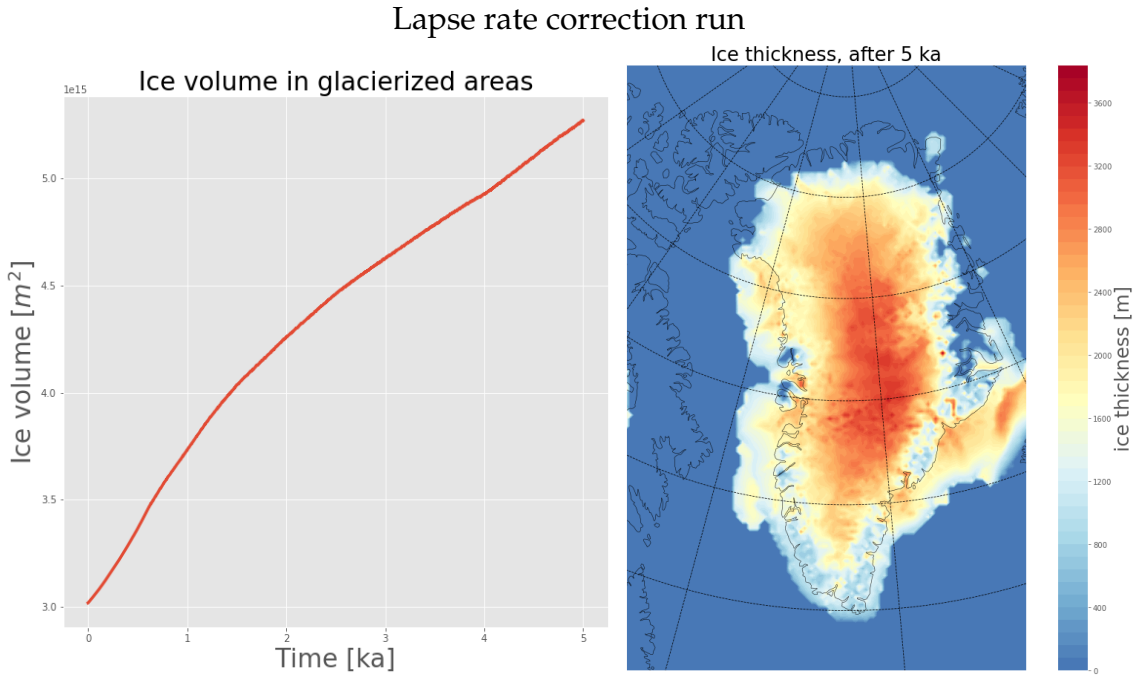

Figure 28: The results from a 5000 year run with a lapse rate correction of $6.5\ \frac{^{\circ}C}{km}$. The first tile shows the evolution of the ice volume in the glacierized area and the second shows the ice thickness after 5000 years at 10 km resolution.

Figure 29 shows the velocity maps of lapse rate correction run. As it can be seen, adding the lapse rate correction results in the model loosing the ability to recreate the ice streams around the coastlines. The hybrid model could to a certain extend recreate these ice streams, as shown in figure 27, but this model only has fast flowing ice, along the southeastern ice front.

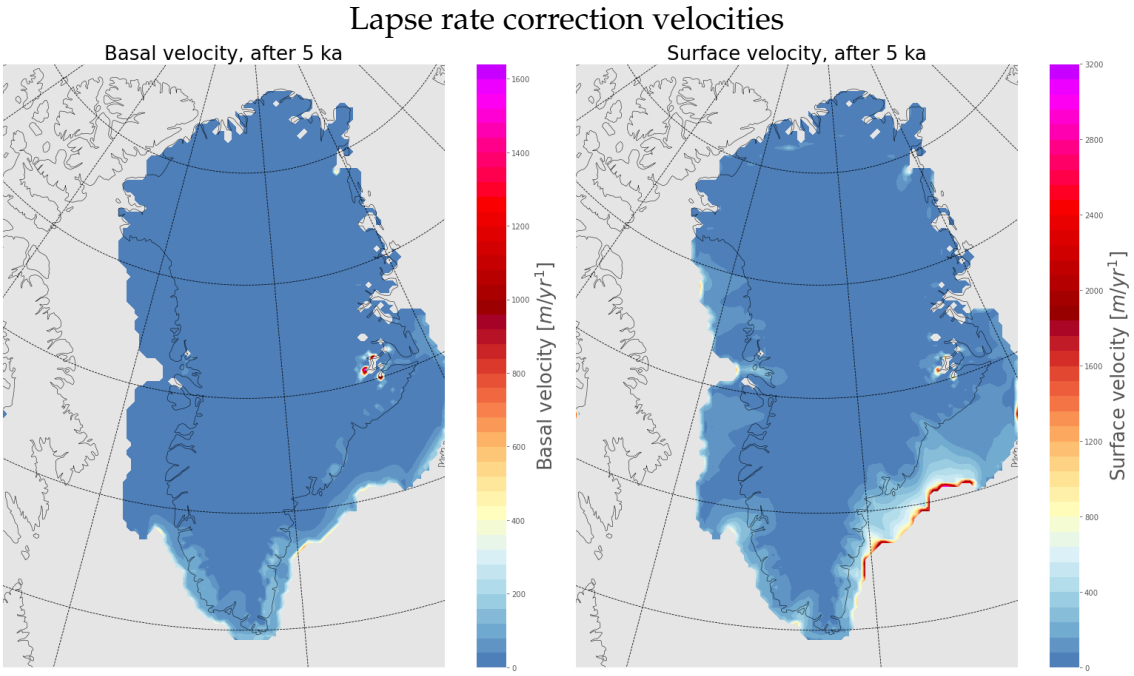

Figure 29: The basal and surface velocity of the ice after 5000 year with a lapse rate correction of 6.5 $\frac{^{\circ}C}{km}$, at 10 km resolution.

6.4 Till friction angle

As mentioned earlier in section 5.3.3 the till friction angle is defined so that deeper areas in the topography has a lower friction angle in order to mimic the effects of weaker sediments collecting in the deeper valleys. For this run the till friction component of the model has been added. The till friction was set to the PISM standards of 15.0,40.0,-300.0 m,700.0 m. The command line for run can be found in appendix D.

Figure 30 shows the ice volume evolution and the ice thickness after 5000 years. The ice sheet is now smaller than for the lapse rate run and the SIA only run, but bigger than the hybrid run. This is because the ice now has a different friction at the bottom, that holds on to the ice more in some places than in others.

Adding the till friction angle makes the sediments in deep valleys softer, the deeper the valley the softer the sediments, and this should result in model being able to recreate some of the ice streams on the GrIS. However this is not the case, as can be seen from figure 31. Adding the till friction term, makes the model better at recreating ice stream, than the lapse rate model, but still not as good as the hybrid stress balance regime run.

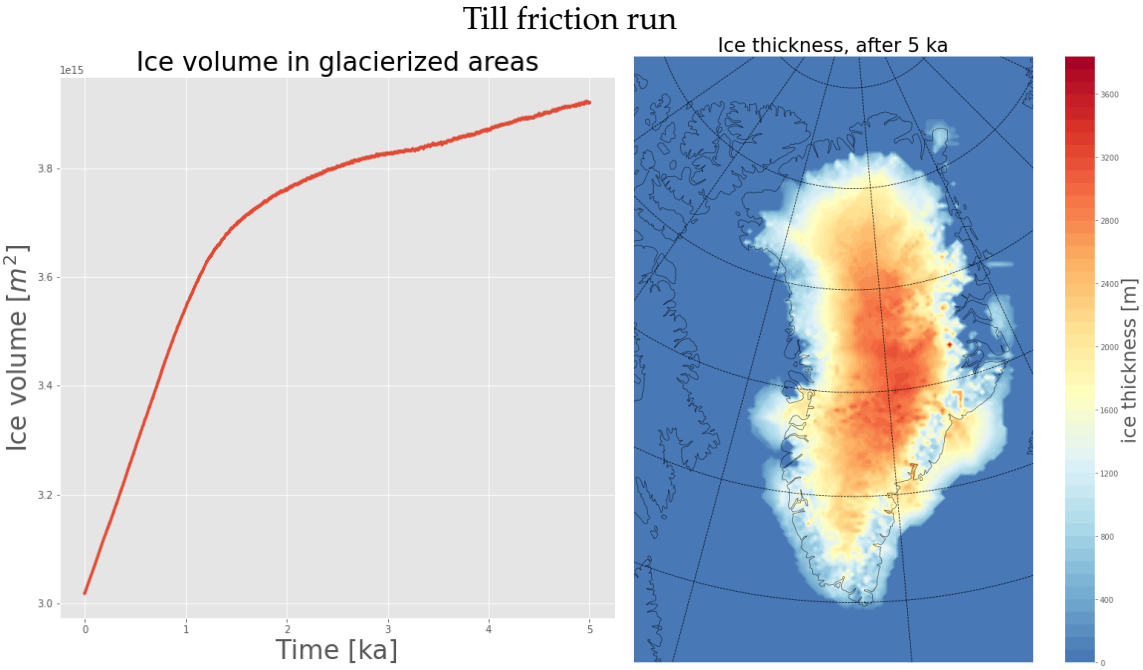

Figure 30: The results from a 5000 year run with till friction angle added. The first tile shows the evolution of the ice volume in the glacierized area and the second shows the ice thickness after 5000 years at 10 km resolution.

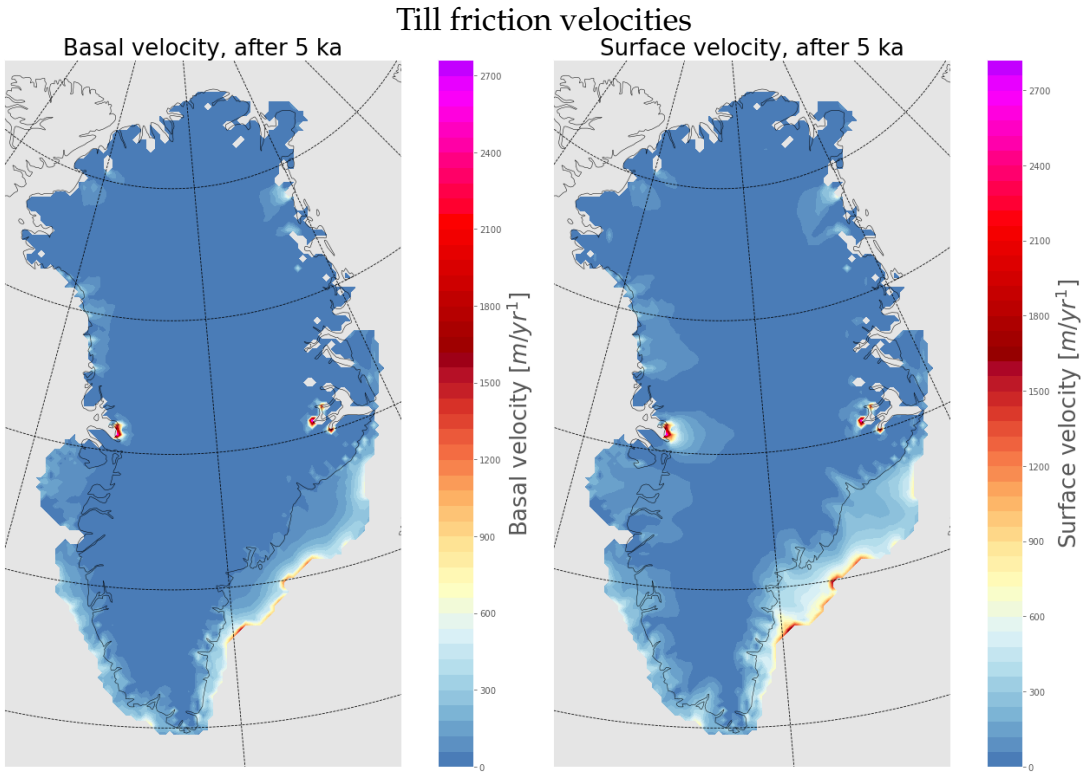

Figure 31: The basal and surface velocity of the ice after 5000 year with till friction angle added, at 10 km resolution.

7 Results

This chapter contains the results from all the PISM runs carried out in this study. It contains plots of the ice thickness, surface and basal velocities and ice volume evolution.

7.1 Present day steady state runs

This section contains all the results from PISM runs using present day or close to present day climate conditions. All the models where run to steady state, where the mass loss and mass gain are equal and the ice sheet is neither growing nor shrinking.

7.1.1 Present day climate

The first step was running PISM with present day climate conditions to steady state. This was done to test the run time of the model and how it performs under known conditions.
The model was run for 20,000 years, using the IBCAO topography, the BedMachine ice thickness, [Shapiro and Ritzwoller, 2004] basal heat flux map and the RACMO temperatures and precipitation. Figure 32 shows the evolution of the ice volume in the glaciarized areas. Here 0 ka is present day and 20 ka is 20,000 years into the future.

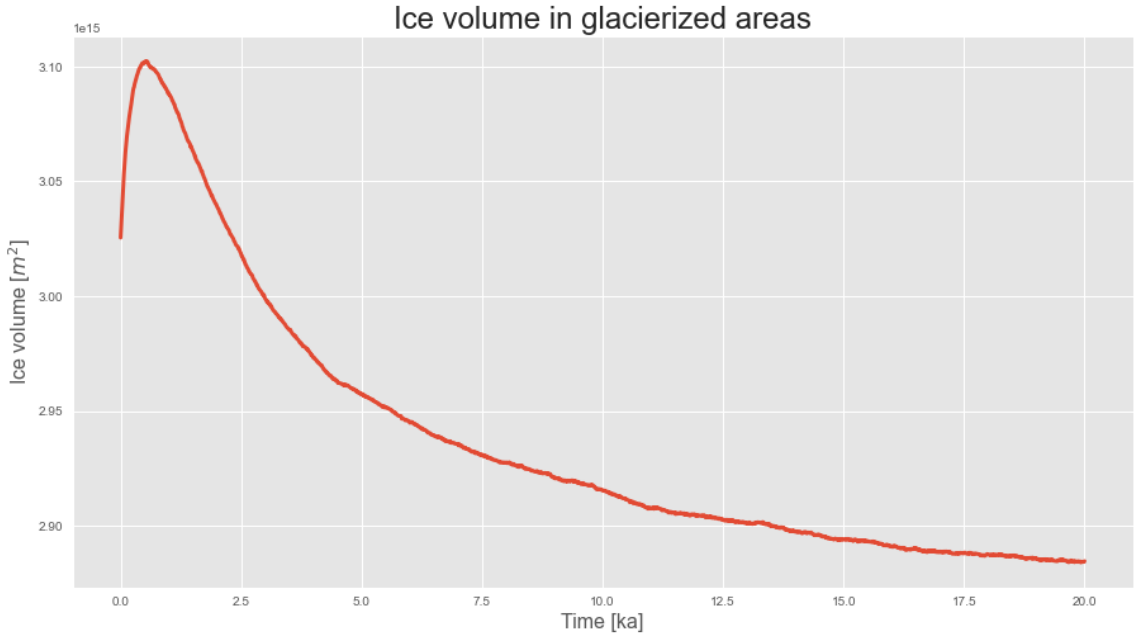

Figure 32: The evolution of the ice volume in the glacierized areas of Greenland, for present day climate conditions, run at a 10 km resolution.

The first panel in figure 33 shows the initial ice thickness over Greenland, before the model was run and the second shows the ice thickness after running the model for 20,000 years using the present day climate conditions from [Noël et al., 2018]. Figure 34 shows the difference between the two, that is the 20,000 years ice thickness minus the the present day ice thickness.

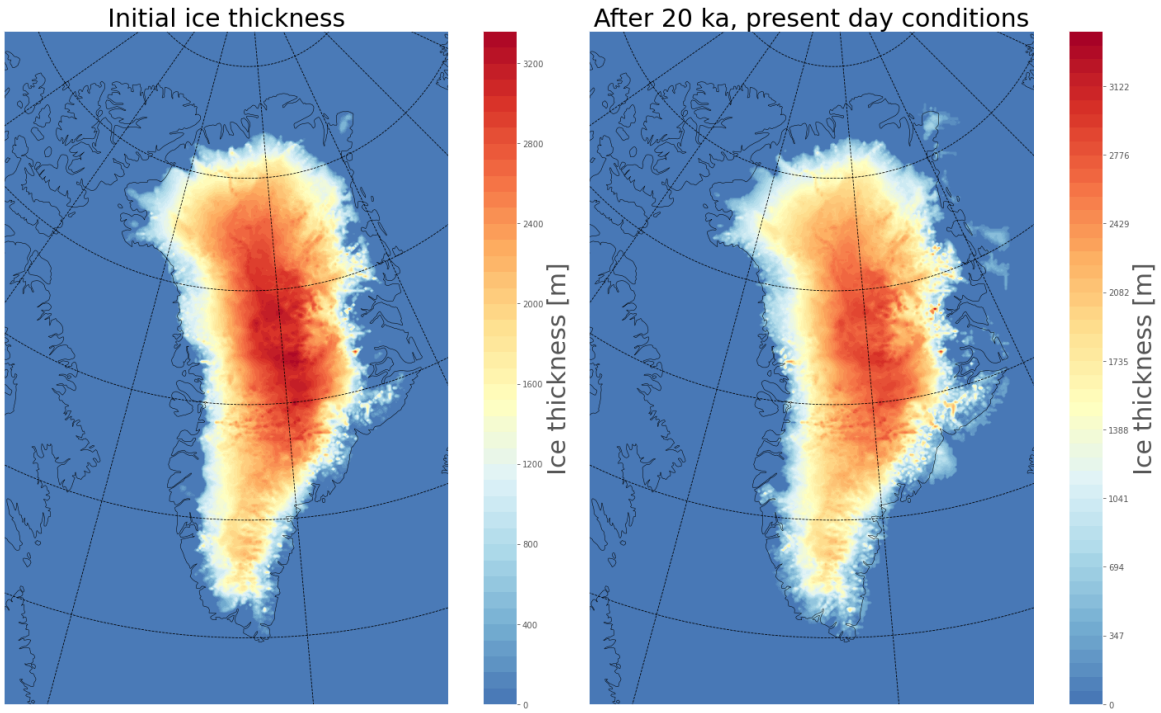

Figure 33: Panel one shows the initial ice thickness of GrIS. Panel two shows the ice thickness after running the model for 20 ka, with present day climate conditions.

After 20,000 years the extent of the ice sheet is bigger than present day. Specifically it seems to have spread into the ocean and created what could look like large ice shelves along the eastern coastline. The thickness of the ice sheet however is lower over most of the ice sheet, especially towards the north and on top of the ice. This means that despite the larger horizontal extent, the total volume of the ice sheet is smaller after 20,000 years.

Figure 35 shows the basal and surface velocity of the ice after 20,000 years. Both the surface and basal velocities are fairly small or non existing in the middle of the ice sheet, but grows larger towards the margins. The velocities are highest around a number of the fjords where outlet glaciers are located today, such as the Jakobshavn isbræ and the Northeast Greenland Ice Stream (NEGIS). These ice streams have contributions from the basal sliding and internal deformation of the ice.

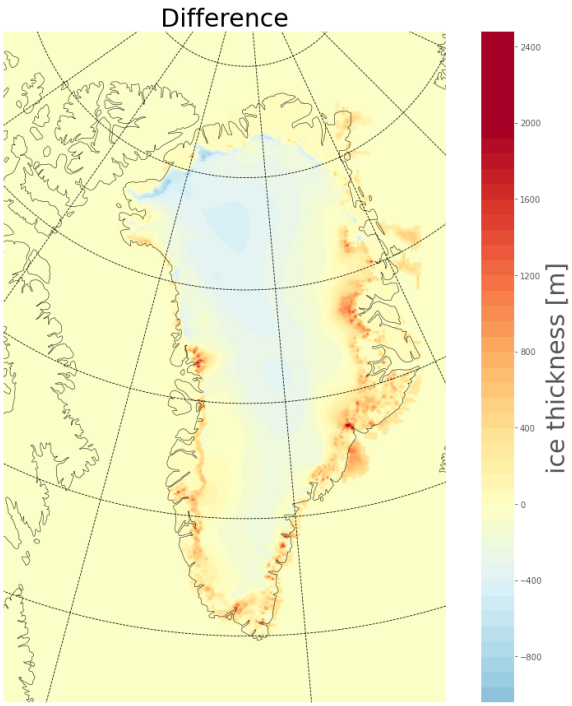

Figure 34: The difference between the two ice thickness plots in figure 33 (after 20 ka - present day).

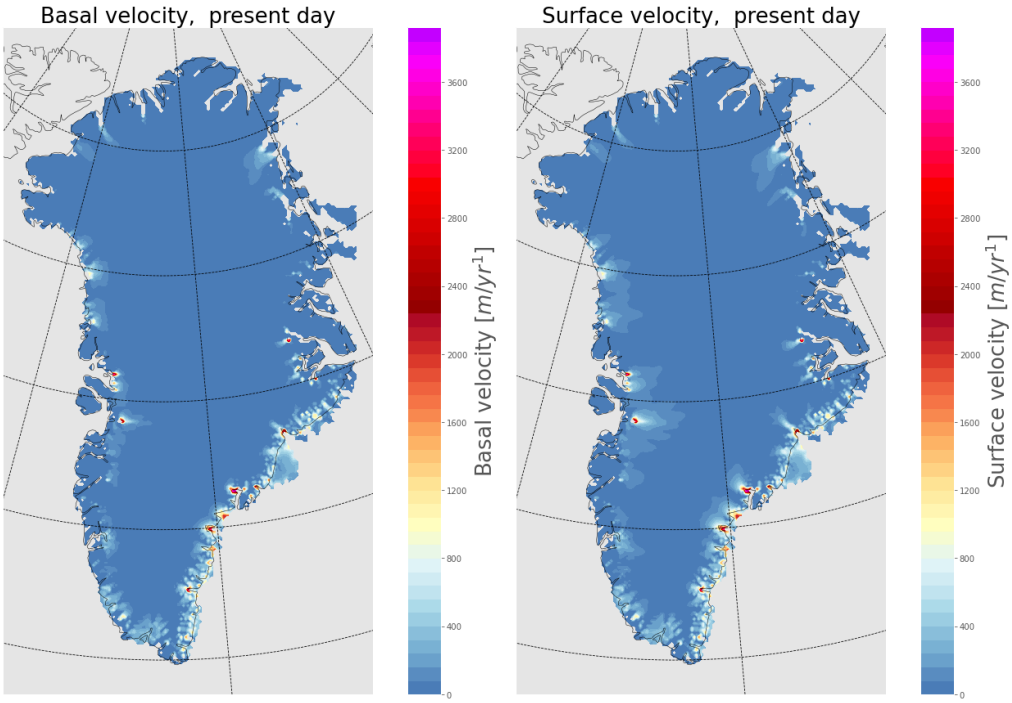

Figure 35: The basal and surface velocity, after 20,000 years, with present day climate.

7.1.2 Warmer temperatures

To test the resistance of the GrIS to changes in temperature, the same experiment was performed, for higher temperatures than present day, but the same precipitation as before. Practically this was done by uniformly increasing the temperature field from RACMO by 2, 4, 8 and 12°C. These specific temperatures were chosen, because +2°C is the global temperature increase from the Paris Agreement [UN, Paris Agreement, 2015] and +4°C $\pm$ 4 is the temperature difference between present day and the Eemian, found from the NEEM ice core [NEEM community members, 2013].
Figure 36 shows the evolution in ice volume, for all 5 different temperature fields, including present day. Here the red curve is the same as can be found in figure 32.

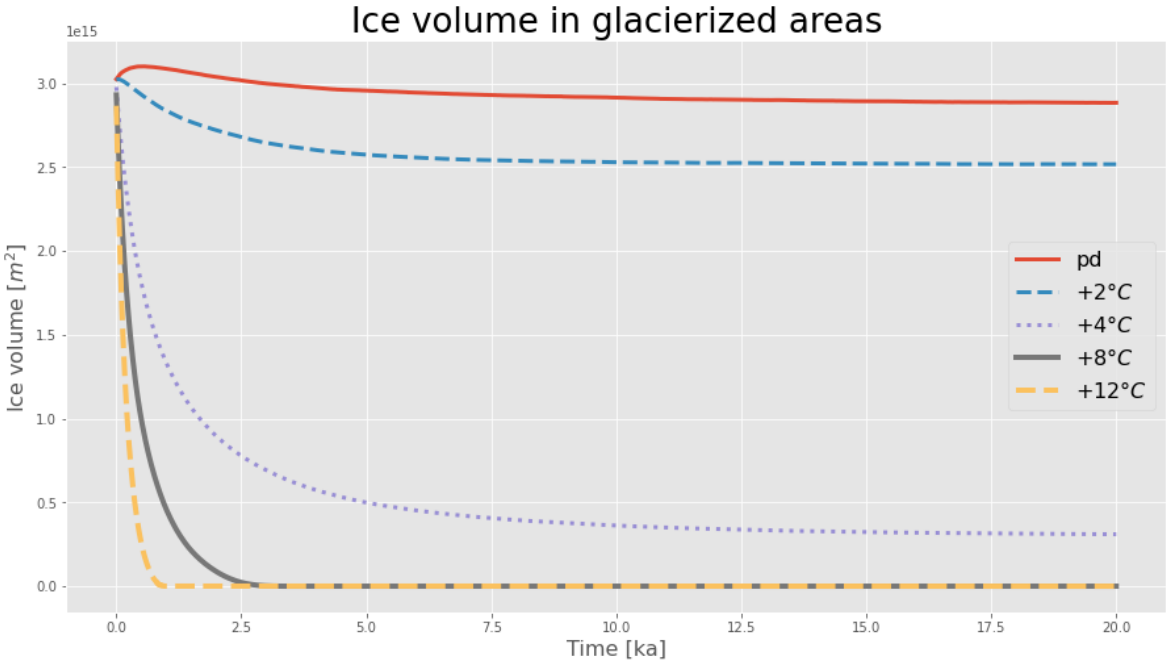

Figure 36: This figure shows the evolution of the ice volume in the glacierized areas for present day temperature and uniformly increased by 2, 4, 8 and 12°C.

As seen in figure 36 only the present day temperature, +2°C and +4°C result in an ice sheet still existing after 20,000 years, however only the present day conditions and +2°C have an ice sheet of a size comparable to the current GrIS, as the + 4°C ice sheet is almost gone.

Temperature increase	Equivalent sea level rise
pd	0.36 m
+ 2 °C	1.29 m
+ 4 °C	6.88 m
+ 8 °C	7.42 m
+ 12 °C	7.42 m

Table 1: Sea level rise equivalent to the mass loss of the ice sheet at 5 different temperatures after 20,000 years.

Table 1 contains the sea level rise equivalent to the mass loss of the ice sheet, for the 5 different temperature fields after 20,000 years. These sea level rises have been calculated using the following equation

$$SLE = \frac{V_{ice}}{A_{ocean}}, \tag{27}$$

where M_{ice} is the mass of lost ice and V_{ocean} is the volume of water required to raise the worlds oceans by 1 mm.

Figure 37 shows results for the 2°C temperature increase. The first panel shows the initial ice thickness and the second panel shows the extent of the ice sheet after running the model for 20,000 years. Figure 38 shows the difference between the two.

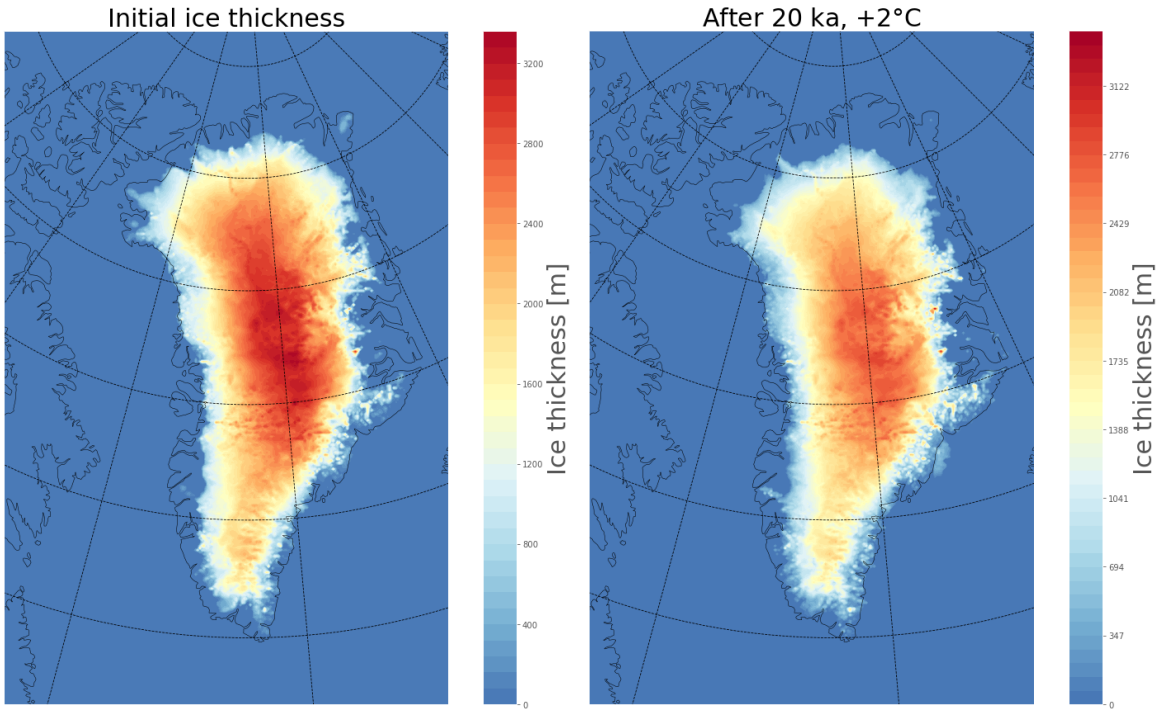

Figure 37: The initial ice thickness and the ice thickness after running the model for 20,00, with present day climate conditions +2°C.

The extent of the ice sheet after 20,000 years is noticeably smaller than the initial ice sheet, but not significantly. Generally on top of the ice sheet it has lost mass resulting in thinning of the ice sheet, but it is especially in the north, that the loss of mass has happened, resulting in a retreat of the ice front.

Along the eastern coastline and a bit along the south-western as well, there has been an increase in mass. It is not as much as for the present day conditions in figure 33, and the ice has not started spreading into the ocean.
There has been significantly more loss of mass than gain of mass in this simulation. This has resulted in a loss of mass equivalent to a total global sea level rise of 1.29 m.
Figure 39 shows the basal and surface velocity of the ice after 20,000 years. Again the velocities are fairly small or non existing in the middle of the ice sheet, but grow larger towards the margins. The velocities are highest around a number of the fjords where

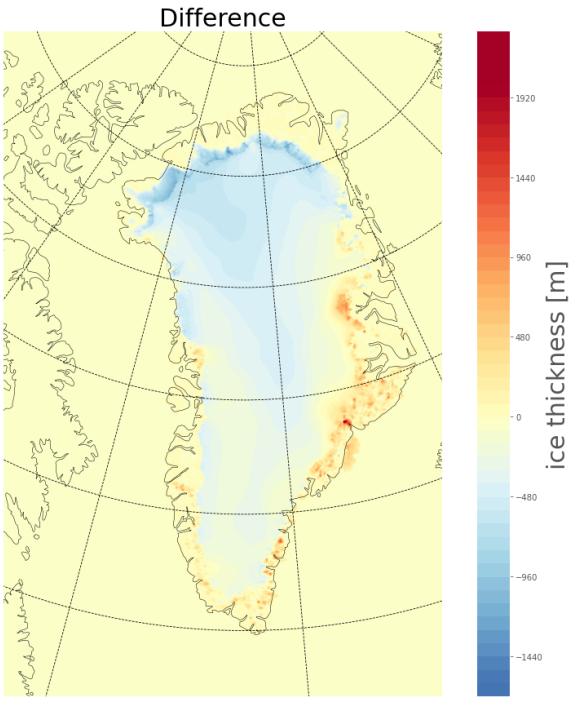

Figure 38: The difference between the two ice thickness plots in figure 37 (after 20 ka - present day).

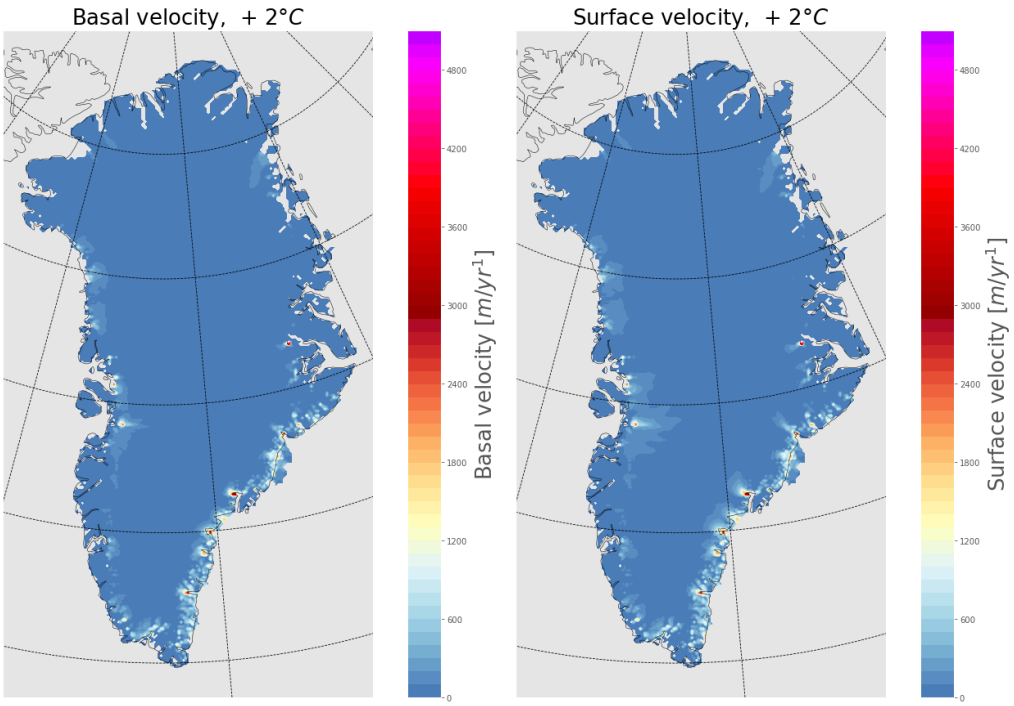

Figure 39: The basal and surface velocity after 20,000 years, with a +2°C increase.

outlet glaciers are located today.

Figure 40 shows the extent of the + 4°C ice sheet after 20,000 years. In this simulation the ice sheet is almost completely gone. Only a collection of ice around the middle of Greenland towards the eastern coastline is remaining. The thickest part of the ice

sheet is only half as thick as the thickest part of the present day ice sheet.
This large loss of mass from the ice sheet would result in a global sea level rise of 6.88 m, which is a very big part of the total equivalent sea level rise, bound in the mass of the GrIS.

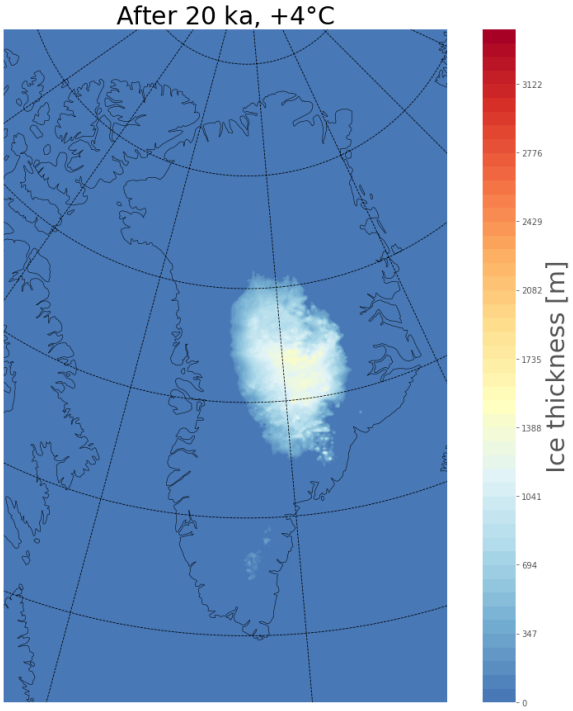

Figure 40: This figure shows the ice sheet thickness and extent after 20,000 years, with a temperature increase of 4°C.

7.2 Glacial steady state runs

This section contains all the results, from PISM runs carried out using glacial or close to glacial conditions. All the models were run to steady state. This was done to test if PISM can produce an ice sheet resembling the ice sheet from LGM. Later these results will be used as the starting point for a glacial cycle simulation.
In these runs the RACMO temperature fields were uniformly lowered by 20°C, which as mentioned earlier was approximately how much colder the glacial climate over Greenland was [Dahl-Jensen et al., 1998]. As mentioned earlier the precipitation was also lower, therefore the precipitation fields were also uniformly lowered to be 25%, 50% and 100% of the present day precipitation.
Also the sea level was lower around Greenland, because so much water was bound in the ice on the continents at this time [Lambeck, 2004], so the sea level of the model was lowered by 130 m.

The model was run for all the three different precipitation fields using the topography maps including and excluding Canada from the computational domain. The two topography maps can be seen in figures 5 and 6 in section 3.1. The only difference between these two maps and what PISM was provided, is that the sea level was 130 m lower.

Figure 41 shows the evolution of the ice volume in the glacierized areas over the domain. In red is shown the three runs including Canada as part of the computational domain. In blue the runs excluding Canada. The solid lines show the runs with 25% precipitation, the dashed lines (- - -) show the runs with 50% precipitation and the dotted line (...) show the runs with 100%. All the models were run for 50,000 years, so they would reach steady state.

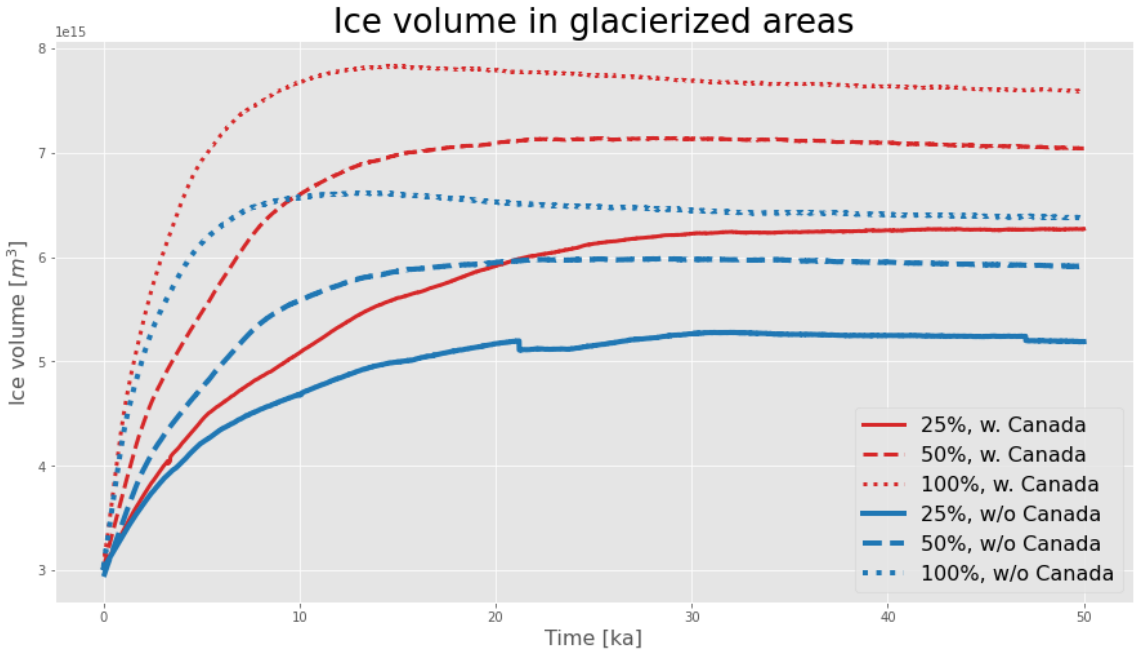

Figure 41: Ice volume evolution in glacierized areas over 50 ka, for different percentages of present day precipitation. Red is runs where Canada is included in the domain, blue is where Canada has been removed. The solid lines show the runs with 25% precipitation, the dashed lines (- - -), show the runs with 50% precipitation and the dotted line (...) show the runs with 100%.

Figure 42 shows the ice thickness and ice sheet extent after 50,000 years, for the runs in figure 41. The first column shows the runs using the 25% precipitation field, second column is 50% and third is 100% precipitation. The top row is including Canada and the bottom row is excluding Canada.
All three runs that include Canada as part of the computational domain, has grown significant amounts of ice on the Canadian land masses. Also in all three runs an ice bridge has developed between the most eastern part of Canada and northern Greenland, effectively connecting the two ice sheets.

All six of the runs have the ice spreading into the ocean on both sides of Greenland. This is especially happening along the whole of the eastern coastline and in the southern part of the western one. The ice sheet has also grown much thicker in the middle of the ice divide throughout all six runs. Both these evaluations are due to the calving criteria, that the ice breaks of when i floats.
For a criteria allowing ice shelves, the ice cap would have been thinner at the ice divide and margins, due to more flow and for a criteria cutting the ice before the ice would have been thicker and the extend smaller for the whole ice sheet.

The three runs excluding Canada from the computational domain have ice that seems to be forming around the areas of the Canadian coastline and no ice where Canada used to be. Other than this they are very similar to the three runs including Canada.

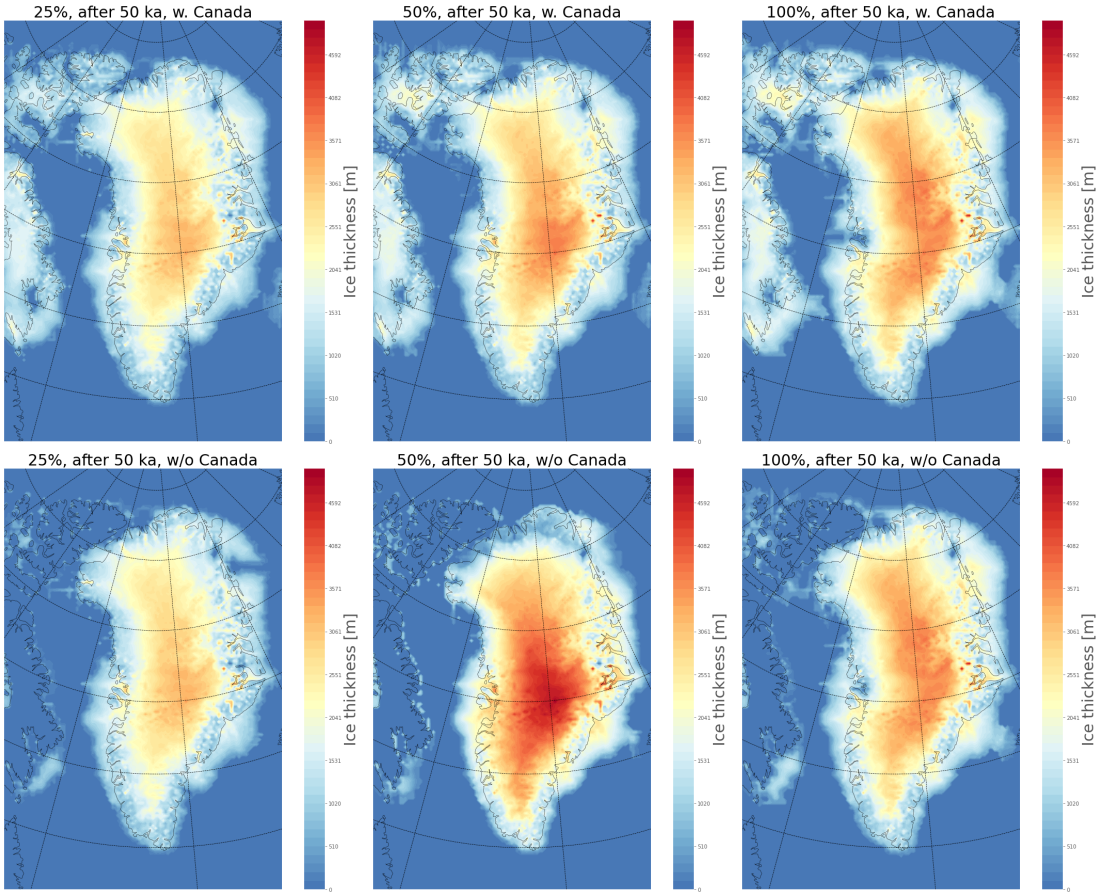

Figure 42: This figure shows the extent and thickness of the ice sheet after 50 ka for different percentages of present day precipitation, with and without Canada in the computational domain. The first column shows the runs using the 25% precipitation field, second column is 50% and third is 100% precipitation. The top row is including Canada and the bottom row is excluding Canada.

7.3 Eemian runs

To recreate the Eemian ice sheet the model was run from 140,000 years ago to present day. This period was chosen, so it includes the end of the glacial period before Eemian in the run. The end of the glacial is included to test whether the ice bridge to Canada has an impact on the extent of the Eemian ice sheet. The model was run all the way to present day, to see if it could recreate the present day ice sheet.

Figure 43 shows the results for running PISM from 140,000 years ago to present day, with three different precipitation scalings and with and without Canada in the domain. The three precipitation scalings used are the SeaRISE scaling, the scaling from [Buchardt et al., 2012] (both can be found in figure 13 in section 3.5) and present day precipitation, scaled according to temperature by PISM.
The sea level was changed over the period, according to the [Lisiecki and Raymo, 2005] marine core, scaled to fit the SeaRISE sea level record. The sea level change can be found in figure 14 in section 3.5. The initial ice sheet was set to be the glacial steady state ice sheet from 42, produced with 25% of present day precipitation, both with and without Canada.

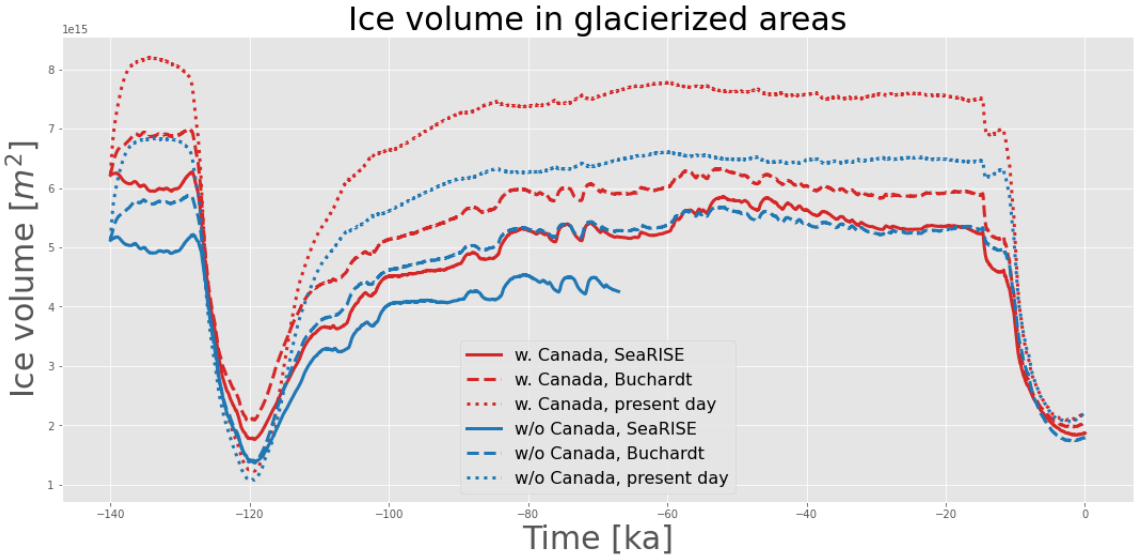

Figure 43: The evolution of the ice volume from 140,000 years ago until present day, for different precipitation scalings. In red are runs including Canada in the domain and in blue excluding Canada. Solid lines are with the SeaRISE scaling, dashed lines (- - -) are with the scaling from [Buchardt et al., 2012] (both are found in figure 13) and dotted lines (...) are the unscaled present day RACMO precipitation.

As it can be seen in figure 43, the minimum ice sheet extent during Eemian happens approximately 120,000 years ago. The ice sheets with constant present day precipitation produce the largest ice sheets during the glacials and the smallest during Eemian times.
The SeaRISE runs produce the smallest ice sheets during the first glacial and almost the smallest during the last glacial. The Eemian ice sheet is located very much in the middle. The SeaRISE run without Canada only ran to 67,000 years ago. This is because the ice sheet became more than 7 km thick and the diffusivity of the ice passed 20,000 $\frac{m^2}{s}$, which is highly nonphysical.

It is suspected that this error occurred due to inconsistencies in the bedrock data, e.g. that bedrock lows are not resolved properly, but further investigations were not conducted.
The Buchardt runs produce ice sheets of a volume between the volumes of SeaRISE and present day precipitation during the glacials and smallest ice sheets during Eem.

Figure 44 shows four different ice sheet extents for the GrIS during the Eemian, using the SeaRISE precipitation scaling without Canada. The first panel shows the ice extent at 130 ka before present, at the beginning of the Eemian. Panel two shows the ice sheet extent at 125 ka before present after the ice has started to retreat. Panel three shows the ice sheet extent at 120 ka before present, at the ice sheet's minimum extent. Panel four shows the ice extent at 115 ka before present, when the ice sheet starts to grow again.
Figure 45 shows the ice sheet extents at the same four time stamps, but in this run Canada was included in the computational domain. The main difference between the two runs, is the ice sheet extent in the north-eastern part of Greenland, where the ice extents into the ocean when including Canada in the domain and not when excluding it.

Figure 46 shows the same four ice sheet extents for the GrIS during the Eemian, using the [Buchardt et al., 2012] precipitation scaling without Canada. Figure 47 shows the ice sheet extents at the same four time stamps, using the [Buchardt et al., 2012] precipitation scaling, but in this run Canada was included in the computational domain.
As for comparing [Buchardt et al., 2012] and the SeaRISE runs the main difference between these two runs, is the ice sheet extent in the north-eastern part of Greenland, where the ice extents into the ocean when including Canada in the domain and not when excluding it.

Figure 48 shows the same four ice sheet extents for the GrIS during the Eemian, using the present day precipitation without Canada. Figure 49 shows the ice sheet extents at the same four time stamps, again using the present day precipitation, but in this run Canada was included in the computational domain.
For these two runs there are no major differences between the ice sheets at any of the time stamps, besides the ice that forms in and around Canada, which affects the isostatic sinking differently. This must be the reason for the different resulting ice sheets. There seems to be slightly more ice in the north-eastern part of Greenland at -125 ka, but this is not present at the later time stamps.

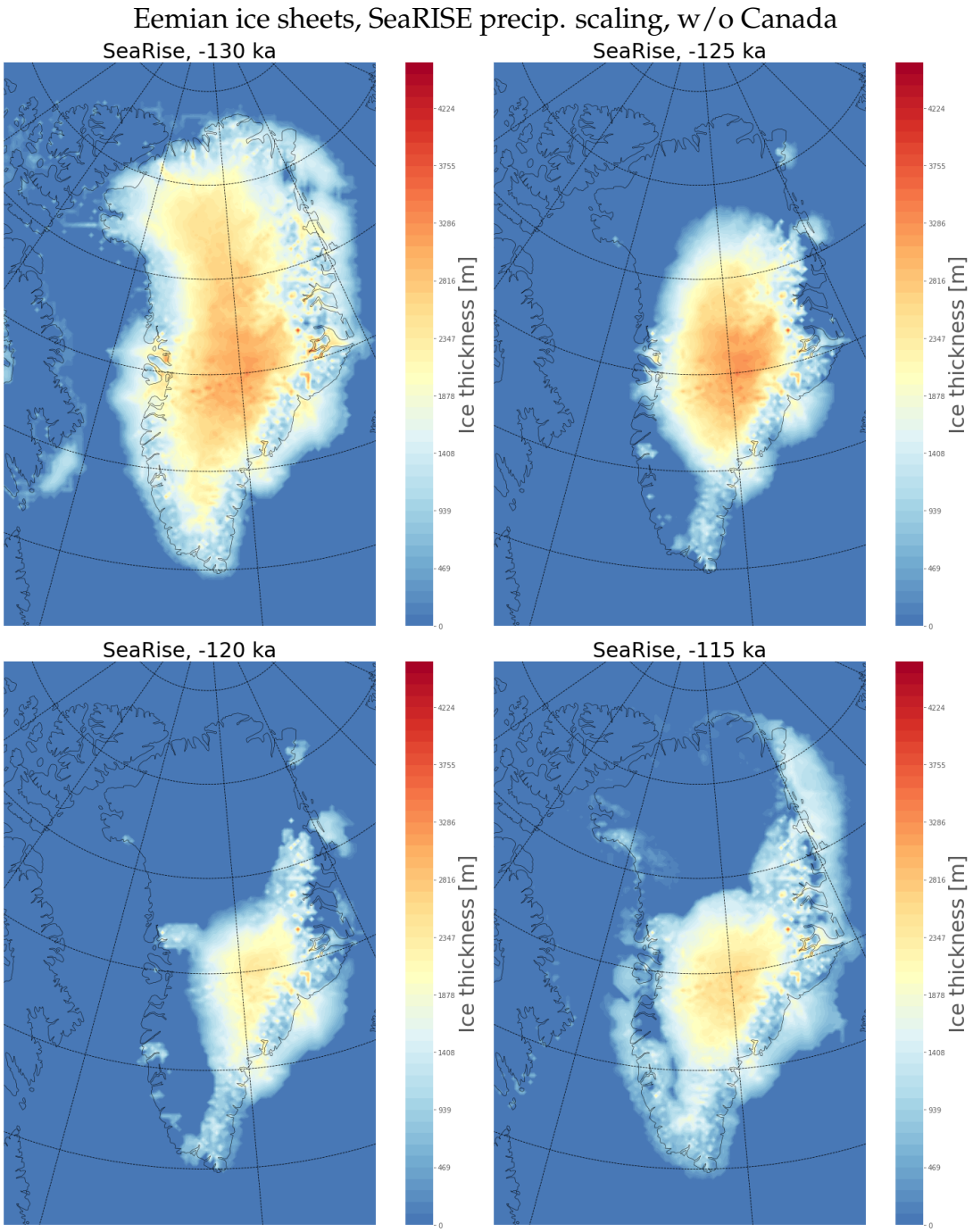

Figure 44: The extent of the Eemian ice sheet, using the SeaRISE precipitation scaling without Canada. The first panel shows the ice extent at 130 ka before present, at the beginning of the Eemian. Panel two shows the ice sheet extent at 125 ka before present after the ice has started to retreat. Panel three shows the ice sheet extent at 120 ka before present, at the ice sheet's minimum extent. Panel four shows the ice extent at 115 ka before present, when the ice sheet starts to grow again.

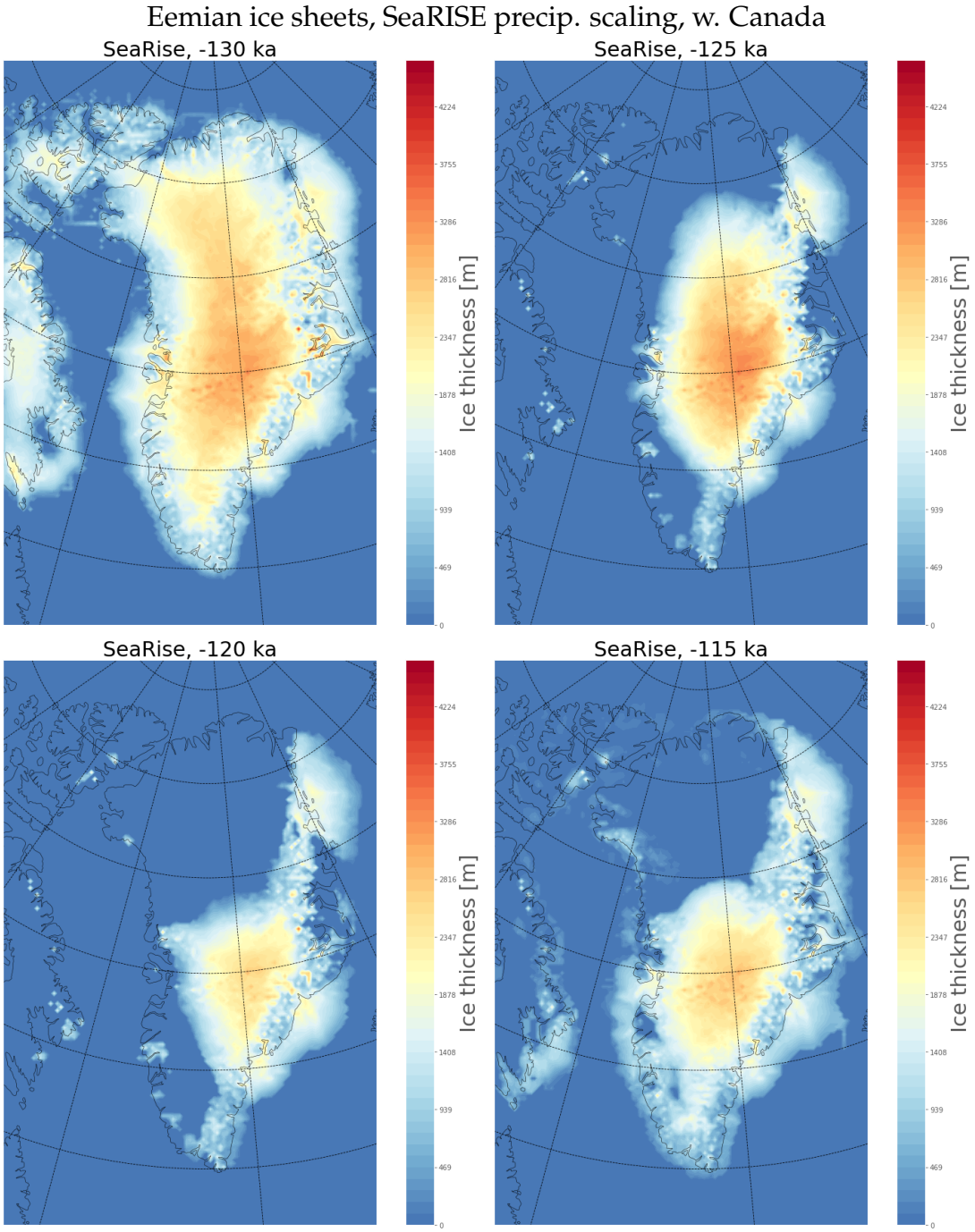

Figure 45: The extent of the Eemian ice sheet, using the SeaRISE precipitation scaling with Canada. The first panel shows the ice extent at 130 ka before present, at the beginning of the Eemian. Panel two shows the ice sheet extent at 125 ka before present after the ice has started to retreat. Panel three shows the ice sheet extent at 120 ka before present, at the ice sheet's minimum extent. Panel four shows the ice extent at 115 ka before present, when the ice sheet starts to grow again.

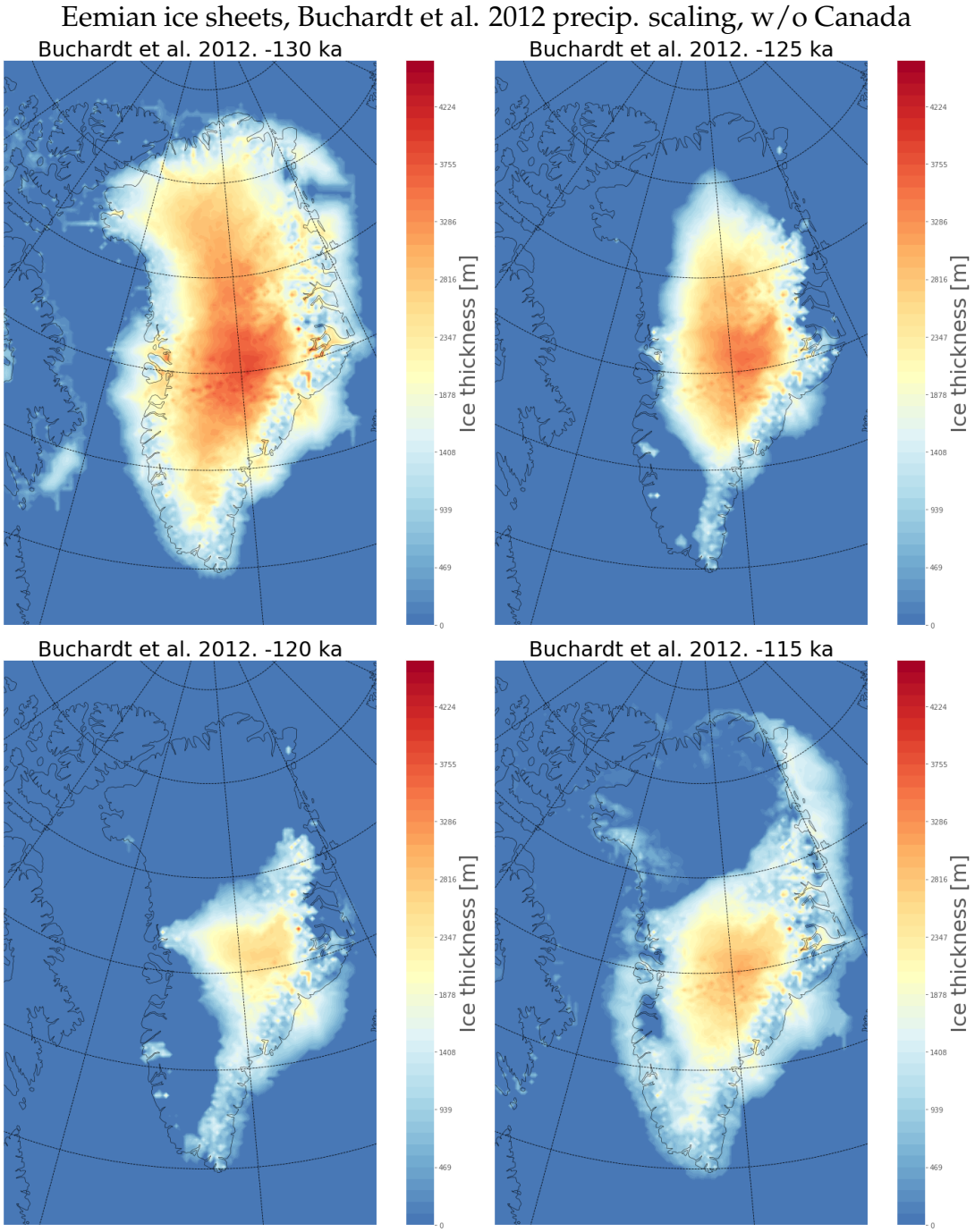

Figure 46: The extent of the Eemian ice sheet, using the [Buchardt et al., 2012] precipitation scaling without Canada. The first panel shows the ice extent at 130 ka before present, at the beginning of the Eemian. Panel two shows the ice sheet extent at 125 ka before present after the ice has started to retreat. Panel three shows the ice sheet extent at 120 ka before present, at the ice sheet's minimum extent. Panel four shows the ice extent at 115 ka before present, when the ice sheet starts to grow again.

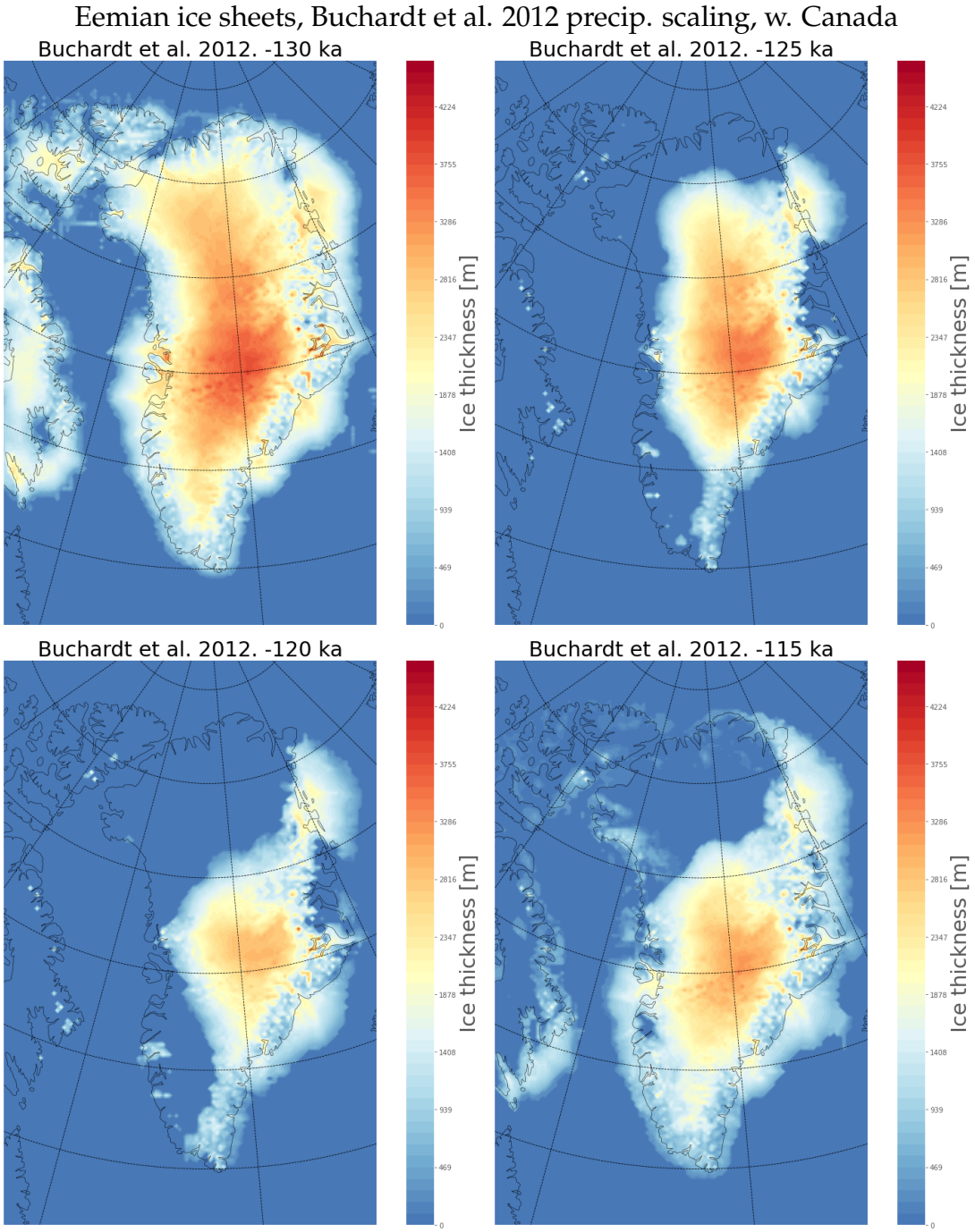

Figure 47: The extent of the Eemian ice sheet, using the [Buchardt et al., 2012] precipitation scaling with Canada. The first panel shows the ice extent at 130 ka before present, at the beginning of the Eemian. Panel two shows the ice sheet extent at 125 ka before present after the ice has started to retreat. Panel three shows the ice sheet extent at 120 ka before present, at the ice sheet's minimum extent. Panel four shows the ice extent at 115 ka before present, when the ice sheet starts to grow again.

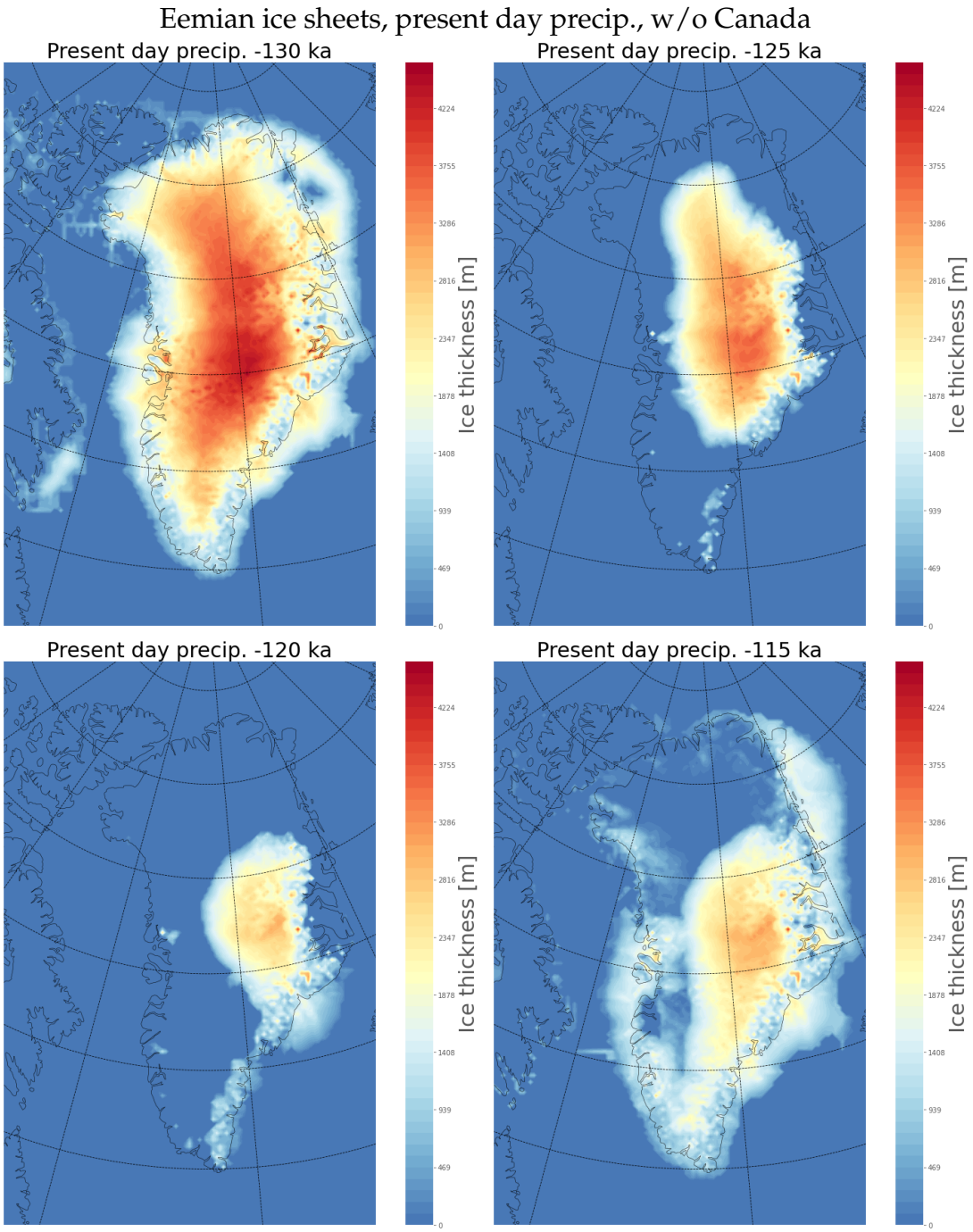

Figure 48: The extent of the Eemian ice sheet, using the present day precipitation, without Canada. The first panel shows the ice extent at 130 ka before present, at the beginning of the Eemian. Panel two shows the ice sheet extent at 125 ka before present after the ice has started to retreat. Panel three shows the ice sheet extent at 120 ka before present, at the ice sheet's minimum extent. Panel four shows the ice extent at 115 ka before present, when the ice sheet starts to grow again.

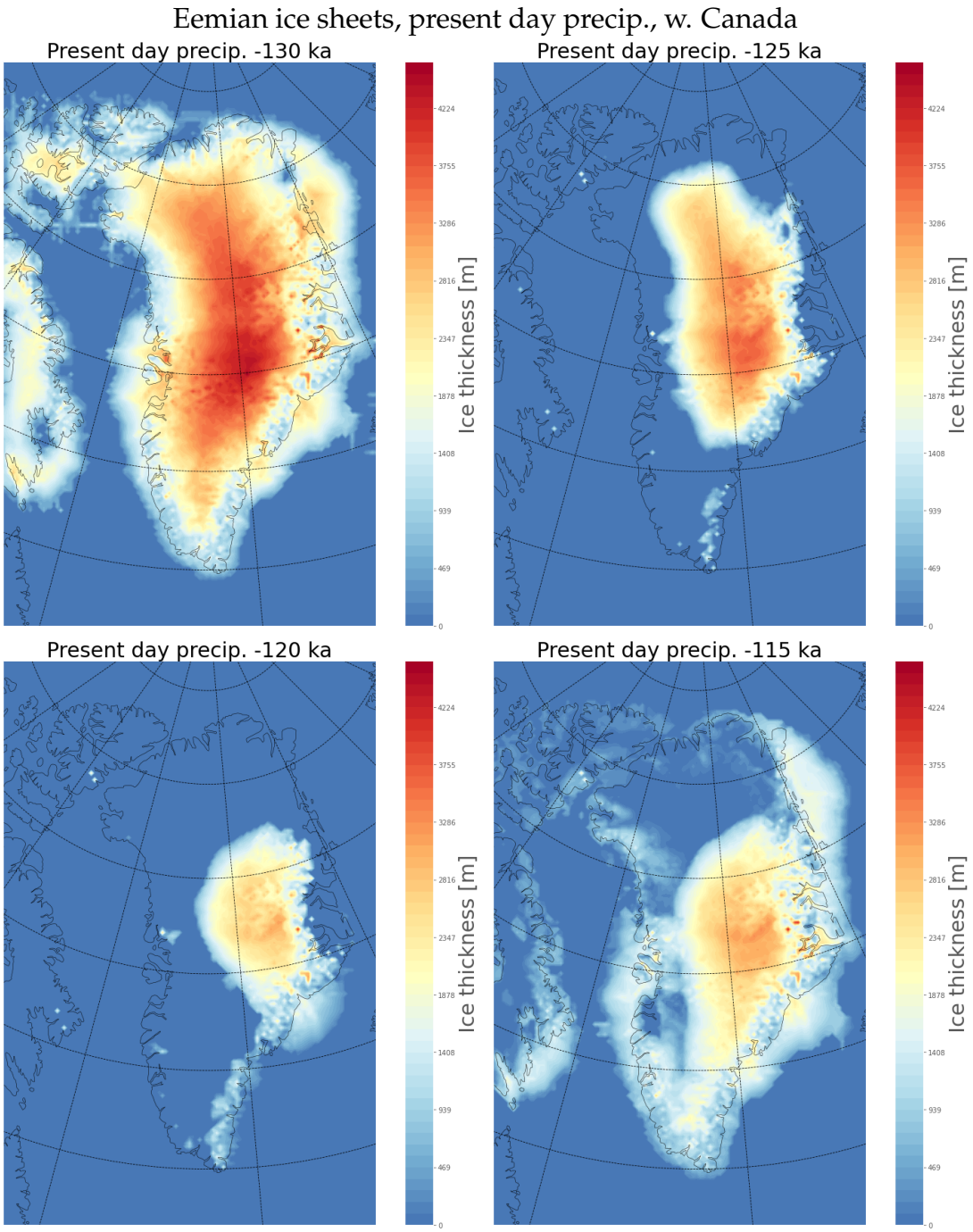

Figure 49: The extent of the Eemian ice sheet, using the present day precipitation, with Canada. The first panel shows the ice extent at 130 ka before present, at the beginning of the Eemian. Panel two shows the ice sheet extent at 125 ka before present after the ice has started to retreat. Panel three shows the ice sheet extent at 120 ka before present, at the ice sheet's minimum extent. Panel four shows the ice extent at 115 ka before present, when the ice sheet starts to grow again.

7.4 Present day ice sheet recreations

Part of the goal of the runs shown in figure 43 was to recreate the present day ice sheet extent. Figure 50 shows the ice sheet extent at present day, using the SeaRISE precipitation scaling and including Canada.
As can be seen from the figure, the ice sheet extent does not match the actual present day ice sheet extent, which can be seen in figure 7. The ice sheet extends less north and less towards the west in southern Greenland. Most places the ice sheet does not reach all the way out to the ocean and generally the ice sheet is also much thinner.

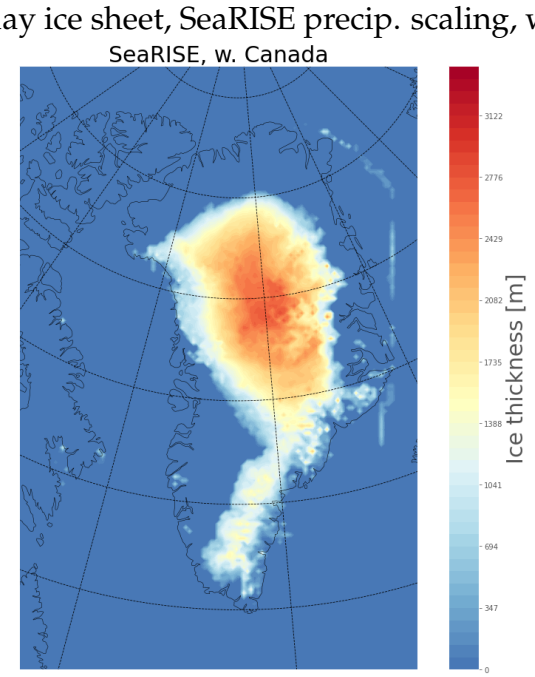

Figure 50: The modelled ice sheet extent at present day, with the SeaRISE precipitation scaling and including Canada in the computational domain.

Figure 51 shows the ice sheet extent at present day, using the [Buchardt et al., 2012] precipitation scaling, both with and without Canada as part of the domain. Both ice sheets are very similar to each other and to the SeaRISE ice sheet in figure 50. The most noticeable difference is the fact that the run excluding Canada has formed two separate ice sheets, whereas the other run has them connected.

Figure 52 shows the ice sheet extent at present day, using the present day precipitation, both with and without Canada as part of the domain. Both ice sheets are also very similar to each other and to the previously shown ice sheets. The run including Canada seems to have a slightly larger extent in the north-east and also generally it is slightly thicker than the run without Canada.

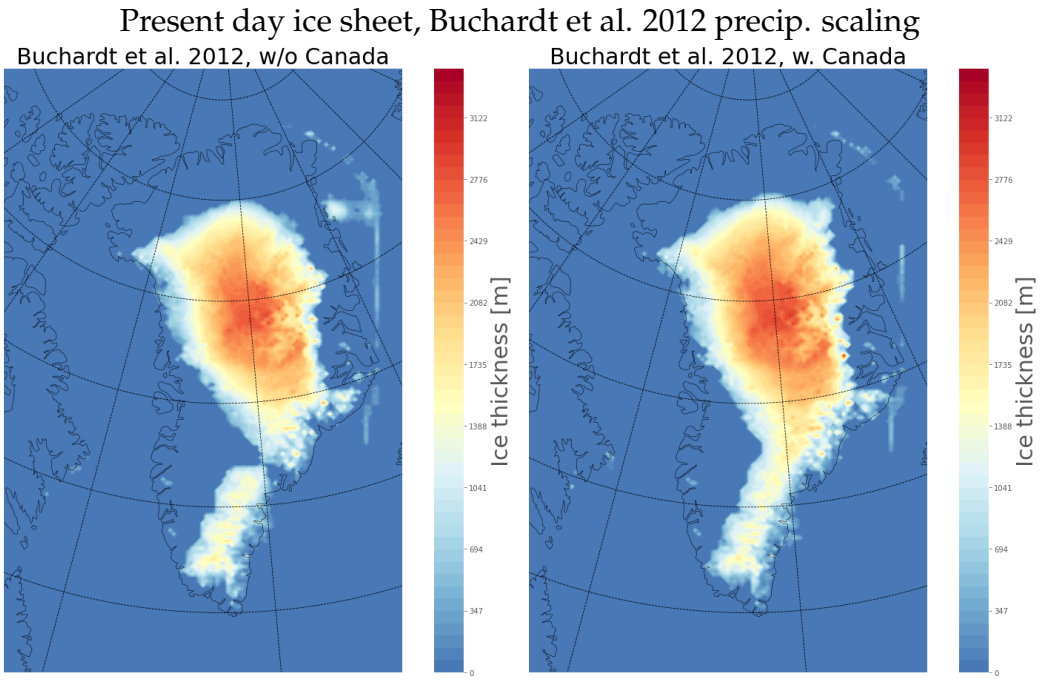

Figure 51: The modelled ice sheet extent at present day, including and excluding Canada. Run with the [Buchardt et al., 2012] precipitation scaling.

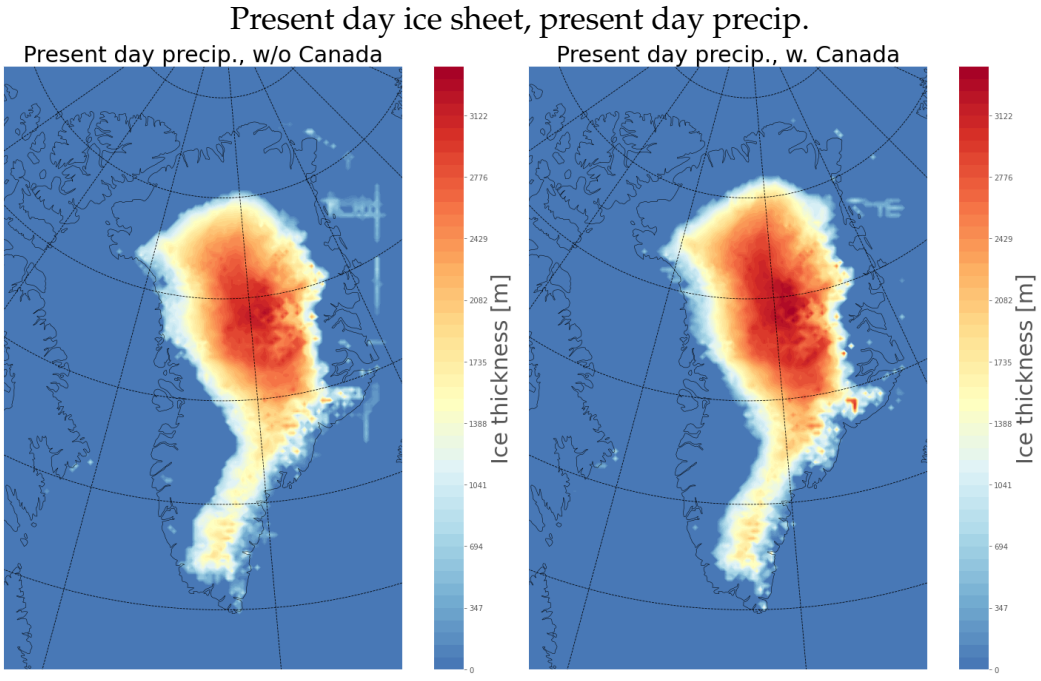

Figure 52: The modelled ice sheet extent at present day, including and excluding Canada. Run with the present day precipitation.

8 Discussion

When running PISM with the present day climate conditions from RACMO we find that the volume of the ice sheet is smaller when it reaches steady state than when the model started. This is expected since we know that the GrIS used to be in approximately steady state, but has been losing mass over the past decades due to increased temperatures on and around Greenland. One would therefore expect that if the temperature and precipitation was kept constant, at present day conditions, that the ice sheet would shrink until it reached a new steady state.
From figure 34 it can be seen that the ice sheet is thinner after 20,000 years, especially around the ice divide and that, despite the loss of mass, it has spread further out than the initial ice sheet. This could have something to do with the fact that the RACMO precipitation is not completely accurate. It is underestimating the amount of precipitation on top of the ice sheet and overestimating at the margins [Fettweis et al., 2020]. This could very well explain why the ice sheet is thinning in the middle and growing at the margins.
Another explanation for this could be that the spacial resolution of the RACMO data is too low. The RACMO data comes on a resolution of 5.5 km, which might not be fine enough to catch the complexity of the precipitation pattern over Greenland, meaning that it could be part of the explanation for why RACMO overestimates the precipitation near the margins and underestimates it near the middle of the ice sheet [Fettweis et al., 2020].

The stress balance regime could also have something to do with the thinning on top and growing at the sides. Because SIA has no basal sliding, it has a tendency to make the ice sheet grow thicker at the margins than an ice sheet would in reality. This is because SIA does not have the surface melt and basal sliding feedback effect to thin the ice near the margins.
When there is surface melt near the margin of an ice sheet, the melting water can penetrate the ice sheet and reach the bottom, resulting in more basal sliding and thus a thinning of the ice here. When the ice then thins, the surface melt becomes larger resulting in a feedback effect. Because SIA has no basal sliding, this thinning will not happen near the margins.

The RACMO precipitation, plotted in figure 9, has the majority of rain and snow fall occur in the southern part of Greenland, specifically on the east coast. This is also the areas with the most accumulation of ice over the 20,000 year period. In the northern part of Greenland there is quite a lot of mass loss. This is probably also do to the precipitation being so small in the north. As can be seen from the RACMO precipitation, there is almost no snow or rain fall happening in this area, meaning that there is next to no accumulation of mass, but ablation still happens due to ice dynamics and melt.

The simulation for present day conditions +2°C, shows a loss of mass over time. The loss of mass is quite significant, since it will result in a global sea level rise of $1.29m$. This specific temperature increase was chosen because it is the total global temperature increase agreed upon as part of the 2015 Paris Agreement [UN, Paris Agreement, 2015]. The loss of mass happening in this simulation is mostly centered around the northern

boundary of the ice sheet, resulting in a retreat of the ice front in this area. Along the other ice fronts the ice is not retreating, in fact at a few places, like along the east coast, the ice is actually thickening and in some areas growing further out.

For both the present day conditions and +2°C, the ice is not retreating from the east coast, meaning that there is still a flux of fresh water running into the Atlantic ocean here. This bodes well for the future of the North Atlantic current and the transportation of warm water to Europe. It seems that there is need for a larger temperature increase if the ice is going to retreat far enough back, to stop the fresh water flux from the ice sheet into the ocean.
For both runs we see a significant thinning of the ice sheet even in top of the ice dome and a retreat of the ice front in the north. A loss of ice thickness in the center of the ice sheet can be quite catastrophic for the ice sheet. If the ice sheet becomes so thin that it starts to reach the equilibrium line, it will be very hard for it to reach a state where it can accumulate as much mass as it losses to melt and calving. If this happens the ice sheet is at risk of melting away completely.

Figure 35 and figure 39 show the velocity fields for the present day and +2°C runs. As it can be seen from these figures, the model is not capable of capturing all the high velocities around NEGIS, Jacobshavn isbræ and The Kangerlussuaq glacier to name a few. They catch some of the flow and all of them have components from both basal sliding and internal deformation, but the ice does not flow quite fast enough [Nagler et al., 2015].
Generally NEGIS is a very hard ice stream to recreate in models. A modelling study by [Smith-Johnsen et al., 2020] found that an exceptionally high heat flux needed to sustain it. Therefore it comes as no surprise, that this model was not able to recreate the velocities of NEGiS.

Generally we believe the Greenland ice sheet to be quite stable and resistant to changes in our climate [Aschwanden et al., 2019] [Shepherd et al., 2020]. Figure 36 shows the evolution of the GrIS for four different temperature fields and from here we see that it might not be as stable as we used to believe.
If we increase the temperature with just 4°C, the minimum temperature difference between present day and Eemian Greenland, the ice sheet almost disappears, but not completely. It reaches steady state after about 15,000 years. If we increase the temperature by 8°C, the ice sheet disappears after around 2500 years and if we increase it by 12°C it is gone before the end of the 21st century.
These temperature increases all result in a significant rise of the global sea level. For +2°C the sea level will increase with 1.29 m, which might not seem like a lot, but can in fact have big consequences in generally flat countries like the Netherlands, the Maldives and even Denmark.
When the temperature is increased even further, the mass loss becomes more significant. For a 4°C increase the global sea level rise becomes 6.88 m, which is almost 93% of the total equivalent sea level rise, bound within the mass of the Greenland ice sheet. An increase in sea level like this could move the coastlines of the previously mentioned countries far inland and would result in a complete loss of landmass in the Maldives, that has a maximum elevation of 2 m [worlddata.info, 2022].

Figure 41 shows the volume evolution of the ice sheet under different glacial conditions. All of them have a temperature of 20°C less than present day, but the precipitation differs. The precipitation was set to be 25%, 50% and 100% of the present day amount. As mentioned earlier it is believed that the precipitation during the glacial was around 25% of the present day, but since the model had a hard time growing ice sheet larger, higher levels were also tested.
Figure 42 shows the ice sheet extent for the runs in figure 41. As it can be seen all the extents are quite similar, in respect to how large of an area they cover. The main difference is the ice sheet thickness. This points towards the conclusion that the ice sheet cannot grow any further out due to the sea level at the time, which was 130 m lower than present day.
It turns out that recreating the ice bridge between Greenland and Canada is very hard, with a precipitation pattern like RACMO. The amount of ice in this area does not seem to get any bigger even when increasing the amount of precipitation. This is probably due to the fact that there is next to no snow fall happening in this area, even at present day conditions. And as we all know from math 25% of nothing is still nothing, meaning that scaling the precipitation to a higher percentage will not make a difference here, because there is nothing to scale. And since it is believed that an ice bridge formed, one conclusion could be that it must have happened under different conditions than we model here, either more accumulation is needed or the ice sheet would form in Canada and flow in towards Greenland from Northwest. The latter is perhaps unlikely due to the relatively flat topography in Canada [Bennike and Björck, 2002].

Figure 43 shows the evolution of the volume for the ice sheet over the past 140,000 years, for different precipitation scalings. As can be seen from this plot, it seems that the main difference in the results happens during the glacial periods and not the Eemian and the Holocene. However the main focus of this project is to model the Eemian ice sheet.
Figures 44 to 49 show the modelled Eemian ice sheet extents for the same precipitation scalings. It can be seen in figure 13 that the SeaRISE scaling results in a larger precipitation during the Eemian and smaller during the two glacials than the scaling from [Buchardt et al., 2012]. This explains why the SeaRISE ice sheet extents further and has a higher thickess than the Buchardt ice sheet is.
The present day precipitation scaled to temperature results in the largest ice sheet during the glacials and the smallest during Eem. This is because it has a larger precipitation during the glacials, but lower during Eem, than the two others.

We do not know much about the precipitation in Greenland during the Eemian, meaning that we might overshoot the amount of accumulation happening at this time. As can be seen from figure 13, both the SeaRISE and the Buchardt precipitations are much higher during Eem than at present, but we do not know if this was actually the case.
We also do not know if the precipitation fell in the pattern as it does today. Maybe more of the snow fell in the north than at present and that could explain why we find evidence of Eemian ice there, but cannot seem to reproduce an ice sheet consistent with this data [Plach et al., 2018].

All the Eemian ice evolutions seem to follow the same pattern. They start retreating in the north and the south-west between -130 ka and -125 ka. Between -125 ka and

-120 ka the ice retreats even further south, resulting in only ice around the middle of Greenland towards the east. After this the ice starts to grow again, but not in the north, mostly in the south and around the coastline.
It is known from the study done by [MacGregor et al., 2015], that can be seen in figure 4, that there is currently Eemian ice at the bottom of the northern part of the Greenland ice sheet. We also know there has been found evidence of Eemian ice in all the deep ice cores in Greenland. This means that there must have been at least some ice in the northern part of Greenland during this time. Because the ice will have had a very hard time moving so far north from the ice sheets shown in figures 44 to 49, due to ice dynamics. This means that the ice sheets modelled in this study probably are not very comparable with how the ice sheet actually looked during the Eemian.
This begs the question, how have they produced ice sheets like the ones shown in figure 3 In the study done by [Plach et al., 2018]? The ice sheet is modelled using a constant sea level and the model is forced using ice front retreat, which does not allow the ice sheet to grow past the extent of the present day ice sheet. This means that the ice sheet cannot grow out into the ocean like the one in this study does.

The reason for not using ice front retreat in this study, is that with this calving parameter, the ice sheet would not be able to grow a bridge to Canada or recreate something resembling a glacial ice sheet, because the ice cannot grow past present day extent. Since part of the aim of this study was to include the transition from glacial to interglacial, to see if including Canada made any kind of difference, this calving parameter could not be used.
Using ice front retreat could have been able to remove all these seemingly random blobs of ice growing into the ocean everywhere, but they are something we will have to deal with, if we want to model the transition from glacial to interglacial.

Another reason that the ice sheets modelled in this study do not resemble the ice sheets in figure 3, is that these studies all grow the Eemian ice sheet, without the transition from glacial to intergalcial. This means that their bedrock topography does not need time to rebound, from being pressed down by the large amounts of ice during the glacial.
This rebound of the bedrock results in lower altitudes and because of the lapse rate correction also warmer temperatures. Because of these higher temperatures the ice sheet is not as resistant to the deglaciation, resulting in the larger and faster retreat of the ice sheet.

This problem with the ice sheet being trapped in the south is not limited to this project. In a study by [Solgaard et al., 2013] they found the same difficulties growing the ice sheet further north from this state. Their problem was due to atmospheric Föhn effect, that resulted in warmer temperatures on the northern side of the ice sheet, preventing it from growing any further north.
In this project the lowering of the bedrock elevation due to the weight of the glacial ice, has resulted in warm temperatures due to the laps rate of the atmosphere. Meaning that the temperature in the north of the ice sheet is so high, that the accumulation of mass in this area is balanced out by surface and basal melt, making it very hard for the ice sheet to grow in that direction.

Figures 50 to 52 show the ice extent at present day for the model runs in figure 43. From this it can be seen that ice sheets produced by these runs are much smaller than the present day ice sheet's actual extent. The reason for this is probably again, that the large amounts of glacial ice in the period before has resulted in a lower bedrock elevation, meaning that due to the lapse rate, the temperatures are higher.
As it can be seen in figure 43, the ice sheet extents start to grow again at the very end, meaning that the bedrock is rebounding and the temperatures over the ice are getting lower. If the model had run for just a couple of thousand years more, the ice sheet could have possibly grown to something resembling the present day ice sheet.
One possible reason for the ice sheet being too small is that the bedrock sinking was too large during the glacial leading to too much surface melting and a smaller ice sheet. This would mean that the glacial ice sheet was too big, and investigating this could be a next step to work on. It is also possible that the bedrock model is not accurate.

The SeaRISE run without Canada has been terminated after 67,000 years due to the non-physicality of the model at this point. The run resulted in an ice sheet of thickness 7 km and a diffusivity of the ice of over 20,000 $\frac{m^2}{s}$. Up until the model enters the last glacial period, the numbers are all on similar levels to the other model runs, therefore it was chosen to not include the results of the Eemian inter glacial.

When modelling an ice sheet of the size of Greenland it is necessary to have a climate model coupled to the ice flow model to create the feedback effect coming from the rest of the climate systems. This includes both the temperature of the atmosphere and the ocean, sea level changes and precipitation patterns. If a climate model had been coupled to PISM in this study, it could have resulted in more realistic results for the Eemian and present day ice sheets.
Doing this would of course also have resulted in a much larger complexity of the project and much higher computational times. And therefore it was ultimately decided, that doing this was not realistic in the time frame set for this project.

9 Conclusion

In this thesis, the PISM ice flow model was used to investigate the evolution and mass balance of the Greenland ice sheet. The stability of the present day ice sheet was tested, for increasing temperatures over Greenland. The results from this showed that small temperature increases can result in a significant loss of mass from the ice sheet.
The model was used to recreated glacial conditions over Greenland, for different percentages of present day precipitation. The results from this showed, that PISM had difficulties recreating an ice sheet of quite the same extend, as the glacial ice sheet was believed to have.
The models were forced using basal heat flux from [Shapiro and Ritzwoller, 2004] and scaled versions of air temperature and precipitation from RACMO [Noël et al., 2018]. A number of runs were conducted using precipitation reconstruction records from [Buchardt et al., 2012] and the SeaRISE project [Huybrechts, 2002], a temperature reconstruction, created by combining δ^{18}O records from [NorthGRIP members, 2004], [NEEM community members, 2013] and [Barker et al., 2011] and a sea level reconstruction record from [Lisiecki and Raymo, 2005], to scale the RACMO data and the sea level trough out a glacial cycle.
The results from these glacial cycle runs, showed a very small ice cap during the Eemian, that had completely retreated from the north of Greenland and could not due to the sunken bed rock grow back in this direction.

Increasing the temperature over Greenland results in an increased mass loss of the ice sheet, leading to an increase in the global mean sea level. Studies show that only a few degrees increase is needed, to result in a significant increase of the global mean sea level.
Table 1 contains the rough estimates of the increase of the global mean sea level at different increased temperatures. Here we see that an increase of just 2°C results in an increase of 1.29 m. This means that if the worlds population manages to stay within the numbers of the Paris agreement [UN, Paris Agreement, 2015], the global mean sea level would still increase by more than a meter, and this number is with out the contribution from the Antarctic ice sheet.
When increasing the temperature over Greenland with 8°C or more, the ice sheet completely disappears, meaning that under temperature conditions resembling the Eemian interglacial, there is a risk of loosing the GrIS all together. However more complex models are needed to investigate the sensitivity of the ice sheets and to determine how quickly the mass loss can occur.

PISM is able to recreate something resembling the ice extent during the LGM, but has a hard time forming an ice bridge between Greenland and Canada. This is probably due to the fact, that the precipitation from the RACMO regional climate model that is used to force the PISM model does not match the glacial precipitation pattern, where more snow might have fallen in the north.
This missing precipitation in the north results in a complete retreat of the Eemian ice sheet from the northern part of Greenland, which is not in agreement with the data found by [MacGregor et al., 2015] and [NEEM community members, 2013], where evidence of Eemian has been found in the northern part of Greenland at present day.

At the end of the Eemian, the ice sheet has a hard time growing towards the north again. This most likely because the bedrock has not fully rebounded, from being pressed down by the previous glacial ice sheet, meaning that the temperature is to high for the ice to evolve in this direction due to increased surface melting..
Since there is precipitation missing in the north, we do not see a significant difference when including Canada in computational domain, compared to when we do not. This is because without snow fall in the north, the connection between the two ice sheets does not reach a size or thickness that is significant enough too have an impact on the later ice retreat.
The model is also not able to recreate the present day ice sheet, after running through a glacial cycle. This is again most likely due to the higher temperatures associated with the lack of rebound of the bedrock.
It could also be related to our glacial ice sheet to be too big, and thereby causing more sinking of the bedrock. We conclude that in order to model the evolution of the Greenland ice in the interglacial periods, the preceding glacials must also be considered due to their significant and delayed effect on the bedrock height.

To further investigate the evolution of the Eemian ice sheet and the present day ice sheet under warmer conditions, there would be a need for a precipitation field of a higher spacial resolution than the RACMO data. This data set does not capture the complexity of the precipitation over Greenland, resulting in a map with no rain or snow fall in the north.
This higher resolution precipitation map will also be a necessity in any further investigations of the importance of including Canada in the computational domain, because it will require a more accurate snow fall pattern for northern Greenland and Canada.

Another problem was related to the calving mechanism.. The model runs presented in this thesis used the option ”float kill”, where floating ice is removed. This option results in these blobs of ice growing out from the coast of Greenland, that are not in agreement with how we believe the ice sheet would evolve. There is a need for a more comprehensive study of the different calving parameters of PISM and when to use these to get the most natural ice sheet growth.
Furthermore PISM would need to be coupled with a climate model, that could model the feedback mechanisms between the ice sheet and the rest the rest of the climate systems. The climate system of Earth is much more complicated than described in this thesis and than PISM can model it as a stand-alone model. Without the feedback mechanisms from the ocean and atmosphere, the ice sheet can just evolve freely, not taking into account that temperature and precipitation changes drastically, when the ice sheet grows or retreats. This should be the main focus of future studies.

This project has yielded some interesting results regarding the evolution of GrIS under warmer conditions. The models show that only a few degrees increased temperature over Greenland can result in a drastic mass loss, where the ice sheet retreats away from the coast line all together.. The loss of mass from the ice sheet can result in increasing sea levels all around the globe and could result in less or no fresh water flux into the Atlantic ocean. Meaning a risk of turning of the North Atlantic Current all together.

References

[Aschwanden et al., 2016] Aschwanden, A., Fahnestock, M., and Truffer, M. (2016). Complex greenland outlet glacier flow captured. *Nature Communications*, 7:10524.

[Aschwanden et al., 2019] Aschwanden, A., Fahnestock, M. A., Truffer, M., Brinkerhoff, D. J., Hock, R., Khroulev, C., Mottram, R., and Khan, S. A. (2019). Contribution of the greenland ice sheet to sea level over the next millennium. *Science Advances*, 5(6):eaav9396.

[Barker et al., 2011] Barker, S., Knorr, G., Lawrence, E. R., Parrenin, F., Putnam, A. R., Skinner, L. C., Wolff, E., and Ziegler, M. (2011). 800,000 years of abrupt climate variability. *Science*, 334 (6054):347–351.

[Bennike and Björck, 2002] Bennike, O. and Björck, S. (2002). Chronology of the last recession of the greenland ice sheet. *Journal of Quaternary Science*, 17:211 – 219.

[Buchardt et al., 2012] Buchardt, S. L., Clausen, H. B., Vinther, B. M., , and Dahl-Jensen, D. (2012). Investigating the past and recent 18o-accumulation relationship seen in greenland ice cores. *Clim. Past*, 8:2053–2059.

[Bueler and Brown, 2008] Bueler, E. and Brown, J. (2008). Shallow shelf approximation as a "sliding law" in a thermomechanically coupled ice sheet model. *Journal of Geophysical Research*.

[Clark et al., 2020] Clark, P., He, F., Golledge, N., Mitrovica, J., Dutton, A., Hoffman, J., and Dendy, S. (2020). Oceanic forcing of penultimate deglacial and last interglacial sea-level rise. *Nature*, 577:660–664.

[Cuffey and Paterson, 2010] Cuffey, K. and Paterson, W. (2010). The physics of glaciers. fourth edition.

[Dahl-Jensen et al., 1998] Dahl-Jensen, D., Mosegaard, K., Gundestrup, G., Clow, G., Johnson, S., Walløe Hansen, A., and Balling, B. (1998). Past temperature directly from the greenland ice sheet. *Science*.

[Fausto et al., 2007] Fausto, R., Ahlstrøm, A., Bøggild, C., and Johnsen, S. (2007). New present day temperature parameterization and degree day model for greenland. *AGU Fall Meeting Abstracts*.

[Fettweis et al., 2020] Fettweis, X., Hofer, S., Krebs-Kanzow, U., Amory, C., Aoki, T., Berends, C. J., Born, A., Box, J. E., Delhasse, A., Fujita, K., Gierz, P., Goelzer, H., Hanna, E., Hashimoto, A., Huybrechts, P., Kapsch, M.-L., King, M. D., Kittel, C., Lang, C., Langen, P. L., Lenaerts, J. T. M., Liston, G. E., Lohmann, G., Mernild, S. H., Mikolajewicz, U., Modali, K., Mottram, R. H., Niwano, M., Noël, B., Ryan, J. C., Smith, A., Streffing, J., Tedesco, M., van de Berg, W. J., van den Broeke, M., van de Wal, R. S. W., van Kampenhout, L., Wilton, D., Wouters, B., Ziemen, F., and Zolles, T. (2020). Grsmbmip: intercomparison of the modelled 1980–2012 surface mass balance over the greenland ice sheet. *The Cryosphere*, 14(11):3935–3958.

[Fowler and Ng, 2021] Fowler, A. and Ng, F. (2021). *Glaciers and Ice Sheets in the Climate System The Karthaus Summer School Lecture Notes: The Karthaus Summer School Lecture Notes*.

[Glen, 1955] Glen, J. W. (1955). The creep of polycrystalline ice, proceedings of the royal society of london series a. *Mathematical and physical sciences*, 228:519–538.

[Huybrechts, 2002] Huybrechts, P. (2002). Sea-level changes at the lgm from ice-dynamic reconstructions of the greenland and antarctic ice sheets during the glacial cycles. *Quat. Sci. Rev.*, 21 (1–3):203–231.

[Imbrie and McIntyre, 2006] Imbrie, J. D. and McIntyre, A. (2006). Specmap time scale developed by imbrie et al., 1984 based on normalized planktonic records (normalized o-18 vs time, specmap.017). *PANGAEA*.

[Jakobsson et al., 2020] Jakobsson, M., Mayer, L., Bringensparr, C., Castro, C., Mohammad, R., Johnson, P., Ketter, T., Accettella, D., Amblas, D., An, L., Arndt, J. E., Canals, M., Casamor, J. L., Chauché, N., Coakley, B., Danielson, S., Demarte, M., Dickson, M.-L., Dorschel, B., and Zinglersen, K. (2020). The international bathymetric chart of the arctic ocean version 4.0. *Scientific Data*, 7:14.

[Johnsen et al., 1992] Johnsen, S., Clausen, H., Dansgaard, W., Gundestrup, N., Hansson, M., Jonsson, P., Steffensen, J., and Sveinbjörnsdottir, A. (1992). A "deep" ice core from east greenland. *MoG Geoscience*, 29.

[Jouzel J., 2007] Jouzel J., e. a. (2007). Orbital and millennial antarctic climate variability over the past 800,000 years. *Science*, 317:793.

[Kirchner et al., 2011] Kirchner, N., Hutter, K., Jakobsson, M., and Gyllencreutz, R. (2011). Capabilities and limitations of numerical ice sheet models: a discussion for earth-scientists and modelers. *Quaternary Science Reviews*, 30(25):3691–3704.

[Kopp et al., 2009] Kopp, R., Simons, F., Mitrovica, J., Maloof, A., and Oppenheimer, M. (2009). Probabilistic assessment of sea level during the last interglacial stage. *Nature*, 462:863–867.

[Lambeck, 2004] Lambeck, K. (2004). Sea-level change through the last glacial cycle: Geophysical, glaciological and palaeogeographic consequences. *External Geophysics*, 336:677–689.

[Lisiecki and Raymo, 2005] Lisiecki, L. and Raymo, M. (2005). Lisiecki, l. e. raymo, m. e. a pliocene-pleistocene stack of 57 globally distributed benthic 18o records. paleoceanography 20, pa1003. *Paleoceanography*, 20.

[MacGregor et al., 2015] MacGregor, J., Fahnestock, M., Catania, G., Paden, J., Gogineni, S., Young, K., Rybarski, S., Mabrey, A., Wagman, B., and Morlighem, M. (2015). Radiostratigraphy and age structure of the greenland ice sheet. *Journal of Geophysical Research: Earth Surface*, 120.

[Morlighem et al., 2017] Morlighem, M., Williams, C., Rignot, E., An, L., Arndt, J., Bamber, J., Catania, G., Chauché, N., Dowdeswell, J., Dorschel, B., Fenty, I., Hogan, K., Howat, I., Hubbard, A., Jakobsson, M., Jordan, T., Kjeldsen, K., Millan, R., Mayer, L., Mouginot, J., Noël, B., O'Cofaigh, C., Palmer, S., Rysgaard, S., Seroussi, H., Siegert, M., Slabon, P., Straneo, F., van den Broeke, M., Weinrebe, W., Wood, M., and Zinglersen, K. (2017). Bedmachine v3: Complete bed topography and ocean bathymetry mapping of greenland from multibeam echo sounding combined with mass conservation. *Geophysical Research Letters*, 44(21):11,051–11,061.

[Nagler et al., 2015] Nagler, T., Rott, H., Hetzenecker, M., Wuite, J., and Potin, P. (2015). The sentinel-1 mission: New opportunities for ice sheet observations. *Remote Sensing*, 7:9371.

[NEEM community members, 2013] NEEM community members (2013). Eemian interglacial reconstructed from a greenland folded ice core. *Nature*, 493:489–494.

[Noël et al., 2018] Noël, B., van de Berg, W. J., van Wessem, J. M., van Meijgaard, E., van As, D., Lenaerts, J. T. M., Lhermitte, S., Kuipers Munneke, P., Smeets, C. J. P. P., van Ulft, L. H., van de Wal, R. S. W., and van den Broeke, M. R. (2018). Modelling the climate and surface mass balance of polar ice sheets using racmo2 – part 1: Greenland (1958–2016). *The Cryosphere*, 12(3):811–831.

[NorthGRIP members, 2004] NorthGRIP members (2004). High-resolution record of northern hemisphere climate extending into the last interglacial period. *Nature*, 431:147–151.

[Plach et al., 2018] Plach, A., Nisancioglu, K. H., Le clec'h, S., Born, A., Langebroek, P. M., Guo, C., Imhof, M., and Stocker, T. F. (2018). Eemian greenland smb strongly sensitive to model choice. *Climate of the Past*, 14(10):1463–1485.

[Praetorius, 2018] Praetorius, S. K. (2018). North atlantic circulation slows down. *Nature*, 556:180–181.

[Shapiro and Ritzwoller, 2004] Shapiro, N. and Ritzwoller, M. (2004). Inferring surface heat flux distributions guided by a global seismic model: Particular application to antarctica. *Earth and Planetary Science Letters*, 223:213–224.

[Shepherd et al., 2020] Shepherd, A., Ivins, E., Rignot, E., Smith, B., Van den Broeke, M., Velicogna, I., Whitehouse, P., Briggs, K., Joughin, I., Krinner, G., Nowicki, S., Payne, A., Scambos, T., Schlegel, N.-J., Aa, G., Agosta, C., Ahlstrøm, A., Babonis, G., Barletta, V., and Wuite, J. (2020). Mass balance of the greenland ice sheet from 1992 to 2018. *Nature*, 579.

[Smith-Johnsen et al., 2020] Smith-Johnsen, S., de Fleurian, B., Schlegel, N., Seroussi, H., and Nisancioglu, K. (2020). Exceptionally high heat flux needed to sustain the northeast greenland ice stream. *The Cryosphere*, 14(3):841–854.

[Solgaard et al., 2013] Solgaard, A., Bonow, J., Langen, P., Japsen, P., and Hvidberg, C. (2013). Mountain building and the initiation of the greenland ice sheet. *Palaeogeography, Palaeoclimatology, Palaeoecology*, 392:161–176.

[Stone et al., 2012] Stone, E., Lunt, D., Annan, J., and Hargreaves, J. (2012). Quantification of the greenland ice sheet contribution to last interglacial sea-level rise. *Climate of the Past Discussions*, 8:2731–2776.

[The PISM authors, 2020] The PISM authors (2020). Pism a parallel ice sheet model, version 1.2.1.

[UN, Paris Agreement, 2015] UN, Paris Agreement (2015). *Adoption of the Paris Agreement : draft decision -CP.21 : proposal*. Geneva :. 2015-12-12. "Annex: Paris Agreement": p. 21-32.

[Veres et al., 2013] Veres, D., L., B., Landais, A., Toyé Mahamadou Kele, H., Lemieux-Dudon, B., Parrenin, F., Martinerie, P., Blayo, E., Blunier, T., Capron, E., Chappellaz, J., Rasmussen, S. O., Severi, M., Svensson, A., Vinther, B., and Wolff, E. W. (2013). The antarctic ice core chronology (aicc2012): an optimized multi-parameter and multi-site dating approach for the last 120 thousand years. *Clim. Past*, 9:1733–1748.

[Vinther and Johnsen, 2013] Vinther, B. and Johnsen, S. (2013). *Greenland Stable Isotopes*, pages 403–409.

[Winkelmann et al., 2010] Winkelmann, R., Martin, M., Haseloff, M., Albrecht, T., Bueler, E., Khroulev, C., and Levermann, A. (2010). The potsdam parallel ice sheet model (pism-pik) - part 1: Model description. *The Cryosphere Discussions*, 4.

[worlddata.info, 2022] worlddata.info (2022). Maldives: country data and statistics. `https://www.worlddata.info/asia/maldives/index.php`. Accessed: 2022-19-05.

Appendices

Appendix A - SIA stress balance regime run

The command line for the SIA only stress balance regime run described in section 6.1.

```
mpiexec -n 20 pismr \
-i topgrafy.nc -bootstrap -Mx 221 -My 333 \
-Mz 101 -Mbz 11 -z_spacing equal -Lz 4300 -Lbz 2000 \
-skip -skip_max 10 \
-grid.recompute_longitude_and_latitude false \
-grid.registration corner \
-ys -5000 -ye 0 \
-atmosphere yearly_cycle,elevation_change \
-atmosphere_yearly_cycle_file atmosphere.nc \
-atmosphere.elevation_change.file atmosphere_elevation_change.nc \
-temp_lapse_rate 6.5 \
-surface pdd \
-calving float_kill \
-sia_e 3.0 -stress_balance sia \
-ts_file ts_outfile.nc -ts_times -5000:1:0 \
-extra_file ex_outfile.nc -extra_times -5000:10:0 \
-extra_vars diffusivity,velsurf_mag,thk,topg,usurf,velbase_mag \
-o outfile.nc
```

Appendix B - Hybrid stress balance regime run

The command line for the hybrid stress balance regime run described in section 6.2.

```
mpiexec -n 20 pismr \
-i topgrafy.nc -bootstrap -Mx 221 -My 333 \
-Mz 101 -Mbz 11 -z_spacing equal -Lz 4300 -Lbz 2000 \
-skip -skip_max 10 \
-grid.recompute_longitude_and_latitude false \
-grid.registration corner \
-ys -5000 -ye 0 \
-atmosphere yearly_cycle,elevation_change \
-atmosphere_yearly_cycle_file atmosphere.nc \
-atmosphere.elevation_change.file atmosphere_elevation_change.nc \
-temp_lapse_rate 6.5 \
-surface pdd \
-calving float_kill \
-sia_e 3.0 -stress_balance ssa+sia \
-pseudo_plastic -pseudo_plastic_q 0.5 \
-ts_file ts_outfile.nc -ts_times -5000:1:0 \
-extra_file ex_outfile.nc -extra_times -5000:10:0 \
-extra_vars diffusivity,velsurf_mag,thk,topg,usurf,velbase_mag \
-o outfile.nc
```

Appendix C - Lapse rate run

The command line for the laps rate correction run described in section 6.3.

```
mpiexec -n 20 pismr \
-i topgrafy.nc -bootstrap -Mx 221 -My 333 \
-Mz 101 -Mbz 11 -z_spacing equal -Lz 4300 -Lbz 2000 \
-skip -skip_max 10 \
-grid.recompute_longitude_and_latitude false \
-grid.registration corner \
-ys -5000 -ye 0 \
-atmosphere yearly_cycle,elevation_change \
-atmosphere_yearly_cycle_file atmosphere.nc \
-atmosphere.elevation_change.file atmosphere_elevation_change.nc \
-temp_lapse_rate 6.5 \
-surface pdd \
-calving float_kill \
-sia_e 3.0 -stress_balance ssa+sia \
-pseudo_plastic -pseudo_plastic_q 0.5 \
-ts_file ts_outfile.nc -ts_times -5000:1:0 \
-extra_file ex_outfile.nc -extra_times -5000:10:0 \
-extra_vars diffusivity,velsurf_mag,thk,topg,usurf,velbase_mag \
-o outfile.nc
```

Appendix D - Till friction run

The command line for the till friction run described in section 6.4.

```
mpiexec -n 20 pismr \
-i topgrafy.nc -bootstrap -Mx 221 -My 333 \
-Mz 101 -Mbz 11 -z_spacing equal -Lz 4300 -Lbz 2000 \
-skip -skip_max 10 \
-grid.recompute_longitude_and_latitude false \
-grid.registration corner \
-ys -5000 -ye 0 \
-atmosphere yearly_cycle,elevation_change \
-atmosphere_yearly_cycle_file atmosphere.nc \
-atmosphere.elevation_change.file atmosphere_elevation_change.nc \
-temp_lapse_rate 6.5 \
-surface pdd \
-calving float_kill \
-sia_e 3.0 -stress_balance ssa+sia \
-pseudo_plastic -pseudo_plastic_q 0.5 \
-topg_to_phi 15.0,40.0,-300.0,700.0 \
-till_effective_fraction_overburden 0.02 \
-tauc_slippery_grounding_lines \
-ts_file ts_outfile.nc -ts_times -5000:1:0 \
-extra_file ex_outfile.nc -extra_times -5000:10:0 \
-extra_vars diffusivity,velsurf_mag,thk,topg,usurf,velbase_mag \
-o outfile.nc
```

Appendix E - Present day steady state run

The command line for the present day steady state runs described in section 7.1.

```
mpiexec -n 20 pismr \
-i topgrafy.nc -bootstrap -Mx 221 -My 333 \
-Mz 101 -Mbz 11 -z_spacing equal -Lz 4300 -Lbz 2000 \
-skip -skip_max 10 \
-grid.recompute_longitude_and_latitude false \
-grid.registration corner \
-ys -20000 -ye 0 \
-atmosphere yearly_cycle,elevation_change \
-atmosphere_yearly_cycle_file atmosphere.nc \
-atmosphere.elevation_change.file atmosphere_elevation_change.nc \
-temp_lapse_rate 6.5 \
-surface pdd \
-calving float_kill \
-stress_balance.sia.max_diffusivity 50000 \
-sia_e 3.0 -stress_balance ssa+sia \
-pseudo_plastic -pseudo_plastic_q 0.5 \
-topg_to_phi 10.0,30.0,-300.0,300.0 \
-till_effective_fraction_overburden 0.02 \
-tauc_slippery_grounding_lines \
-ts_file ts_outfile.nc -ts_times -20000:10:0 \
-extra_file ex_outfile.nc -extra_times -20000:100:0 \
-extra_vars diffusivity,temppabase,tempicethk_basal,bmelt,tillwat,
   velsurf_mag,mask,thk,topg,usurf,hardav,velbase_mag,tauc \
-o outfile.nc
```

Appendix F - Glacial steady state runs

The command line for the Glacial steady state runs described in section 7.2.

```
mpiexec -n 20 pismr \
-i topgrafy.nc -bootstrap -Mx 111 -My 167 \
-Mz 101 -Mbz 11 -z_spacing equal -Lz 6000 -Lbz 2000 \
-skip -skip_max 10 \
-grid.recompute_longitude_and_latitude false \
-grid.registration corner \
-ys -50000 -ye 0 \
-atmosphere yearly_cycle,elevation_change \
-atmosphere_yearly_cycle_file atmosphere.nc \
-atmosphere.elevation_change.file atmosphere_elevation_change.nc \
-temp_lapse_rate 6.5 \
-surface pdd \
-calving float_kill \
-stress_balance.sia.max_diffusivity 50000 \
-sia_e 3.0 -stress_balance ssa+sia \
-pseudo_plastic -pseudo_plastic_q 0.5 \
-topg_to_phi 10.0,30.0,-300.0,300.0 \
-till_effective_fraction_overburden 0.02 \
-tauc_slippery_grounding_lines \
-ts_file ts_outfile.nc -ts_times -50000:10:0 \
-extra_file ex_outfile.nc -extra_times -50000:100:0 \
-extra_vars diffusivity,temppabase,tempicethk_basal,bmelt,tillwat,
   velsurf_mag,mask,thk,topg,usurf,hardav,velbase_mag,tauc \
-o outfile.nc
```

Appendix G - Eemian runs

The command line for the Eemian runs described in section 7.3.

```
mpiexec -n 20 pismr \
-i topgrafy.nc -bootstrap -Mx 111 -My 167 \
-Mz 101 -Mbz 11 -z_spacing equal -Lz 6000 -Lbz 2000 \
-skip -skip_max 10 \
-grid.recompute_longitude_and_latitude false \
-grid.registration corner \
-ys -140000 -ye 0 \
-atmosphere yearly_cycle,elevation_change,delta_T,frac_P \
-atmosphere_yearly_cycle_file atmosphere.nc \
-atmosphere.elevation_change.file atmosphere_elevation_change.nc \
-atmosphere_delta_T_file temperature_change_file.nc \
-atmosphere_frac_P_file precipitation_change_file.nc \
-temp_lapse_rate 6.5 \
-surface pdd \
-ocean constant -sea_level constant,delta_sl \
-ocean_delta_sl_file sealevel_change_file.nc \
-calving float_kill \
-stress_balance.sia.max_diffusivity 50000 \
-sia_e 3.0 -stress_balance ssa+sia \
-pseudo_plastic -pseudo_plastic_q 0.5 \
-topg_to_phi 10.0,30.0,-300.0,300.0 \
-till_effective_fraction_overburden 0.02 \
-tauc_slippery_grounding_lines \
-ts_file ts_outfile.nc -ts_times -140000:10:0 \
-extra_file ex_outfile.nc -extra_times -140000:1000:0 \
-extra_vars diffusivity,temppabase,tempicethk_basal,bmelt,tillwat,
   velsurf_mag,mask,thk,topg,usurf,hardav,velbase_mag,tauc \
-o outfile.nc
```